Characterization and selective manipulation of GnRHR-expressing neurons in the periaqueductal gray of female mice (*Mus musculus,* Linnaeus 1758)

Characterization and selective manipulation of GnRHR-expressing neurons in the periaqueductal gray of female mice (Mus musculus Linnaeus 1758)

Dissertation

zur Erlangung des Doktorgrades der Naturwissenschaften

vorgelegt von

Roberto de Angelis

geboren am

3. April 1983 in Rom, Italien

Institut für Experimentelle und Klinische Pharmakologie und Toxikologie der Medizinischen Fakultät der Universität des Saarlandes

Homburg (Saar)

2016

Referent: Professor Dr. Ulrich Boehm

Korreferent: Professor Dr. Frank Zufall

Tag der Abgabe der Dissertation: 23.11.2016

Zusammenfassung

Das Gonadotropin-freisetzendes Hormon (GnRH) ist der Hauptregler der Fortpflanzungsphysiologie bei Wirbeltieren. GnRH wird von einer kleinen Untergruppe von Hypothalamus Neuronen freigesezt. In die Hypophyse es auf gonadotrope zellen wirkt, die selektiv den Gonadotropin freisetzenden Hormonrezeptor (GnRHR) exprimieren. Das GnRHR-Signal in den gonadotrope zellen ist dann entscheidend für die Gonadenfunktion und damit die Fruchtbarkeit. Darüber hinaus haben klassische Studien an Ratten gezeigt, dass GnRH das weibliche Sexualverhalten fördert, da es direkt im Gehirn wirkt. Insbesondere verstärken GnRH-Infusionen im dorsalen periaqueduktalen Grau (PAG) die weibliche sexuelle Empfänglichkeit. Zuvor wurde in unserem Labor ein Mausmodell erzeugt, dass die zuverlässige Visualisierung der neuronalen Ziele von GnRH über Cre-abhängige Expressionen von τGFP in GnRHR-exprimierenden Zellen erlaubt. GnRHR Neuronen sind weit verbreitet in Bereichen des Gehirns der männlichen Maus, die an geschlechtsspezifischem Verhalten beteilgt sind, einschließlich des PAG. Darüber hinaus konnte GnRH eine Erhöhung des intrazellularen Kalzium induzieren und die Frequenz der Aktionspotentiale in GnRHR-Neuronen modulieren. Die Rolle von GnRHR-Neuronen im Verhalten blieb jedoch unerforscht. Durch die Verwendung des gleichen binären gentischen Ansatzes, hatte ich zunächst das Ziel, das GnRHR Netzwerk in dem PAG des weiblichen Gehirns der Maus bei gleichaltrigen Gruppen zu beschreiben. Ich fand eine breite Verteilung der GnRHR Neuronen spezifisch in der dorsalen und den seitlichen Teilen des PAG, jedoch nicht in dem ventrolateralen PAG. Darüber hinaus nimmt die Anzahl der GnRH Neuronen mit dem Alter zu, was auf eine späte Errichtung des GnRHR-Netzes in das PAG hindeutet. Des weiteren versuchte ich die genetische Ablation von GnRHR Neuronen im dorsalen PAG. Um dies zu tun, injizierte ich ein Adeno-assoziierten Virus im PAG, der die cre-abhängige Expression einer konstitutiv aktiven Form von Caspase-3 vermittelt. Auf diese Weise konnte ich den programmierten Zelltod in den PAG-GnRHR-Neuronen induzieren. Überraschenderweiße beeinflusste die Ablation die weibliche sexuelle Empfänglichkeit nicht. Darüber hinaus habe ich die Aktivität der GnRH Neurone in Bezug auf das weibliche Sexualverhalten mit dem Marker c-fos untersucht. Ich fand eine stark hochregulierte c-fos Aktivität im PAG, jedoch nicht in GnRHR Neuronen.

In einer parallelen Studie untersuchte ich die Rolle des metabotropen Rezeptors 5 (mGluR5) beim Einstzen der Pubertät. Die neuroendokrinen Mechanismen, die den Beginn der Pubertät regulieren, werden weitgehend erforscht, sind aber immer noch unzureichend verstanden. Beweis dafür zeigte die Rolle von Glutamat bei der Regulation von GnRH-Neuronen. Weibliche Mäuse, denen das metabotrope Rezeptor 5 (mGluR5) Gen fehlte, zeigten einen verzögerte Pubertät und eine verminderte Fertilität. Zur Analyse der Gonadotropinfunktion in Abwesenheit von mGluR5 analysierte ich die Serumprofile der gesamten Hypophysenhormone. Ich fand reduzierte Mengen von Follikel-stimulierenden Hormones, jedoch blieb die Menge von luteinisierenden Hormones gleich. Beim Hormonspiegel von Schilddrüsen-stimulierenden Hormones bei weiblichen Mäusen, denen das mGluR5-Gen fehlte, konnte ich jedoch einen Anstieg feststellen. Diese Ergebnisse könnten neue Einsichten in die Mechanismen liefern, die die Fruchtbarkeit regulieren und helfen kann dazu beitragen, neue Therapien für Pubertätsstörungen zu entwickeln.

Abstract

The gonadotropin-releasing hormone (GnRH) is the main regulator of reproductive physiology in vertebrates. GnRH is released by a small subset of hypothalamic neurons. In the pituitary gland it acts on gonadotropes, which selectively express the Gonadotropin-releasing hormone receptor (GnRHR). The GnRHR signal in gonadotrope cells is then crucial for gonadal function and thus fertility. Furthermore, classical studies in rats indicated that GnRH strongly facilitates female sexual behavior, by acting directly in the brain. In particular, GnRH infusions within the dorsal periaqueductal gray (PAG) augmented female sexual receptivity. Previously our lab has generated a mouse model that allowed for the reliable visualization of the neural targets of GnRH, *via* Cre-dependent expression of τGFP in GnRHR-expressing cells. GnRHR neurons are widely present in the male mouse brain in areas involved in sex-specific behaviors, including the PAG. Furthermore, GnRH could elicit calcium responses and modulate firing activity in GnRHR neurons. However, the role of GnRHR neurons in behavior remained unexplored. By using the same binary genetic approach, I first aimed to describe the GnRHR network in the PAG of the female mouse in age-matched groups. I found a wide distribution of GnRHR neurons specifically in the dorsal and lateral parts of the PAG, but not in the ventrolateral PAG. Furthermore, the number of GnRHR neurons increased during age, suggesting a late establishment of the GnRHR network within the PAG. Secondly, I aimed to genetically ablate GnRHR neurons in the dorsal PAG. In order to do that, I injected in the dorsal PAG an adeno-associated virus that mediates cre-dependent expression of a constitutively active form of caspase-3. In this way, I could induce programmed cell death only in PAG-GnRHR neurons. Surprisingly, ablation did not affect female sexual receptivity. Moreover, I investigated GnRHR neural activity following female sexual behavior by using the marker c-fos. I found a strong c-fos up-regulation in the PAG, but not in GnRHR neurons.

In a parallel study I have explored the role of metabotropic glutamate receptor 5 (mGluR5) in the initiation of puberty. The neuroendocrine mechanisms that regulate the initiation of puberty have been largely explored but still poorly understood. Evidence revealed a role of glutamate in the regulation of GnRH neurons. Female

mice lacking the metabotropic receptor 5 (mGluR5) gene exhibited delayed puberty and reduced fertility. To analyze gonadotropin function in the absence of mGluR5 I analyzed the whole pituitary hormone serum profiles. I found reduced levels of follicle stimulating hormone but not luteinizing hormone, together with higher thyroid-stimulating hormone levels in female mice lacking the mGluR5 gene. These results could provide new insights into the mechanisms that can regulate fertility and help to develop new therapies for puberty disorders.

Table of contents

List of figures

List of tables

List of abbreviations

3V	Third ventricle
µl	Microliter
µm	Micrometer
µM	Micromolar
°C	degree Celsius
ACSF	Artificial cerebrospinal fluid
ACTH	Adrenocorticotropic hormone
AHA	Anterior hypothalamic area
AOB	Accessory olfactory bulb
Aq	Aqueduct
Arc	Arcuate nucleus
AVPV	Anteroventral periventricular nucleus
bp	Base pair
cDNA	complementary deoxyribonucleic acid
ACSF	Artificial cerebrospinal fluid
AAV	Adeno-associated virus
AAV-Cas3	AAV5- flex-taCasp3-TEVp
BL	Barley lectin
BNST	Bed nucleus stria terminalis
ChR2	Channelrhodopsin2
CMV	Cytomegalovirus
CTg	Central tegmental nucleus
d	Day
DAG	Diacylglycerol
DLPAG	Dorsolateral periaqueductal gray
DMPAG	Dorsomedial periaqueductal gray
DNA	Deoxyribonucleic acid
dPAG	Dorsal periaqueductal gray
DpMe	Deep mesencephalic nucleus
DR	Dorsal raphe
DRC	Dorsal raphe cap

DTA	Diphtheria toxin A fragment
DTg	Dorsal tegmental nucleus
DTR	Diphtheria toxin receptor
D3V	Dorsal third ventricle
E.	Embryonic day
e.g.	*exempli gratia*, for example
ERE	Estrogen responsive element
ERα	Estrogen receptor alpha
ERβ	Estrogen receptor beta
ESP1/22/24	Exocrine gland secreting peptide 1/22/24
Esr1	Estrogen receptor 1
et al.	*et altera*
FACS	Fluorescent activated cell sorting
FSH	Follicle stimulating hormone
g	Grams
GFP	Green fluorescent protein
GnRH	Gonadotropin releasing hormone
GnRHR	Gonadotropin releasing hormone receptor
GPR54	G-protein coupled receptor 54
GRIC	GnRHR-IRES-Cre
αGSU	Glycoprotein alpha subunit
hpg	Hypothalamus-pituitary-gonadal axis
hPLAP	human placental alkaline phosphatase
hr(s)	Hour(s)
i.e.	*Id est*, that is
IHC	Immunohistochemistry
i.p.	Intraperitoneal
IP_3	Inositol triphospate
IRES	Internal ribosome entry site
IV	Fourth (ventricle)
KO	Knock-out
LC	Locus ceruleus
LDTg	Laterodorsal tegmental nucleus

LH	Luteinizing hormone
LPAG	Lateral periaqueductal gray
LS	Lateral septum
LV	Lateral ventricle
M	Molar
ME	Median eminence
MeA	Medial amygdala
mg	Milligram
mGluR5	metabotropic glutamate receptor 5
min(s)	Minute(s)
ml	Milliliter
mM/mMol	Millimolar
MOB	Main olfactory bulb
mRNA	Messenger ribonucleic acid
MS	Medial septum
NaCl	Sodium chloride
NaOH	Sodium hydroxide
nm	Nanometer
OB	Olfactory bulb
ORF	Open reading frame
OVLT	Organo vasculosum lamina terminalis
OVX	Ovariectomy
P	Progesterone
PAG	Periaqueductal gray
PBS	Phosphate buffered saline
PCA	Principal component analysis
PCR	Polymerase chain reaction
Pe	Periventricular nucleus
PFA	Paraformaldehyde
pH	potentium Hydrogenii
PKC	Protein kinase C
PMCO	Posteromedial cortical amygdalar nucleus
POA	Preoptic area

PR	Progesterone receptor
PRL	Prolactin
RNA	Ribonucleic acid
ROSA	Reverse oriented splice acceptor
RT	Room temperature
R26-DTA	Rosa26-Diphtheria toxin A
SDS	Sodium dodecyl sulfate
sec(s)	Second(s)
SF-1	Steroidogenic factor 1
Su3	Supraoculomotor central gray
Tris	Tris-(hydroxymethyl)-aminomethane
TRPC2	Transient receptor potential C2
TSH	Thyroid stimulating hormone
UkS	Universitätsklinikum Saarland
V	Volume
VLPAG	Ventrolateral periaqueductal gray
VMH	Ventromedial nucleus of the hypothalamus
VMHdm	dorsomedial part of the ventromedial nucleus of the hypothalamus
VMHvl	ventrolateral part of the ventromedial nucleus of the hypothalamus
VNO	Vomeronasal organ
wo	Weeks old
wt	Wild Type
YFP	Yellow fluorescent protein

1 Introduction

1.1 The reproductive axis

Reproduction in vertebrates depends on the coordinated action of three components: the hypothalamus, the pituitary gland and the gonads, that together form the hypothalamus-pituitary-gonadal (hpg) axis. The hpg axis is essential for many aspects of reproductive function during the life span of an organism, such as gonadal development, the onset of puberty and the maintenance of fertility in the adult (Sisk and Foster, 2004). The hpg axis is organized hieratically under strict control of the central nervous system especially by a small subset of hypothalamic neurons scattered throughout the preoptic area (POA) which synthesize and release from their nerve terminals in the median eminescence (ME) the gonadotropin hormone-releasing hormone (GnRH) in a pulsatile manner. The GnRH peptide then reaches (through the hypophyseal portal vasculature) the anterior pituitary where it regulates the synthesis and release of luteinizing hormone (LH) and follicle-stimulating hormone (FSH) from gonadotrope cells, which express the GnRH receptor (GnRHR). LH and FSH in turn are released in the circulation and regulate gonadal function, such as follicle maturation and ovulation in females, and production of sperm in males. LH and FSH also affect steroid hormones production from gonads, which are released into the bloodstream providing feedbacks at the level of the brain and the pituitary (fig.1.1).

1.1.1 GnRH is the key molecule in the reproductive axis function

The genetic evidence of GnRH function came from the hypogonadic (*hpg*) mouse which has a loss-of-function mutation in the GnRH gene. Injections of GnRH or transplantation of hypothalamic portions containing GnRH neurons restored gonadotropin secretion and rescued the hypogonadic phenotype, demonstrating the hypothalamic origin of the central control by GnRH in the maturation of gonads and their proper function (Charlton, 2004). GnRH (pGlu-Hys-Trp-Ser-Tyr-Gly-Leu-Arg-Pro-Gly-NH_2) is a short peptide originally encoded as a pre-prohormone of 92 aminoacids (Maggi et al., 2016). The peptide was initially isolated from porcine and ovine hypothalamic extracts (Baba et al., 1971; Schally et al., 1971), but can be found in all vertebrates from the lamprey to humans (Kavanaugh et al., 2008). In humans, the

GnRH gene (GNRH1) is located on the short arm of chromosome 8 (Maggi et al., 2016). A variety of additional GnRH isoforms exists among different species (Kavanaugh et al., 2008). For example, in humans and monkeys GnRH-II is also present and encoded by a different gene and interestingly, belongs to a distinct neuronal population with respect to GnRH-I (Maggi et al., 2016), although with unclear functions. In fish models such as zebrafish (*Danio rerio*) or medaka (*Oriza*

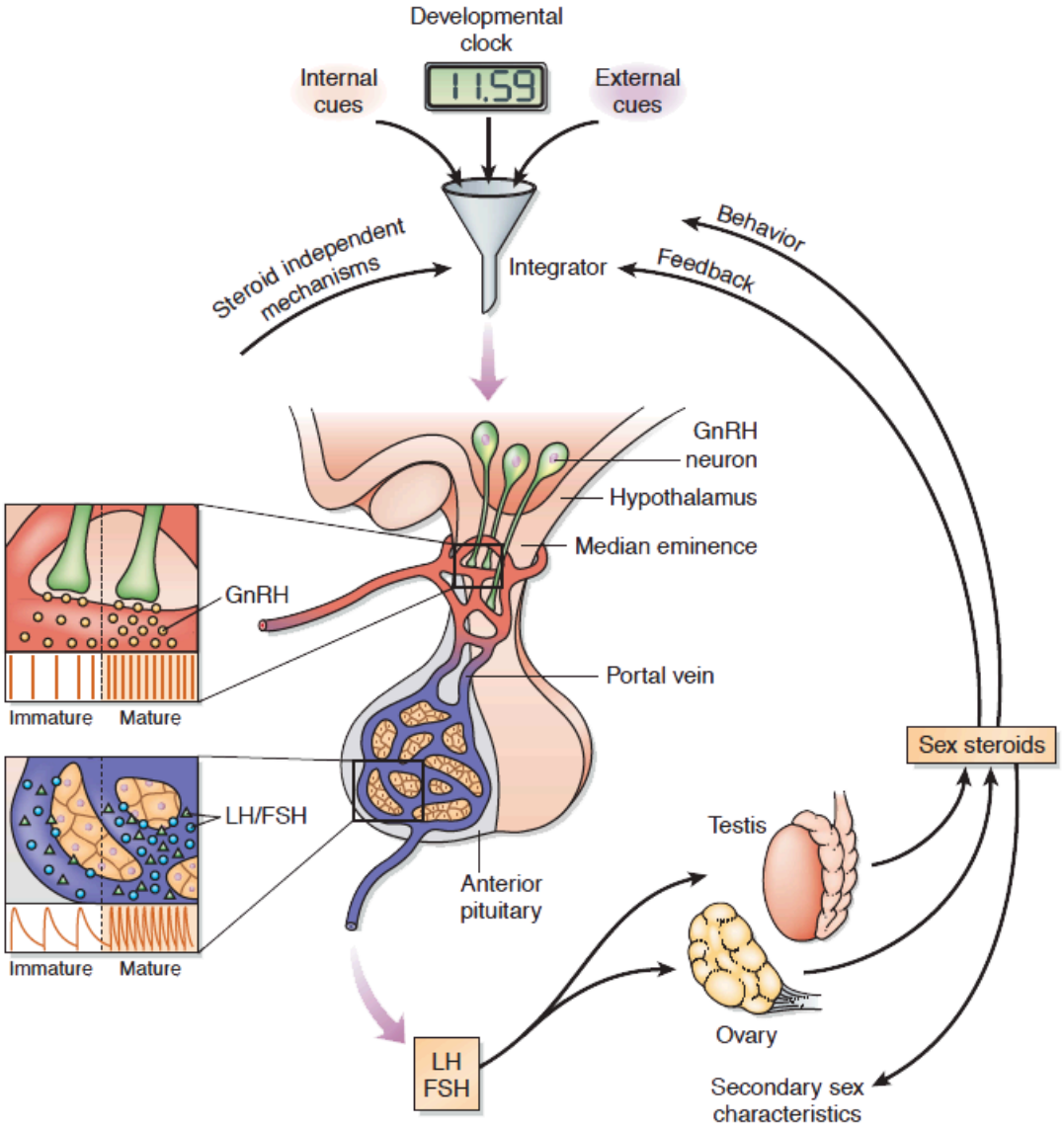

Figure 1.1 Representation of the hpg axis showing patterns of GnRH neurosecretion and gonadotropins (LH and FSH) pulsatile release in before and after puberty. Multiple permissive cues converge on the GnRH resulting in the modulation of steroid hormones feedbacks from the gonads on physiology and behavior. From Sisk and Foster, 2004.

latipes) GnRH-III is also present in addition to GnRH-I and GnRH-II, and neurons expressing this variants display anatomical segregation (Okuyama et al., 2014). In

mice however, only the GnRH-I gene is present, therefore in this manuscript "GnRH" refers to GnRH-I.

1.1.1.1 GnRH neurons distribution

There are about 800 GnRH neurons in the adult mouse brain (Wu et al., 1997) and these are mainly distributed in the preoptic area (POA) of the hypothalamus, but are also present in a continuum along their migratory pathway (Merchenthaler et al., 1984). Neurons are found anterior to the POA in the diagonal band of Broca and in the medial septum (MS), and a small number of neuronal somata in the olfactory bulb (OB). Towards the median eminescence, few GnRH neurons are found in the anterior hypothalamic area (AHA) (Herbison, 2015).

1.1.1.2 GnRH projections inside and outside the reproductive axis

GnRH neurons exert their role in regulating fertility by projecting to the median eminescence (ME) (Parkash et al., 2015). GnRH terminals are in close apposition with blood vessels within the median eminescence and tanycytes, a specialized population of glial cells at the level of the third ventricle (Parkash et al., 2015). GnRH neurons exhibit unusual neurite morphology, sharing features of both axonal and dendritic projections (Herde et al., 2013). Surprisingly, retrograde tracing studies report only the 50% to 70 % of GnRH neurons to be “hypophysiotropic”, *i.e.* project into the hypophyseal portal vasculature (Campos and Herbison, 2014). The organum vasculosum of the lamina terminalis (OVLT) is rich in GnRH processes (Herde et al., 2011), and GnRH-immunoreactive long-distance processes are also found in several areas of the rat brain, such as the hippocampus, the amygdala, the stria terminalis and in the midbrain in the posterior commissure and the periaqueductal gray (Merchenthaler et al., 1984). These data raises the possibility that GnRH has several other targets other than gonadotropes, and may modulate neural activity.

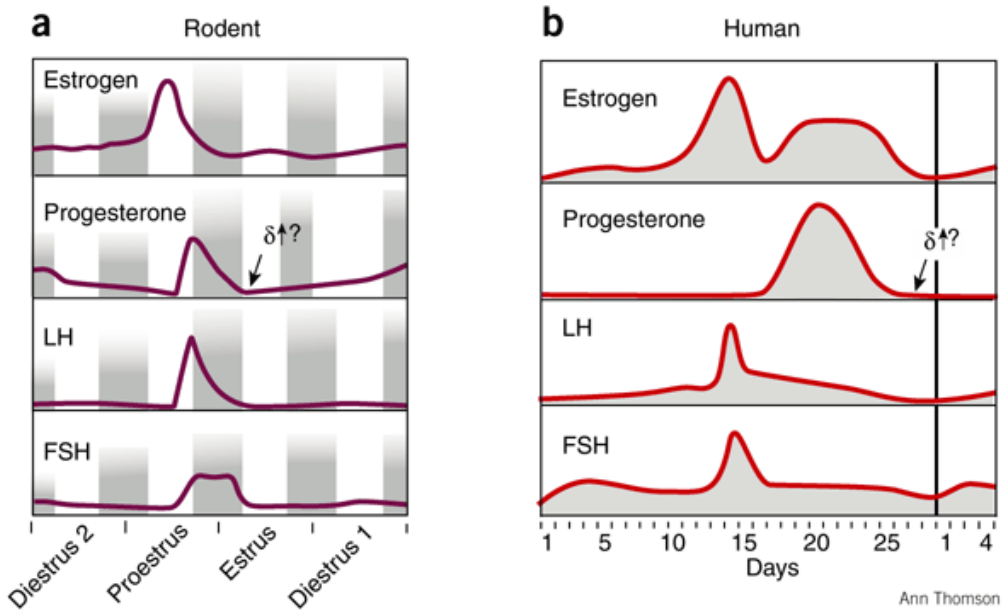

Figure 1.2 Fluctuations of circulating estradiol, progesterone, and gonadotropins (LH and FSH) during the different estrus cycle stages in rodents (a) and humans (b). From Staley and Scharfman, 2005.

1.1.2 Control of ovulation in rodents and humans by the reproductive axis

In female mammals, gametes (oocytes) and steroid hormones production from the ovaries are cyclically regulated by gonadotropins (Walmer et al., 1992). Each oocyte is surrounded by a cellular structure, the ovarian follicle. FSH signaling acts on follicular cells to promote follicle maturation. The growing follicle starts to secrete estradiol into the circulating system (Fortune, 2003). The increase in estradiol concentration in the bloodstream reaches a peak, and is followed by a preovulatory LH surge, timed with ovulation (Bingel, 1974; Smith et al., 1975). The estrus cycle is conserved regarding hormonal profiles but, whereas in humans is 28 days long, in mice lasts 4-5 days (fig.1.2) (Staley and Scharfman, 2005). Estrus in mice and rats is also strictly linked to the 24 hours light-dark cycle (fig.1.2), suggesting gonadotropin regulation from the internal circadian clock (Chu et al., 2013). Four stages can be identified in mice and rats, according to changes in the vaginal cytology: proestrus, estrus, metestrus (or diestrus 1) and diestrus (Caligioni, 2009; Hubscher et al., 2005). Estradiol gradually rises during diestrus and reaches the peak in the morning of proestrus (Smith et al., 1975), whereas the surge in LH occurs on the afternoon of proestrus (fig.1.2) (Bingel, 1974; Smith et al., 1975).

1.1.2.1 The GnRH pulse generator

Pulsatile profile of LH in the circulating system was first analyzed in rhesus monkeys and later in several other species of mammals, including rats and mice (Campos and Herbison, 2014; Maeda et al., 2010). LH pulses are coordinated with pulsatility of GnRH in the hypothalamus (Ordog and Knobil, 1995), which is regulated by bursts of the GnRH neuron (Campos and Herbison, 2014). A rapid and sharp raise in LH serum concentration can be triggered by GnRH neurons stimulation *in vivo* (Campos and Herbison, 2014). However, endogenous pulse generation is indirectly mediated by estradiol (Ordog and Knobil, 1995; Radovick et al., 2012). Global ERα KO, but not ERβ KO mice exhibit increased pituitary expression of the LHβ gene, similarly to OVX females (Couse et al., 2003). It is thought that estradiol feedback is mediated mainly by two distinct populations of ERα-expressing hypothalamic neurons upstream to GnRH neurons (Kumar et al., 2015; Smith et al., 2006). The major upstream regulator of GnRH release so far described is kisspeptin, a neuropeptide that in mice is produced mainly by neurons in two distinct hypothalamic neurons, the arcuate nucleus (Arc) and the antero-ventral periventricular nucleus (AVPV) (Clarkson et al., 2009). Inactivating mutations in the gene encoding for kisspeptin or its receptor GPR54 lead to hypogonadotropic hypogonadism and infertility both in humans and mice (d'Anglemont de Tassigny et al., 2007; de Roux et al., 2003; Seminara et al., 2003; Topaloglu et al., 2012). Kisspeptin signaling is also critical for the timing of puberty (Seminara et al., 2003). Conditional knockout of ERα in kisspeptin neurons dramatically advanced puberty onset in mice, due to disregulated increase of LH at prepubertal age (Mayer et al., 2010), indicating that a negative estradiol feedback acts on kisspeptin neurons population to actively restrain LH release.

1.1.3 Hormonal control of reproductive behavior

Male and female sexually-related behaviors are strongly influenced by the direct action of gonadal steroid hormones within the central nervous system (Ferrero and Liberles, 2013). The seminal work of Donald Pfaff provided substantial description of the neural circuits underlying the hormonal control of behavior by studying the female sexual response, the lordosis behavior (fig1.3). The *lordosis reflex* is a posture in response to the male mounting behavior in which the female remains still with the back arched to

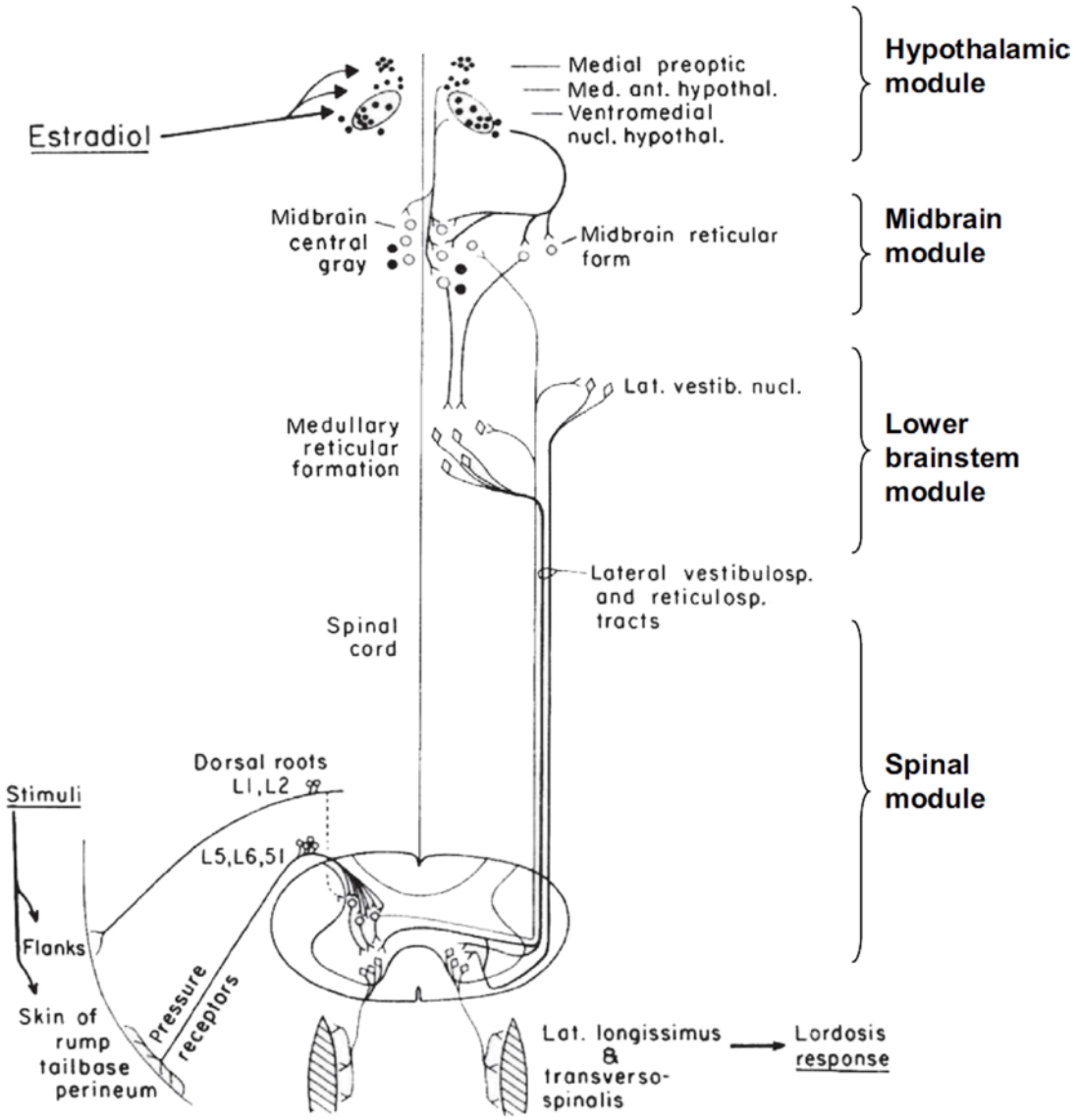

Figure 1.3 Modular control of sexual behavior. Diagram showing the model of activation of lordosis behavior in female rats. Estradiol acts both on VMH and PAG to switch the sensory cues from the stimuli on the flanks to a lordosis response and suppresses defensive rejections. From Knobil and Neill´s Physiology of reproduction, 4th edition.

ensure penetration from the male, thus to maximize impregnation (Hardy and Debold, 1971). However, a female shows lordosis to a male mounting only at appropriate levels of estradiol and progesterone; in cycling females lordosis appears during the periovulatory period together with "proceptive" behaviors towards the male (Pfaus et al., 2003), when estradiol and progesterone reach their peak concentration in the bloodstream; as expected, in rats, OVX females don´t exhibit sexual behavior unless they are primed with estradiol and progesterone (Pfaff and Sakuma, 1979b), implicating a coordinatory role by sexual hormones between the reproductive axis and behavior (fig.1.1). Estradiol action on lordosis is driven mainly by the ERα isoform,

since ERα KO female mice exhibit strong deficits in sexual receptivity (Ogawa et al., 1998), whereas ERβ KO female mice are normal (Ogawa et al., 1999). In the hypothalamus, the ventromedial hypothalamus (VMH) exhibits dense ERα expression (Lee et al., 2014) and is thought to be the main mediator of the estradiol control on lordosis behavior. Lesions in the VMH impaired lordosis responsiveness under estradiol and progesterone priming (Mathews and Edwards, 1977; Pfaff and Sakuma, 1979a) whereas electrical stimulation of the VMH enhanced the estradiol effect on lordosis in female rats in an estrogen dose-dependent manner (Pfaff and Sakuma, 1979b). Progress in genetic targeting allowed selective functional characterization and the identification of the estradiol-responsive neurons within the VMH. Unilateral optogenetic stimulation of the *Esr1*+ (ERα gene) neuron subpopulation in the ventrolateral part of the VMH (VMHvl) in male mice is sufficient to elicit rapid aggression or mating in a scalable manner, suggesting an estradiol-mediated neural switch within the VMHvl through ERα (Lee et al., 2014). Expression silencing of ERα in the VMH induces decrease in VMH-specific PR expression and is sufficient to abolish lordosis behavior in females, together with increase in rejections (Musatov et al., 2006). Progesterone appears to be required for full sexual behavior expression (Pfaus et al., 2003). Recently, genetic identification of progesterone receptor (PR) neurons in mice revealed sexual dimorphism in neural targets of progesterone within the VMHvl and a requirement for sexual behavior in both males and females in sexual behavior, whereas ablation of VMHvl PR neurons disrupts also aggression in males (Yang et al., 2013). The VMH is very well known to send extensive projections to the dorsal periaqueductal gray (dPAG) in the midbrain, as shown by anterograde tracing studies by Swanson´s group in the rat (Canteras et al., 1994). Both the VMHvl and the dorsomedial aspect (VMHdm) send projections mainly to the dPAG (Canteras et al., 1994). VMH is known to process other information such as fear: social fear and predator fear are distinctly coordinated by VMHdm and VMHvl, respectively. However, they are both impaired by electrical attenuation of the dorsal PAG (Silva et al., 2013), suggesting both anatomical and functional overlap at the level of the PAG.

1.1.3.1 The central hub for sexual behavior: the periaqueductal gray

The periaqueductal gray (PAG) plays a pivotal role in the integration of painful stimuli, by influencing pain perception (Bandler and Shipley, 1994). PAG is also

known to receive fear information from both the hypothalamus and amygdala (Kim et al., 2013; Silva et al., 2013). PAG is organized in four columns that extend longitudinally, along the rostrocaudal axis, surrounding the whole aqueduct until its end (Bandler and Shipley, 1994; Beitz and Shepard, 1985). During the estrus cycle, progesterone strongly influences pain responsiveness in rats, correlated with altered neural activity (Devall and Lovick, 2010) and selective GABA subunit expression within the PAG (Lovick and Devall, 2009). In female rats, electrical stimulation of the PAG at different coordinates enhances the effect of estradiol on lordosis in a dose-dependent manner (Sakuma and Pfaff, 1979). The sites where lordosis is facilitated match the localization of the projections from the VMH, mainly in the dorsal, dorsolateral and lateral PAG, however with no precise localization (Canteras et al., 1994; Morrell and Pfaff, 1982; Sakuma and Pfaff, 1979). At certain intensities, such stimulations can produce aversive responses (escape reactions) usually at most lateral parts of the PAG (Sakuma and Pfaff, 1979). As reported by Pfaff, lordosis facilitation requires long stimulations that cannot be fulfilled by the inputs from VMH alone (Sakuma and Pfaff, 1979). Surprisingly, VMH lesions did not affect electrical PAG stimulations, indicating that PAG can act independently of the ventral hypothalamic inputs on the estradiol-mediated induction of sexual receptivity (Sakuma and Pfaff, 1979). Ascending somatosensory cues from the medulla also affected PAG neural activity (Sakuma and Pfaff, 1980a), suggesting convergence of hormonal and sensory cues within the PAG (Sakuma and Pfaff, 1980a, b), with the PAG being the major integration site for sexual receptivity. Other studies report the presence of a lordosis-inhibiting system mediated by POA and lateral septum (LS) projections to the ventrolateral PAG (Arendash and Gorski, 1983; Floody and DeBold, 2004). Retrograde tracing revealed the caudal LPAG neurons to be connected with gigantocellular neurons in the medulla that project to the lordosis producing muscles (Daniels et al., 1999). Notably, c-fos is significantly up-regulated in medulla-projecting LPAG neurons following sexual behavior in rats (Yamada and Kawata, 2014). Nevertheless, PAG neurons express ERα (Loyd and Murphy, 2008), suggesting that estradiol action may act at the level of the PAG as well.

1.1.4 GnRH integrates vomeronasal inputs with the neural substrates that drive female sexual behavior

1.1.4.1 Pheromonal control of reproductive physiology and behavior

In mammals, the neuroendocrine status is strongly influenced by pheromone detection. A striking example of modulation of reproductive physiology by pheromones is the Bruce effect, first observed in laboratory rodents and recently confirmed in wild primates (Boehm, 2006; Roberts et al., 2012), in which pregnancy is blocked and the estrus cycle restored in a female exposed to urine of an unfamiliar male. In mice, exposure of grouped juvenile females to male urine advanced puberty (Lombardi and Vandenbergh, 1977), or could induce estrus in grouped females (Bronson and Whitten, 1968). The relative pheromones that mediate these effects belong to different class of molecules, such as heptanone found in female urine, α-pharnesene that induces estrus in male urine (Jemiolo et al., 1986; Novotny et al., 1986; Novotny et al., 1999) or major histocompatibility complex I (MHC I) protein ligands (Leinders-Zufall et al., 2004; Leinders-Zufall et al., 2014). The responsible of these effects is the vomeronasal

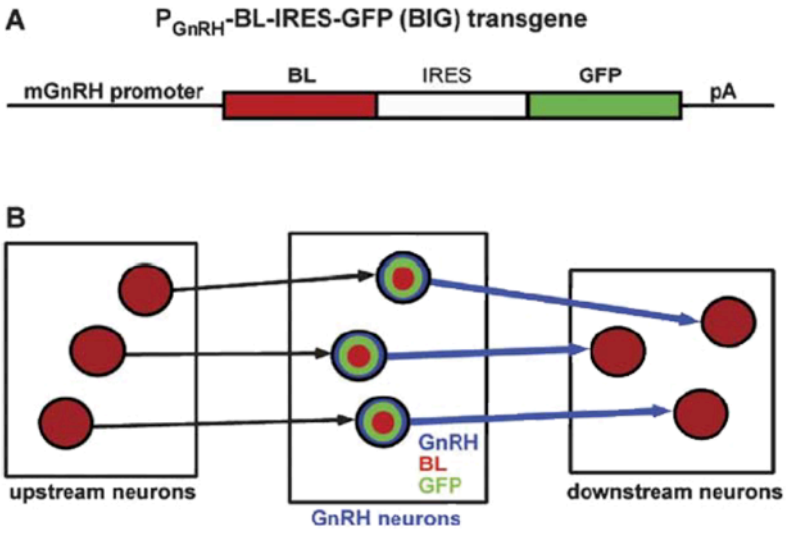

Figure 1.4 Genetic tracing of GnRH neurons. A: Trangenic construct carrying the mammalian GnRH promoter upstream to the Barley Lectin (BL) gene, Internal Ribosome Entry Site (IRES) and Green Fluorescent Protein (GFP). B: BL is transferred from active synapses and travels along neurons both retrogradely to presynaptic neurons or anterogradely, to postsynaptic neurons. From Boehm et al, 2005.

organ (VNO), an olfactory subsystem within the nose. The VNO detection is also important in the modulation of reproductive behavior. In mice, surgical removal or

gene knockout of vomeronasal signal transduction genes (such as TRPC2 -/-) abolishes female sexual behavior (Dulac and Kimchi, 2007; Saito and Moltz, 1986). The male pheromone ESP1 as well can induce lordosis in female mice through a specific vomeronasal receptor (Haga et al., 2010), whereas the juvenile-specific ESP22 inhibits sexual behavior (Ferrero et al., 2013).

Previous studies hypothesized that vomeronasal system is functionally connected to the reproductive axis through GnRH neurons (Meredith, 1998). The visualization of selective GnRH neurons connectivity (Boehm et al., 2005) was allowed by a mouse model in which the expression of the transneuronal tracer barley lectin (BL) is restricted to GnRH neurons (fig.1.4). BL was found to be transferred from GnRH neurons to neurons in several brain areas. In particular, input neurons to GnRH neurons were identified in VMH and exhibited strong sexual dimorphism. BL neurons were also found in medial amygdala (MeA) and PMCO and show c-fos responses to α-pharnesene exposure in females, indicating direct information to GnRH neurons from pheromonal cues. These results together indicate that GnRH neurons receive information from several brain areas, including areas that process olfactory and pheromonal information and areas responsible for driving sexual behavior.

1.1.4.2 GnRH as a modulatory neurotransmitter in female sexual behavior. Cooperation or necessity?

GnRH was found to stimulate male and female sexual behavior in many species (Boyd and Moore, 1985). In rodents, has been proposed that GnRH participates in modulation of behavior by acting on the neural substrates of sexual behavior. Initial studies in rats report a direct involvement of GnRH in promoting sexual receptivity in females. Ovariectomized (OVX) and hypophysectomized females treated with sub-threshold doses of estradiol (*i.e.*, not sufficient to elicit receptivity) showed enhanced lordosis behavior when co-treated with GnRH (Pfaff, 1973). A parallel study (Moss and McCann, 1973) showed that systemic LH and FSH failed to elicit a lordosis response in ovariectomized female rats. Together, these findings implicate that the enhancing effect of GnRH is not due to any increase in LH and/or FSH, nor -indeed- to any feedback from the ovarian hormones.

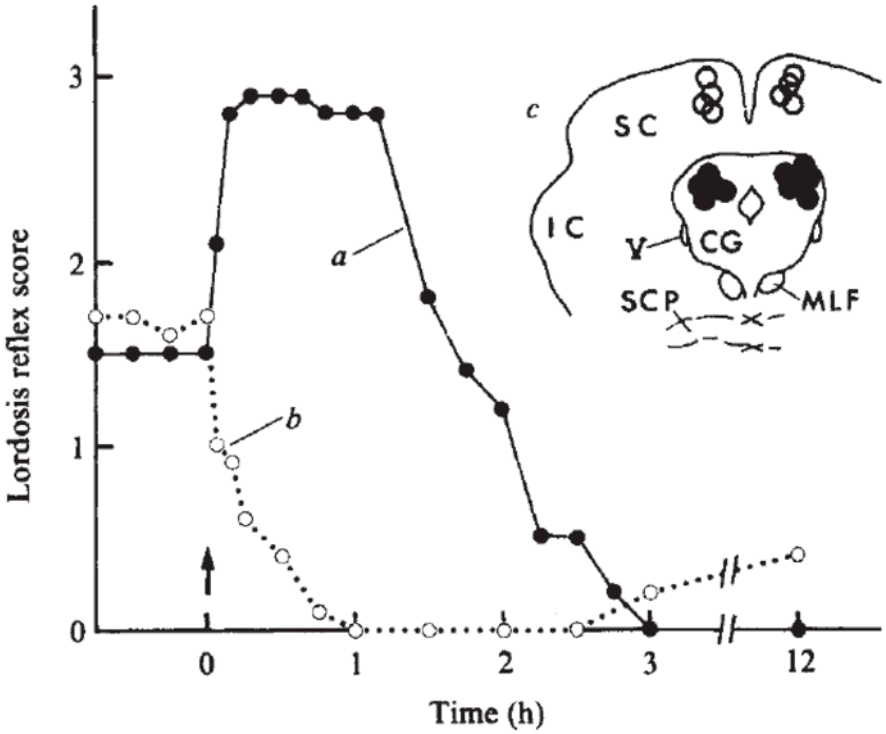

Figure 1.5 Female sexual behavior before and after GnRH (A) or anti GnRH globulin (B) infusion in the dorsal PAG of the rat. White circles in (C) show ineffective GnRH infusions in the superior colliculus (SC). From Sakuma and Pfaff, 1980.

Consistent with this, Sakuma and Pfaff (Sakuma and Pfaff, 1980c) showed that bilateral injections of GnRH directly in the periaqueductal gray -but not in the superior colliculus- of OVX female rats primed with estradiol induced a potent, fast and long-lasting raise in the lordosis reflex comparable to PAG electrical stimulations (Sakuma and Pfaff, 1979) (fig.1.5. A and C). Moreover, female sexual response disappeared following injection of a GnRH antagonist (fig.1.5.B). Further evidences from different labs supported this idea. Lordosis responses in female rats were abolished upon surgical VNO removal (Saito and Moltz, 1986). Subcutaneous administration of estradiol and progesterone partially restored lordosis in VNO-ablated rats, but only subcutaneous estradiol together with GnRH fully restored lordosis to the level of controls, when treated with sub-threshold estradiol (Saito and Moltz, 1986). The authors suggested interplay of estradiol and GnRH in the modulation of the neural substrates in VMH and PAG, to induce the lordosis response at maximal levels. GnRH administered intracerebroventricularly (icv) relieved sexual behavior deficits following VNO removal (Meredith and Howard, 1992), suggesting the cerebrospinal fluid as a vehicle for the modulatory role of GnRH in female sexual behavior. Consistent with this, GnRH was detected in ewes cerebrospinal fluid at

concentrations comparable to the hypophyseal portal blood (Caraty and Skinner, 2008; Skinner et al., 1997), showing both pulsatile and surge profiles coherently with reproductive status. Ward and Charlton (Ward and Charlton, 1981) conducted behavioral experiments in *hpg* female mice. *hpg* females show a loss of sexual receptivity when primed with estradiol alone, similarly to OVX females. When primed with estradiol and progesterone, lordosis quotient was recovered in *hpg* mice, however, with a prominent delay (in the order of weeks) with respect to wild type OVX females. Systemic GnRH injections (together with estradiol and progesterone priming) fully restored behavioral deficits at the level of wild type OVX, estrogen and progesterone primed. These results suggest that GnRH is required to fully restore sexual responsiveness in female mice. However, a reactivation of the hpg axis by subcutaneous GnRH cannot be ruled out in this experiment. Together, these results establish that despite the permissive role of genomic estradiol in unleashing the sexual responsiveness, the local GnRH action in the dorsal PAG represents the most potent stimulus that brings the lordosis response to maximal levels. However, the question whether the *endogenous GnRH is necessary* for efficient sexual responsiveness is still opened. To date, techniques so far used to dissect the behavioral GnRH lacked of genetic specificity. Despite intense work, the neural circuits of sexual behavior that sense GnRH remained unknown.

1.2 The GnRH receptor (GnRHR)

Gonadotropin releasing hormone receptor (GnRHR) is the downstream effector of GnRH. It is specifically expressed on the surface of gonadotrope cells and has ben found to be expressed in the brain and other tissues (Maggi et al., 2016). "Loss of function" mutations within the human GnRHR gene were identified in patients affected with normosmotic (normal sense of smell) hypogonadotropic hypogonadism or Kallmann syndrome (de Roux et al., 1997). The GnRHR protein (fig.1.6) belongs to the seven transmembrane G-protein coupled receptor family (GPCRs). Its structure is unique because despite canonical GPCRs, it lacks the intracellular C-terminal domain, leading to a slower desensitization and internalization rates (Maggi et al., 2016). GnRH binds and activates GnRHR through the N-terminal domain and triggers the G-protein $G\alpha_{q/11}$ signal cascade. The $G\alpha_{q/11}$ intracellular signal activates the phopholipase C which triggers the increase in diacylglycerol (DAG) and inositol 1,4,5, diphosphate (IP_3). IP_3 then induces mobilization of internal calcium stores and DAG the activation of the protein kinase C (PKC). During adulthood, GnRHR mRNA is up regulated prior ovulation and returns to basal levels in diestrus (Bauer-Dantoin et al., 1993), however its regulation seems to be independent from the action of ERα and ERβ (Couse et al., 2003). GnRHR onset of expression is defined early in development by the transcriptional regulator SF-1 (Parker et al., 2002). Transgenic mice which express the human placental alkaline phosphatase reporter gene (hPLAP) under the control of a 3,3 kb fragment from the rat GnRHR promoter showed hPLAP expression in pituitary and also in several brain areas, such as hippocampus, the lateral septum (Granger et al., 2004). However, due to differences between rat and mouse, authors could not exclude ectopic and aberrancies in rat GnRHR promoter expression (Granger et al., 2004). Indeed, most studies on GnRHR function involved either immortalized tumor-derived cell line (αT3-1 and LβT2 cell lines) (Maggi et al., 2016), or transgenic heterologous expression, far from being close to physiological conditions. Genetic targeting of the GnRHR gene with an IRES-Cre cassette allowed unambiguous visualization and characterization of GnRHR cells (Wen et al., 2008).

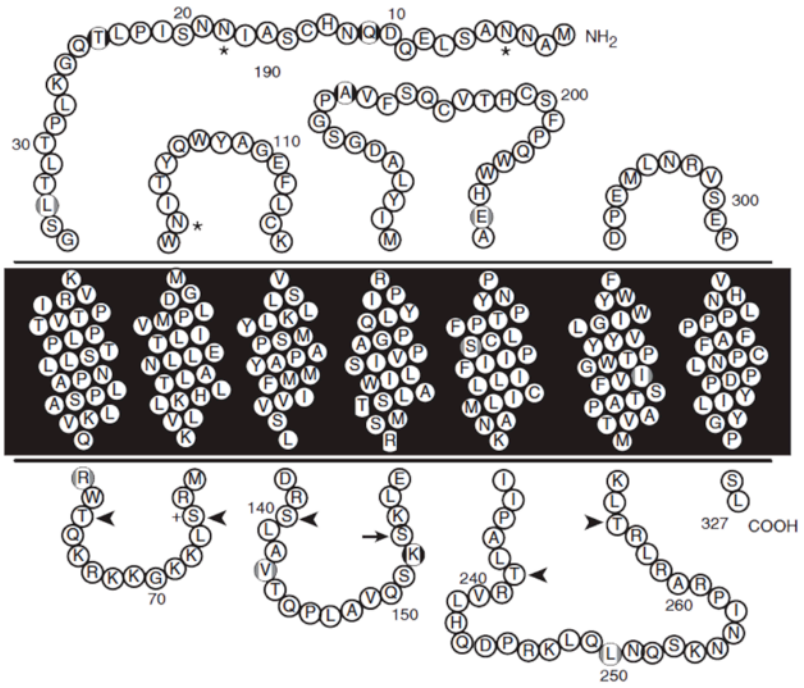

Figure 1.6 Diagram of the rat GnRHR protein (Kaiser et al., 1992)**.**

1.2.1 The GnRHR-IRES-Cre mouse

In order to study the expression of the *allelic* GnRHR, the GnRHR-IRES-Cre (GRIC) mouse line was generated previously in our lab (Wen et al., 2008). The endogenous GnRHR gene was targeted at the end of the last exon (gene targeting approach), ensuring that expression of the bacterial Cre recombinase is dependent only the regulation and activity of the endogenous GnRHR promoter and moreover, on the actual GnRHR protein synthesis (Candlish et al., 2015). The internal ribosome entry site (IRES) between the GnRHR and Cre recombinase sequence ensures bicistronic mRNA expression, so the GnRHR and the Cre will be synthesized as two separate proteins. GRIC mice were crossed with ROSA26-YFP mice to attain fluorescent visualization of genetically defined gonadotropes (fig.1.7.A). ROSA26-YFP mice bear a targeted insertion of the YFP downstream a loxP-flanked transcriptional stop signal in the ubiquitously expressed ROSA26 locus within the mouse genome (Soriano, 1999). Cre-dependent excision of the stop signal allows faithful YFP expression (dependent on the constitutively active ROSA promoter), independent from the highly fluctuating GnRHR expression. Fluorescent visualization allowed to selectively characterize gonadotropes within the highly heterogeneous pituitary gland. YFP+ signal in GRIC/R26-YFP mice is restricted in the anterior pituitary (fig.1.7.B).

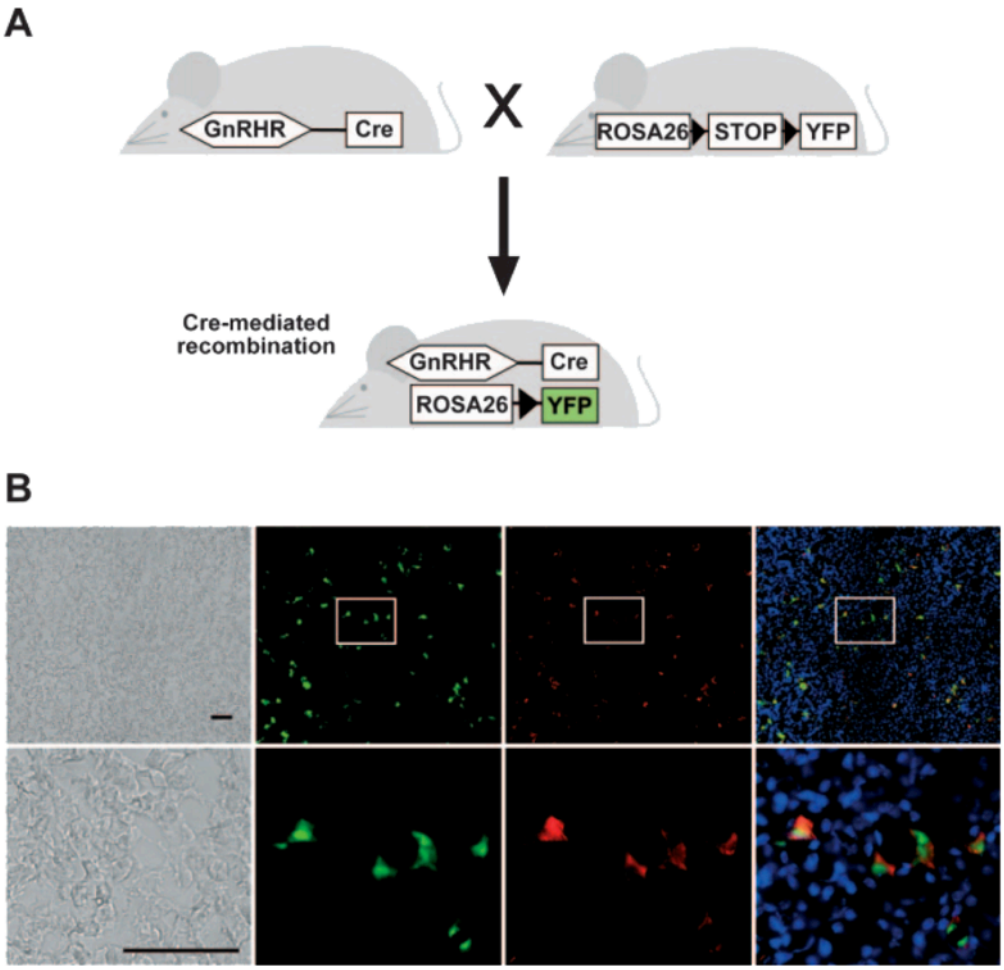

Figure 1.7 Binary genetic approach to visualize GnRHR cells. A: Coexpression of GnRHR-restricted Cre and cre-depenent ROSA26-YFP leads to cre-mediated recombination of the loxP-flanked transctiptional stop signal upstream to the YFP ORF, leading to YFP expression in GnRHR cells, enabling visualization B: Fluorescent YFP labeling (green) is restricted in gonadotropes, highlighted by LH and FSH immunoreactivity (red). From Wen et al., 2008.

Indeed, 99,98% of YFP+ were LH/FSH+, confirming the gonadotrope identity of YFP+ cells (Wen et al., 2008). Importantly, almost all YFP+ gonadotropes (23/25 cells) showed increase in intracellular Ca2+ after GnRH application, indicating the presence of a functional GnRHR (Wen et al., 2008). Improved fluorescence was obtained in our lab with the generation of the conditional eR26-τGFP line (Wen et al., 2011). The eR26 (enhanced ROSA26) is a ROSA locus targeted with a CAGS cassette, which contains the chicken β-actin promoter and the cytomegalovirus (CMV) enhancer (Okabe et al., 1997), to achieve enhanced expression of the downstream τGFP. τGFP is a green fluorescent protein (GFP) fused with the microtubule-associated protein tau (τ), which targets the GFP to microtubules (Rodriguez et al., 1999). The GRIC/eR26-τGFP line allowed the visualization of substantial morphological and spatial plasticity

during critical reproductive stages in the whole pituitary gonadotrope population as well as at single cell level, suggesting adaptations in response to hormonal changes (Alim et al., 2012). Fluorescent labeling of gonadotropes allowed also Fluorescent Activated Cell Sorting (FACS) and the whole trascriptome sequencing of male and females gonadotrope cells was revealed. It was found extensive remodeling in gonadotrope expression profiles during several reproductive stages (Qiao et al., 2016), together with a massive body of information about gonadotrope genetics.

1.2.1.1 GnRHR neurons are present in the periaqueductal gray of the male mouse and in other mesencephalic regions

The GRIC/R26-YFP+ mouse model enabled the identification of the long-time hypothesized neuronal targets of GnRH in the periaqueductal gray. In our lab has been characterized the brain of GRIC/R26-YFP males and observed YFP+ neurons mainly in the DM/DLPAG and LPAG, matching with the previously identified location where GnRH was effective in eliciting lordosis in female rats (fig.1.8.A). Also VMH contains GnRHR neurons, proposing the ventromedial nucleus of the hypothalamus for an additional modulatory site of GnRH concerning sexual receptivity. Surprisingly, YFP+ neurons are also found in the superior colliculus (fig.1.8.B-C)(Wen et al., 2011), where GnRH was ineffective in lordosis facilitation (Sakuma and Pfaff, 1980c).

1.2.1.2 Additional GnRH target areas revealed by fluorescent visualization of GnRHR neurons

YFP+ neurons were identified in areas that process main olfactory inputs, such as the pyriform cortex (Pyr) and the anterior cortical amigdala (CoA). Also MeA and PMCO were found YFP+ neurons, suggesting regulation by GnRH signaling of vomeronasal information. Scattered YFP+ neurons were found in hypothalamic areas, such as arcuate nucleus (Arc), periventricular nucleus (Pe). POA also contains YFP+ neurons, which are in close vicinity to GnRH neurons, however none of the GnRH neurons are YFP+, suggesting no autocrine feedbacks on GnRH neurons (Wen et al., 2011).

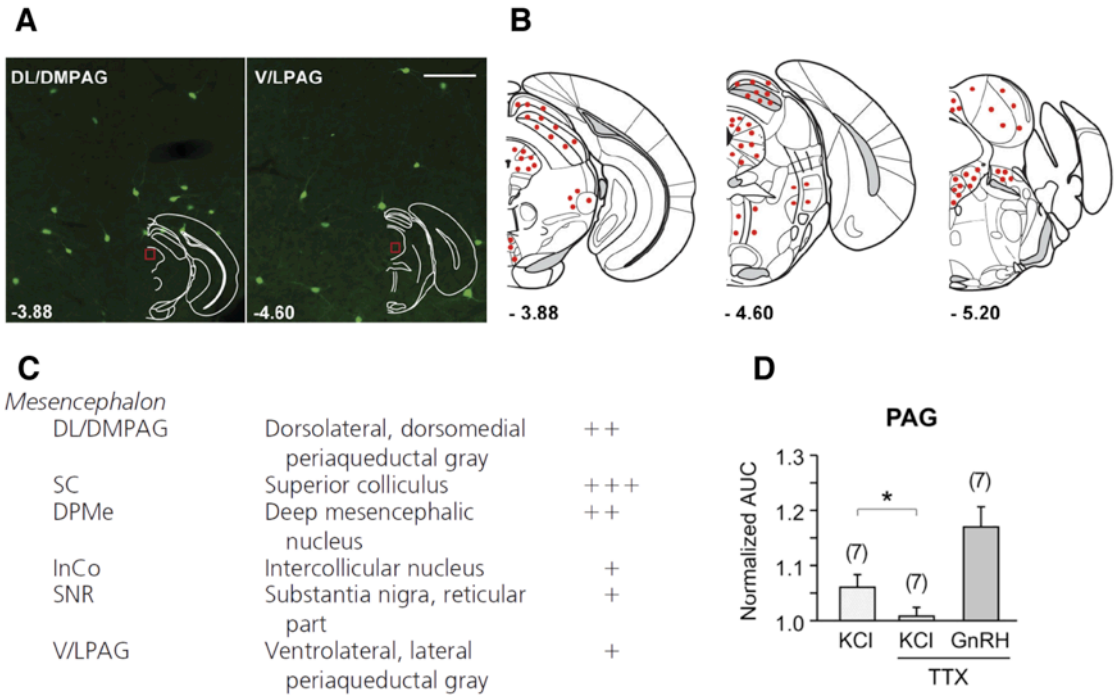

Figure 1.8 GnRHR neurons visualization in the PAG and midbrain of the GRIC/eR26-YFP male A: sections showing the dorsal and ventrolateral columns of the PAG. B: GnRHR neurons are widely distributed in the midbrain at different coordinates. C: GnRHR are clustered in the superior colliculus and the dorsal part of the PAG.D: Normalized area under the curve (AUC) showing Ca^{2+} responses following GnRH application independent on action potentials. TTX: tetrodotoxin. Modified from Wen et al., 2011.

1.2.1.3 Neuronal GnRHR signaling enabled by reliable fluorescent visualization of GnRHR neurons revealed neural code modulation in synchrony with the estrus cycle by GnRH.

The employment of the GRIC/eR26-τGFP mouse line allowed bright visualization of GnRHR neurons in brain slices. It was found that GnRH elicited Ca2+ responses in GnRHR neurons in the PAG (fig 1.8.D), Pe and in the Arc (Wen et al., 2011). Electrophysiological recordings of GnRHR neurons in the Pe revealed spontaneous activity (Schauer et al., 2015). Clusters analysis and principal component analysis (PCA) revealed that GnRHR neurons exhibit distinct patterns of firing activity defined by the different estrus cycle stages. During metestrus GnRHR neurons were mainly bursting (92%), whereas in proestrus 63% of the measured GnRHR neurons was observed in a tonic pattern. Bursting neurons decreased over proestrus and GnRH application was found sufficient to trigger a switch from a burst firing to a tonic firing in GnRHR neurons, and cetrorelix, a GnRHR antagonist, reversed the GnRHR tonic firing back to a burst firing (Schauer et al., 2015). Together, these data indicate that τGFP neurons express functional GnRHRs on neuronal membranes in the adult brain,

and that they modulate the neural activity in response to GnRH, coherently with ovulation. GnRHR neurons somata and their projections (highlighted by the τGFP reporter) in the Pe revealed close contacts both with GnRH terminals and capillaries, suggesting multiple sources of the peptide GnRH. These findings not only further support a role of GnRH involved as a neuromodulatory transmitter, but also uncovered the neurons in the PAG that are modulated by GnRH, together with other areas involved in processing social information.

1.3 Novel genetic tools to study neural correlates in behaving mammals

In the recent years, the establishment of the cre/loxP system in mouse models led to the explosion of not only cre-dependent genetic tools for fluorescent labeling, but also to perturb cellular and neuronal function, together with the development of novel strategies for genetic delivery *in vivo*.

1.3.1 Recombinant adeno-associated viruses

Recombinant adeno-associated viruses (r-AAVs) are widely used as vectors for genetic delivery *in vivo*. AAVs can efficiently infect neuronal cells therefore are suitable for stereotaxic delivery in the brain. An aspect in the employment of AAVs is their capability of being both directly and retrogradely up taken by neurons and transported along axons to the nucleus, allowing retrograde tracing from projection areas (Campos and Herbison, 2014; Low et al., 2013). Several AAVs were designed so far to deliver cre-dependent gene expression and can be employed in the vast array of cre mouse lines (Tsai et al., 2009). Among hundreds of serotypes, the variants 2/2 and 2/5 of the serotype 2 are the most widely used and characterized AAVs as they efficiently transfects neurons, therefore are largely employed as vectors for several genetic tools, such as optogenetic tools (Yizhar et al., 2011). Notably, serotype 2/5 (abbreviated as AAV5) has been successfully employed in mice, with a wider spread in the brain tissue respect to serotype 2/2 (AAV2) (Yizhar et al., 2011). The AAV5-flex-taCasp3-TEVp viral construct can trigger apoptosis of cre expressing cells, and was successfully employed for the ablation of progesterone receptor neurons in the ventromedial hypothalamus (VMHvl) *in vivo* (Yang et al., 2013). This AAV contains the genetic information for an engineered form procaspase 3 protein, whose cleavage into the

active form caspase 3 induces apoptosis in the host cell. In physiological conditions, the procaspase 3 proteins contains the cleavage site for upstream caspases, that drives the active form of caspase 3 (taCasp3). This engineered version of procaspase 3 lacks the caspase cleavage site to avoid endogenously driven activation, but has a cleavage site for the heterologous enzyme tobacco etch virus (TEVp). A peptide-encoding sequence (T2A) between the two ORFs, ensures bicistronic expression of pro-taCasp3 and TEVp (Yang et al., 2013). The bicistronic sequence is flanked by a combination of mutated and wild type loxP sites similar to the DiO strategy, named as "flip-excision", FLEX, in order to drive the protein expression only in cre-expressing cells (Atasoy et al., 2008).

1.4 Scientific aims and strategies

Aim 1: Characterization of GnRHR neurons in the female brain

Previous studies suggest that GnRH is necessary in promoting female reproductive behavior by acting directly in the PAG. Genetic targeting of the GnRHR gene in mice neurons allowed both the visualization and the manipulation of GnRHR cells. Consistent with this, I aimed to analyze *in vivo* the role of GnRH signaling in female sexual behavior by selective ablation of GnRHR neurons and subsequently characterize the behavior. To do this, I first elaborated a map of GRIC/eR26-τGFP neurons in the PAG of the female. Secondly, I stereotaxically delivered a cre-dependent AAV encoding for procaspase, to trigger programmed cell death in GnRHR neurons locally in the dorsal PAG of GRIC/eR26-τGFP female mice according to the obtained mapping results, without affecting gonadotropes in the pituitary, nor the endogenous GnRH. In parallel I analyzed whether GnRHR neurons are activated during female sexual intercourse, by analyzing the expression of c-fos, the primary early gene whose activation is dependent on neural activity.

Aim 2: Studying the role of mGluR5 in reproductive physiology

In collaboration with Dr. Ioana Inta I analyzed the pituitary hormone profile of female mice lacking the mGluR5 gene. Puberty disorders and infertility were identified in female mice lacking the mGluR5 gene. To understand whether these effects are due to a deregulated gonadotropin release, I performed simultaneous analysis of pituitary

hormones in serum of wt, heterozygous and homozygous knockout for the mGluR5 gene.

2 Materials and Methods

2.1 Role of GnRHR neurons in female sexual behavior

2.1.1 Antibodies, solutions and reagents

Table 2.1 Primary antibodies list

Name	Company	Catalogue No.	Dilution
Rabbit anti-GFP IgG	Life technologies	A11122	1:1000
Chicken anti-GFP Igγ	Aves Labs	GFP-1020	1:1000
Rabbit anti-c-fos IgG	Santa Cruz Biotechnology	sc-52	1:300
Goat anti-c-fos IgG	Santa Cruz Biotechnology	sc-52-G	1:300
Rabbit anti-GnRH IgG	ThermoFischer Scientific	PA1-121	1:800
Rabbit anti-Erα IgG	Millipore	06-935	1:1000
Rabbit anti-nNOS IgG	ThermoFischer Scientific	61-7000	1:300
Rabbit anti-Tph2 IgG	Abcam	ab111828	1:500
Rabbit anti-mCherry (home made), 0,3 mg/ml	provided by Prof V. Flokerzi, UkS	-	1:200

Table 2.2 Secondary antibodies list

Name	Company	Catalogue No.	Dilution
Donkey anti-rabbit 488-conjugated IgG Fab Fragment	Jackson Labs	711-547-003	1:500
Donkey anti-rabbit 488-conjugated IgG F(ab')2 Fragment	Jackson Labs	711-546-152	1:500

Donkey anti-rabbit Cy3-conjugated IgG Fab Fragment	Jackson Labs	711-167-003	1:500
Donkey anti-rabbit Cy5-conjugated IgG Fab Fragment	Jackson Labs	711-177-003	1:500
Donkey anti-goat Cy3-conjugated IgG Fab Fragment	Jackson Labs	705-167-003	1:500
Donkey anti-chicken 488-conjugated IgG F(ab')2 Fragment	Jackson Labs	703-546-155	1:500

Table 2.3 Blocking

Name	Company	Catalogue No.
Normal donkey serum	Jackson Labs	017-000-121

Table 2.4 General solutions

Name	Composition
Blocking solution	5% normal donkey serum 0,3% Triton x-100 0,02% Sodium Azide PBS 1X
Antibody solution	0,5% λ-carrageenan 0,02% Sodium Azide 1x PBS
PBS 1X (0,01M)	10 mM Na2HPO4 1,37 mM NaCl 2 mM KH2PO4 2,7 mM KCl
ACSF	25mM NaHCO3 1,25 mM NaH2PO4 0,8 mM MgCl 6x H2O 5 mM Glucose 124 mM NaCl 8 mM KCl

	1mM CaCl2 2xH20
PFA 4%	4% PFA 1x PBS

Table 2.5 Reagents list

Name	Company	Catalogue No.
Methylene Blue 0,05 % w/v, in H2O	Sigma-Aldrich	319112-100ML
bisBenzimide H 33258	Sigma-Aldrich	B-1155
λ-carrageenan	Sigma-Aldrich	22049-F
Sodium Azide	Sigma-Aldrich	S2002
Progesterone	Abcam	ab141252
β-Estradiol	Sigma-Aldrich	E8875
Cholesterol	Sigma-Aldrich	C8667
Na2HPO4	VWR	28029.292
NaCl	VWR	27810.364
KCl	Grüssing	Z12008
KH2PO4	Sigma-Aldrich	P5655
NaHCO3	Sigma-Aldrich	S-6297
NaH2PO4	Sigma-Aldrich	S7907
MgCl 6XH2O	Sigma-Aldrich	M2393
Glucose	Sigma-Aldrich	G-5146
CaCl	Sigma-Aldrich	C-5080
Sucrose	AppliChem	131621.1211
PFA	Sigma-Aldrich	P-6148
Triton X-100	AppliChem	A4975,1000
Sesame Oil	Sigma-Aldrich	S3547
NaOH	Grüssing	Z12155

2.1.2 Mice

In order to visualize and to be able to manipulate *in vivo* GnRHR-expressing neurons, in the present study were used adult (10-14 weeks old) and sexually naive GRIC/eR26-τGFP females. GRIC/eR26-τGFP females were obtained by crossing GnRHR-IRES-Cre (GRIC) homozygous mice (Wen et al., 2008) with eR26-**τ**GFP homozygous mice (Wen et al., 2011). Mice were kept under at standard light/dark cycle (12:12-h; lights-on at 07:00 h; lights-off at 19:00 h) with food and water *ad libitum*. For behavioral studies, mice were kept at inverted light/dark cycle for at least three weeks (12:12-h; lights-on at 22:00 h; lights-off at 10:00 h) before the experiments. Mouse experiments were carried out in accordance with the German Animal Welfare Act, European Communities Council Directive 2010/63/EU, and the institutional ethical and animal welfare guidelines of the University of Saarland. All the surgical procedures, including perfusion and organ collection were approved by the Animal Protection Committee of the University of Saarland.

2.1.3 Mouse genotyping

Genomic DNA was obtained from ear biopsies. Ear biopsies were lysed in 100 µl ear lysis buffer (Table 2.6) added with Proteinase-K, overnight at 55°C on shaker (MHR 23, Ditabis). Mice were genotyped by PCR (Polymerase Chain Reaction). The PCR mix is listed in the table below. PCR is then performed with a thermal cycler (T100, Biorad). PCRs for Cre-recombinase, enhanced ROSA26 locus (which insertion of the targeted τGFP construct) and wild type ROSA26 locus were performed all in one tube (multiplex, see tables 2.7 and 2.8). PCR for the GnRHR-IRES-Cre was performed in a separate reaction (tables 2.7-2.8).

Table 2.6 Ear lysis buffer

Reagent	Concentration
Tris (pH 8.0)	50 mM
NaCl	100 mM
NP40	0,20%
Tween 20	0,20%
EDTA (pH 8.0)	1 mM

Table 2.7 PCR Mix

Cre+eR26+R26 multiplex PCR mix	**µL**
dH20 (MilliQ)	4
MyTaq™ HS Red Mix	6,25
R26 (common) Forward	0,25
eR26 Reverse	0,25
Wild type R26 Reverse	0,25
Cre Forward	0,25
Cre Reverse	0,25
DNA	1
Total	12,5

GnRHR-IHRES-Cre (GRIC) PCR mix	**µL**
MilliQ	4,5
MyTaq™ HS Red Mix	6,25
GnRHR-IHRES-Cre (common) Forward	0,15
GnRHR Wild Type Reverse	0,3
GnRHR Knock-IN Reverse	0,3
DNA	1
Total	12,5

Table 2.8 List of primers

Primer	**Sequence**
R26 (common) Forward	GGA AGC ACT TGC TCT CCC AAA G
eR26 Reverse	GGG CGT ACT TGG CAT ATG ATA CAC
Wild type R26 Reverse	CTT TAA GCC TGC CCA GAA GAC TC
Cre Forward	GCG GTC TGG CAG TAA AAA CTA TC
Cre Reverse	GTG AAA CAG CAT TGC TGT CAC TT
GRIC (common) For.	TGA CAG TCG CAT TCG CTA CC
GRIC K.I. Rev.	AAC TCG CGC CCT GGA AG
GRIC wt Rev.	GAA GGT CTT CTG AAG CTC TAA CAA C

Table 2.9 PCR reaction

Genes	PCR cycle	PCR Product
Cre, eR26, R26 wt	95°C: 2 min 95°C: 30 sec 56°C: 4 min } 25 X 10°C: infinite	Cre: 102 bp eR26: 495 bp R26 wt: 256 bp
GRIC, GnRHR wt	95°C: 2 min 95°C: 15 sec 60°C: 15 sec 72°C: 8 sec } 35 X 10°C: infinite	GRIC K.I.: 539 bp GnRHR wt: 349 bp

2.1.4 Surgery

2.1.4.1 Ovariectomy (OVX)

Ovariectomy was performed to all females used for behavioral analysis in order to prevent pregnancy and especially to avoid variability due to hormonal changes during the different stages of the estrus cycle. Mice were anesthetized with Isofurane (Forene, AbbVie, Deutschland) and kept under continuous isofurane with a mouse stereotaxic mask (Stoelting, Cat. No. 51625M), on top of a heating pad at 37°C. Intra-peritoneal (*i.p.*) injection of a 5 mg/kg saline solution of Carprofen (Rimadyl 50 mg/ml, Pfizer) was performed to relief post-operative inflammation and pain; eye gel (Gent-ophtal, Dr. Winzer Pharma GmbH) was applied to prevent eye drying during anesthesia. On each side, the area rostrally the iliac crest was shaved and washed with disinfectant, then a small incision was made on the skin. A little dissection was made on the tissue underneath until the abdominal cavity is reached. The ovary was pulled out gently with forceps and a ligation is made at the level of uterine horns with absorbable suture thread (Vicryl, VCP391H). The ovary was cut and the remaining tissue was put back inside the abdominal cavity. The internal and external wounds were closed with three suture points with absorbable suture thread (Vicryl, VCP391H). Another incision medially on the neck was made and a 5-mm-long silastic capsule (inner diameter: 1.57 mm; outer diameter: 2.41 mm) containing crystalline 17β-estradiol (E_2, E8875, Sigma) diluted 1:1 with cholesterol (C8667, Sigma) was inserted subcutaneously. The wound was closed with absorbable suture thread (Vicryl, VCP391H). After surgery the mouse

was put back in a clean home cage on top of a 37°C heater. 24 hours after surgery the mouse was injected again intra- *i.p* with a 5 mg/kg saline solution of Carprofen (Rimadyl 50 mg/ml, Pfizer). Recovery form surgery was 14 days at least.

2.1.4.2 Viruses

In this study, *AAV5-EF1a-DiO-hChR2(H134R)-mCherry-WPRE-pA* (titer: 5,2 x 10^{12}, UNC Vector Core) was stereotaxically injected into the dorsal PAG in order to visualize acute GnRHR expression and *AAV5-flex-taCasp3-TEVp:* (titer 5,3 x 10^{12}, UNC Vector Core) to induce acute genetic ablation of GnRHR expressing neurons. The AAV5-EF1a-DiO-hChR2(H134R)-mCherry-WPRE-pA encodes for the Channelrhodopsin2 (H134R), fused with mCherry. The ChR2-mcherry is a Double floxed inverted Open reading frame (DiO), consisting in a combination of mutated and wild type loxP sites (Cardin et al., 2009). Cre-recombination brings the ORF in the *sense* orientation, allowing the expression under the EF1a promoter. Once expressed, the ChR2-mCherry fusion protein will target to the neuron membrane (due to the ChR2 moiety) highlighting cell bodies and projections in Cre-expressing neurons.

2.1.4.3 Stereotaxic injections

The mouse is placed on a stereotaxic device (Stoelting Co.) on top of an heating pad at 37°C, and maintained under continuous Isofurane (Forene, AbbVie, Deutschland); intra-peritoneal (*i.p.*) injection of a 5 mg/kg saline solution of Carprofen (Rimadyl 50 mg/ml, Pfizer) is performed to relief post-operative inflammation and pain; eye gel (Gent-ophtal, Dr. Winzer Pharma GmbH) is applied to prevent eye drying during anesthesia. Once correctly placed, the mouse is shaved on the head. Then, the skin is sterilized with disinfectant and gently opened with a scalpel and the skull exposed. The skull surface is washed with low percentage (3%) H_2O_2 to remove connective tissue and to highlight the skull junctions then washed with saline solution (0,9% NaCl) to stop H_2O_2 reaction. According to the "mouse atlas in stereotaxic coordinates" (Paxinos), two small bilaterally symmetrical holes are drilled with a dentist drill (MH-170, Foredrom) and bilateral injections are performed with an Hamilton Microliter syringe (#62 RN) with a 34 gauge needle (NDL ga34/20mm or 10mm/pst4, Hamilton)

into the dorsal part of the periaqueductal gray (PAG, Antero-posterior coordinate: -4,9 mm from Bregma; Lateral coordinate= ±0,4 mm from Bregma; Dorso-ventral coordinate; 2,1 mm from Bregma); when the needle reached the correct position, is left in place for 3 minutes, AAV5-flex-taCasp3-TEVp (1 μl/side), AAV5-5EF1a-DiO-hChR2(H134R)-mCherry-WPRE (0,2 μl/side), ACSF or Methylene Blue 0,05% solution (1 μl/side) was injected at the rate of 100 nl/min (10 minutes) for each side by mean of the Quintessential Stereotaxic Injector (Stoelting, Cat. No. 33311). The injected volumes were determined according to previous reports (Lohman et al., 2005; Yang et al., 2013). At the end of the injection the needle is left in place for an additional time of 5 minutes. The needle then is retracted slowly and the skin closed with absorbable suture thread (Vicryl, VCP391H). The mouse is removed from the stereotaxic apparatus and placed in a clean home cage on top of a 37°C heater. 24 hours after surgery the mouse is injected again *i.p.* with a 5 mg/kg saline solution of Carprofen (Rimadyl 50 mg/ml, Pfizer). Recovery form surgery is from 7 to 10 days.

2.1.5 Mouse tissue preparation

Mice were anesthetized with a solution of 100 mg/kg of ketamine (Ketavet, Zoetis) and 20 mg/kg of xylazine (Rompun 2%, Bayer) xylazine in PBS. After anesthesia mice were transcardially perfused with 15 ml of PBS at room temperature followed by 25-35 ml of ice-cold 4% PFA in PBS. Brains were harvested and soaked in ice-cold 4% PFA for 2 hours. Brains were then transferred in 30% sucrose solution in PBS for 48 hours for cryo-protection, then freezed in tissue embedding medium (Leica) in disposable plastic tissue embedding molds (Peel-a-way, Cat#:18646A) and stored at -80°C until use. 14 or 25 μm sections were achieved from the frozen tissues in series of 5 (to allow parallel staining procedures) with a cryostat (CM3050 S, Leica) at a temperature of -16/-18°C, and collected on glass slides (Superfrost Plus, Langenbrinck). Sections were stored at -80°C until used.

2.1.6 Behavior

2.1.6.1 Female sexual behavior assessment

All behavioral tests were performed during the dark phase (from 13:00 to 19:00). 3-4 hours prior the behavioral session, OVX females were injected subcutaneously (*s.c.*)

with 500 μg Progesterone (P-0130, Sigma) dissolved in sesame oil (5 mg/ml solution, S3547, Sigma), as described (Brock et al., 2011; DiBenedictis et al., 2012). Behavioral sessions were conducted in Plexiglas chambers (35 cm long x 25 cm high x 19 wide cm), provided by Prof. Julie Bakker. First, sexual experienced males were transferred from their cages to the chamber for 30 minutes for habituation. Subsequently, females were transferred from the cage to the chamber and were let with the males for 30 minutes (for the "c-fos" experiment) or for 10 minutes (for the "ablation" experiment). The males used for the behavior were trained to mount wild type OVX + E_2, Progesterone-injected wild type females for 1-2 encounters, 30 minutes each. Only males that performed >20 mounts in 30 minutes during the training session were used for the experimental sessions. During sessions male mounting, intromissions, ejaculations and female lordosis and rejective behavior events were scored. At the end of the session, both males and females were returned to their cages. *Lordosis* was defined as a firm posture of the female with the back slightly arched, the paws all on the ground while the head can be elevated at various extents, with no defensive reactions while the male was approaching for mounting. *Mounting* was defined as the male using its forepaws to clamp the female flanks from the back for copulating. *Intromission* was scored when the male was repetitively thrusting his pelvis towards the female ano-genital area for more than 6 s (Haga et al., 2010). *Ejaculation* was scored when a male stopped intromitting and remained still onto the female for several seconds. *Rejective* behavior was defined as a defense or escape reaction when the male was approaching for mounting. The lordosis quotient was calculated as:

$$\frac{\text{Lordosis events}}{\text{Mounting events}} * 100$$

and used as an index of sexual receptivity (Sakuma and Pfaff, 1979). Additional parameters were eventually quantified to better characterize sexual receptivity, such as *total time spent in lordosis*, *single lordosis event duration*, *latency to mount*, *latency to lordosis.*

2.1.6.2 c-fos expression following sexual behavior

GRIC/eR26-τGFP littermate females were ovariectomized, estrogen-primed at 10

weeks old (as described above) and tested at 14 weeks old. In the day of the session females were introduced in the behavioral chamber for 30 minutes with a previously introduced sexually experienced male (*lordosis* group) or clean bedding (*control* group). Only females that showed clear signs of sexual receptivity (for example, successful male intromissions) and clear lordosis behavior were used for c-fos immunohistochemistry experiments. After 90 minutes females were anesthetized then perfused and the brains collected, as reported elsewhere for behavioral studies involving c-fos protein expression (Boehm et al., 2005; Halem et al., 2001).

2.1.6.3 Female sexual receptivity following GnRHR neurons ablation in the dorsal PAG

GRIC/eR26-τGFP littermate females were ovariectomized at 14-15 weeks old and stereotaxically injected at 17-18 weeks old with AAV5-flex-taCasp3-TEVp (1 µl/side) or ACSF in the dorsal PAG. Animals were tested after 21 days after the injection, for 2 sessions 10 minutes each, one every four days, similarly to previously reported experimental protocols (Bakker et al., 2002). Behavior was recorded with IR video-camera and scored as described above. At 23 weeks old females were perfused and brains were collected to quantify ablation efficiency.

2.1.7 Immunohistochemistry protocols

Slides were kept at room temperature for 20 minutes before the staining, then washed with PBS 10 minutes for three times at room temperature, incubated for 20 minutes in cold methanol at room temperature to quench endogenous auto-fluorescence, washed again three times with PBS 10 minutes at room temperature and incubated in normal donkey serum blocking for 1 hour at room temperature. The sections were then directly incubated in primary antibody solution overnight (ON) at 4°C. The next day sections were washed again 10 minutes for three times in fresh PBS at room temperature and incubated for 2 hours at room temperature in 1:500 secondary antibody solution. Sections were then washed three times 5 minutes each at room temperature with PBS, incubated in 5 µg/ml nuclear labeling solution for 5 minutes at room temperature, then washed again three times 5 minutes each at room temperature with PBS and finally mounted with FluoroMount-G mounting medium and glass

coverslips (Langenbrinck). All double labelings are performed "sequentially", *i.e.* the staining for each antigen was performed one after another and not at the same time, according to Jackson Labs guidelines (*www.jacksonimmuno.com*). The blocking step was repeated before each primary ON incubation in order to limit the background.

2.1.8 Imaging

Stained sections were imaged with a Axio Imager *epi*-fluorescence microscope (Zeiss) through the AxioVision software (version 4.8.3, Zeiss). Images were quantified and processed with ImageJ, Adobe Photoshop and Adobe Illustrator CS6.

2.1.9 Statistical analysis

All data are displayed as means S.E.M. Different experimental groups were compared using one-tailed student's t test, with Prism 5 (GraphPad software). Differences were considered significant with p values < 0,05.

2.2 Role of mGluR5 in puberty initiation

This project was in collaboration with Dr. Ioana Inta and Prof. Dr. med. Markus Bettendorf from the Division of Paediatric Endocrinology and Diabetes, University Children's Hospital Heidelberg and Prof. Dr. Peter Gass from the Department of Psychiatry and Psychotherapy, Central Institute of Mental Health, Medical Faculty Mannheim. Mice housing, handling, treatment, sacrifice, blood collection and plasma preparation were performed Drs. Ioana Inta at the University of Mannheim. I then performed the hormonal analysis in our lab at the Homburg Uniklinikum, University of Saarland.

2.2.1 Pituitary hormones measurements

Wild type (wt), mGluR5 KO heterozygous (+/-) and homozygous (-/-) knockout (KO) littermate females from the mGluR5 gene KO mouse strain (Lu et al., 1997) were used. Blood from P30, P32 and P34 wild type (wt), heterozygous (+/-) and homozygous (-/-) knockout (KO) mGluR5 female mice was collected after deep anesthesia. Blood samples were centrifuged at 5000 rpm for 10 minutes at 4°C, serum

was collected and stored at -80°C until use. From 10 µl of serum, gonadotropins (LH, FSH), adrenocorticotrophic hormone (ACTH), growth hormone (GH), prolactin and thyrotrophic hormone (TSH) were simultaneously quantified with an xMAP technology multiplex assay (Luminex). This assay is a fluorescent immuno-based system using antibody-coated magnetic beads, allowing multiple antigens detection within one well, using minimal amounts of serum. Measurements were performed with the MAGPIX instrument (Luminex) using the Milliplex MAP Mouse Pituitary Magnetic Bead Panel Kit (MPTMAG-49K, Merck Millipore). The assay limits of detection (minimum detectable concentrations -MinDC- provided with the kit) were 1,9 pg/ml for LH, 9,5 pg/ml for FSH, 1,7 pg/ml for ACTH, 1,7 pg/ml for GH, 46,2 pg/ml for prolactin, 1,9 pg/ml for TSH. The inter and intra-assay coefficients of variation % (CV%) were < 16,4 % and < 6%, respectively. The *inter assay* coefficient was calculated from the mean of the CVs % of the two quality controls (one at low concentration and one at high concentration) across 7 different assays. The *intra assay* was calculated as the mean between the CVs of the reportable results within one plate. The inter assay and intra assay reported from Millipore for this plate for ON incubation across 8 assays were <20% and <15%. Results at the end of an assay were processed with the Analyst software (Merck Millipore). Standard curves were generated by the Analyst software (Merck Millipore) with 7 serial 1:4 dilutions starting from the "standard" sample (provided with the kit), by fitting them with a logarithmic five parameters curve. R^2 values for each curve are comprised between 1 and 0,998. Each samples was run in duplicates in each assay, a signal output in median fluorescence intensity (MFI) was background-subtracted and converted in pg/ml. The final value used for subsequent statistical analysis was the mean of the two duplicates. A CV % value is reported for each sample by the Analyst software (Merck Millipore). Samples with a CV % higher than 15% were not included in the analysis. Data below the minimum or above the maximum detection range were theoretically estimated by the standard curve fitting. All data are shown as means ± S.E.M. Different experimental groups were compared with two-tailed student's t test, using Prism 5 software (GraphPad software). Differences were considered significant with *p* values <0,05.

3 Results

3.1 Role of GnRHR neurons in female sexual behavior

3.1.1 Characterization of τGFP neurons in the PAG of GRIC/eR26-τGFP female mice.

The GRIC/eR26-τGFP mouse model offered a unique opportunity to dissect the endogenous GnRH signaling, by directly manipulating downstream GnRH-target neurons in the brain *in vivo*. I therefore aimed to ablate specifically GnRHR neurons that reside in the PAG of a female mouse, and evaluate female sexual behavior. In order to do this, I first elaborated a detailed map of GnRHR-expressing neurons in the PAG of the female adult mouse from the GnRHR-IRES-Cre/eROSA26-τGFP (GRIC/eR26-τGFP) reporter line. It was previously found in our lab that GnRHR neurons are scattered in the PAG of an adult (12 weeks old) male (Wen et al., 2011). However, detailed information is still missing about the distribution in the PAG of a female. However, GnRHR neurons were not detected in the brain before postnatal day 16 (P16) (Wen et al., 2011), suggesting an adult onset of GnRHR expression in the brain. Consistent with this, I hypothesized a variability in the distribution at different ages in the adult brain. Two ages to analyze were then considered: 10 weeks old and 19 weeks old.

3.1.1.1 Post-pubertal, adult, age-dependent increase of τGFP-expressing neurons in the PAG of GRIC/eR26-τGFP female mice.

In order to quantify τGFP neurons in the PAG, 14 μm sections were collected from bregma -5,20 mm to bregma -2,54 mm, which are the coordinates that span the PAG according to Paxinos Atlas. Brains (within a single experiment) were then aligned using clear hallmarks that could define a certain distance from the bregma, such as, caudally, the facial nerve root (7n) at -5,68 mm, the onset of superficial gray of superior colliculus (SuG) at bregma -4,84 mm, and rostrally the invagination of the dorsal third ventricle (D3V) in the diencephalon to form the aqueduct, at bregma -2,3 mm. A bregma value was assigned to each section, taking eventually into account the dorso-ventral displacement. Among all the brains, sections with the most similar

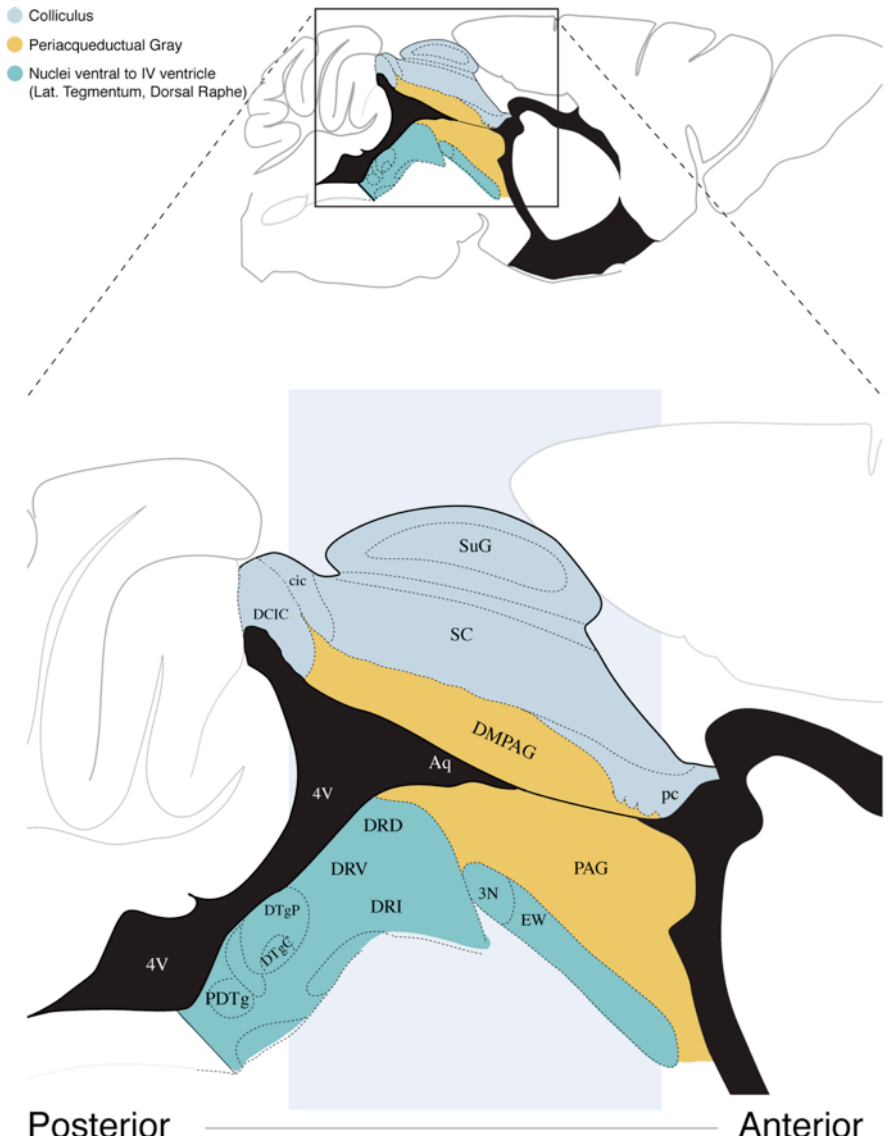

Figure 3.1 Sagittal view of the midbrain and pons of the adult mouse brain adapted from the Mouse Brain Atlas (Paxinos). Aq: Aqueduct. PDTg: posterodorsal tegmentum. DTgC: dorsal tegmentum, central part. DTgP: dorsal tegmentum, posterior part. DRV: dorsal raphe, ventral part DRI: dorsal raphe, internal part. DRD: dorsal raphe, dorsal part. 3N: oculomotor nerve or its root EW: Edinger-Wetsfal nucleus. SuG: superficial gray, superior colliculus. SC: superior colliculus. DCIC: dorsal cortex, inferior colliculus. cic: commissure inferior colliculus. pc: posterior commissure.

bregma value were aligned, and a mean bregma value was calculated. For each experimental group, the number of τGFP neurons for each bregma position, the total number and mean number of neurons per section were calculated. The pontine "region ventral to the IV ventricle" comprises regions at the borders of the more ventral part of the PAG, facing the aqueduct: from bregma -5,34 mm to -4,96 mm the latero-dorsal tegmentum (LDTg) and the central tegmentum (CTg), the locus coeruleus (LC) and medially the internal dorsal raphe (DR) extends below the ventral wall of the IV ventricle. From bregma -4,84 mm to -4,24 mm the subdivisions of the dorsal raphe

nucleus (DR) and raphe cap (RC). From -4,24 mm to -3,64 mm the supraoculomotor central gray and cap (Su3, Su3C) and the Edinger-Westafal nucleus (EW). From -4,24 mm to -2,54 at the end of the PAG the EW and Darkschewitsch nucleus (Dk). Dorsal to the PAG: the inferior colliculus subdivisions (DCIC, CIC ECIC) until -4,16 mm, the superior colliculus subdivisions (SC) from -4,84 mm to -2,92 mm, the optic tectum (OT) and part of the deep mesencephalic nucleus (DpMe) from -2,92 to -2,54 mm were displayed together as "colliculus" (fig.3.1).

Surprisingly, I found a limited number of neurons along the whole PAG at 10 weeks old of age (179±19,14; fig.3.2.A, left column). In 19 weeks old females the total number of τGFP neurons was increased >2 fold in the whole PAG (385±44,84; fig.3.2.A. **: $p<0,01$). To determine whether this effect was replicated elsewhere in the brain, I have counted τGFP neurons also in the regions nearby the PAG. Similarly, τGFP neurons increased significantly in the colliculus of 19 weeks old females (10 wo: 248,3±35,8 vs 19 wo: 481±60,35; fig. 3.2.B. *: $p<0,05$). Conversely, no change in neuron number was observed in the areas that form borders with PAG and the IV ventricle (10 wo: 105±11,53 vs 19 wo: 119,3±22,36; fig.3.2.C $p=0,2997$). Analysis performed for each bregma position confirmed that any change in number of neurons occurs in the ventral part of the IV ventricle at any bregma coordinate (fig.3.2.G), whereas a significant increase can observed in the posterior part of the PAG (positions -4,93, -4,84 and -4,75 mm, fig.3.2.E, *: $p<0,05$) and more anteriorly (-3,74 to -3,26 mm, fig.3.2.E), although a trend of higher number of τGFP neurons was observed homogenously along the whole length of the PAG. Similarly, τGFP neurons increased significantly at the onset of superior colliculus (from -4,84 mm, fig.3.2.F), until its end (-3,16 mm in these data). Significant increase was observed also within the deep mesencephalic nucleus (DpMe, around -3,01 mm in these data). Analysis was extended more in detail for the PAG subdivisions (fig.3.3), respectively dorsomedial periaqueductal gray (DMPAG), dorsolateral and lateral periaqueductal gray (DL/LPAG), and ventrolateral periaqueductal gray (VLPAG). τGFP neurons significantly increased in the DMPAG and the DL/LPAG of 19 weeks old GRIC/eR26 τGFP females with respect 10 weeks old (fig.3.3.A and B) by ≈ 2,5 fold (10 wo: 43,67±4,41 vs 19 wo: 109,7±7,881; ***: $p<0,001$) and >2 fold (10 wo: 85,67±13,35 vs 19 wo: 184,7±37,57; *: $p<0,05$), respectively.

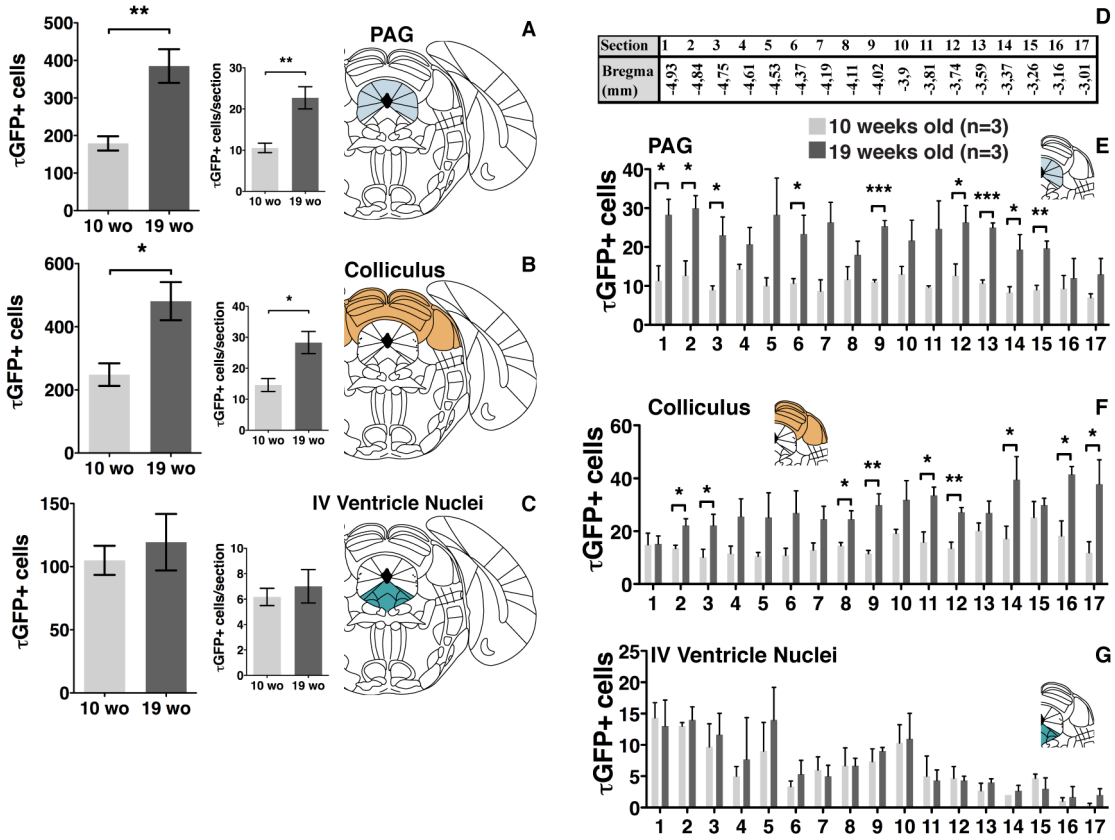

Figure 3.2 Comparison of the number of τGFP neurons in the midbrain of 10 and 19 weeks old females from the GRIC/eR26-τGFP line. A: periaqueductal gray (PAG) total number of neurons and neurons per section. B: Colliculus total number of neurons and neurons per section. C: IV ventricle nuclei total number of neurons and neurons per section. D: alignment legend. E-F-G: statistical comparison for each bregma position. Columns represent mean ±S.E.M. Student's t test: *: p<0,05; **: p<0,01; ***: p<0,001.

Conversely, VLPAG of younger and older females were similar to each other (10 wo: 16±4,73 vs 19 wo: 25±3,79; p=0,1057, fig. 3.3.C). Among the three subdivisions, VLPAG appeared much less populated than DMPAG and DL/LPAG in both ages (10 and 19 weeks old), along the whole length (as shown in fig.3.3.D, E and F). The PAG/Superior colliculus area of 10 weeks old and 19 weeks old female brain is visualized in figure 3.4. This data show that distribution of τGFP neurons is relatively poor among the areas analyzed at 10 weeks old, with a major density in the superior colliculus and, relatively to the PAG subdivisions, in the DMPAG and DL/LPAG. Overall, comparison with older females revealed that an age-dependent increase of GnRHR-expressing neurons is occurring during adulthood in females within a relatively short time during the life-span of a female mouse, restricted to some nuclei and only in DMPAG and DL/LPAG subdivisions of the PAG, but not in the VLPAG.

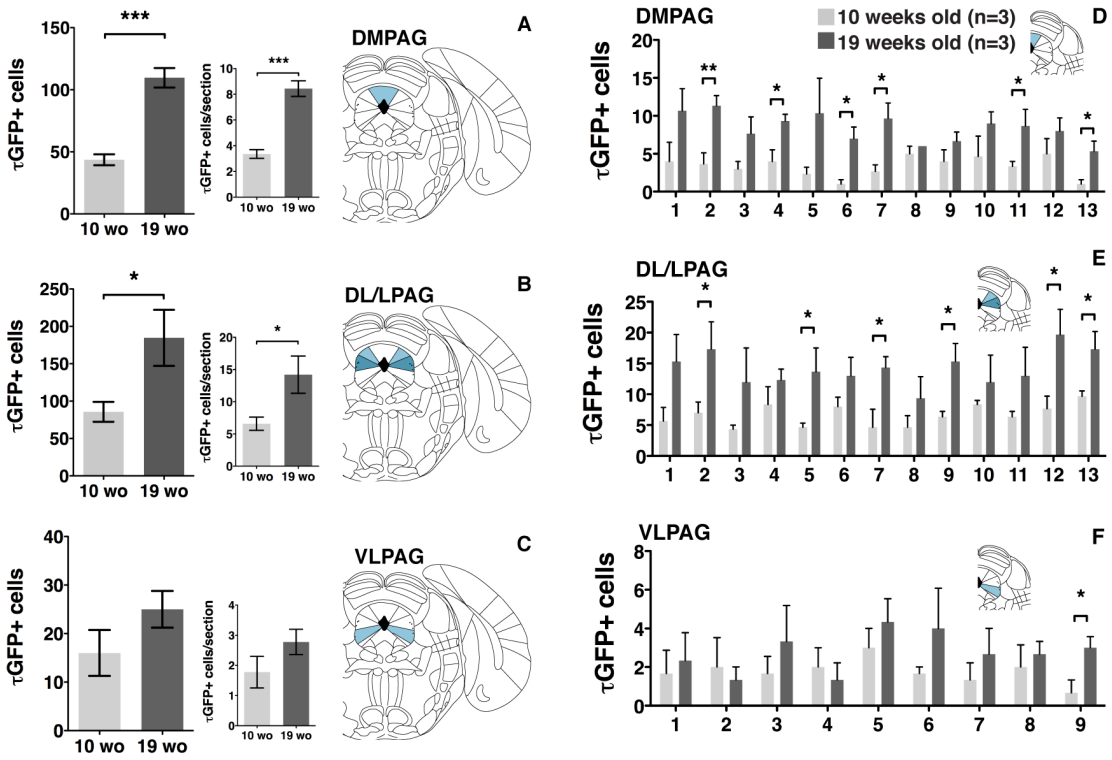

Figure 3.3 Comparison of the number of τGFP neurons within the PAG columns of 10 and 19 weeks old females from the GRIC/eR26-τGFP line. Columns represent mean ±S.E.M. DMPAG: dorsomedial periaqueductal gray. DL/LPAG: dorsolateral and lateral periaqueductal gray. VLPAG: ventrolateral periaqueductal gray. Student's t test: *: p<0,05; **: p<0,01; ***: p<0,001.

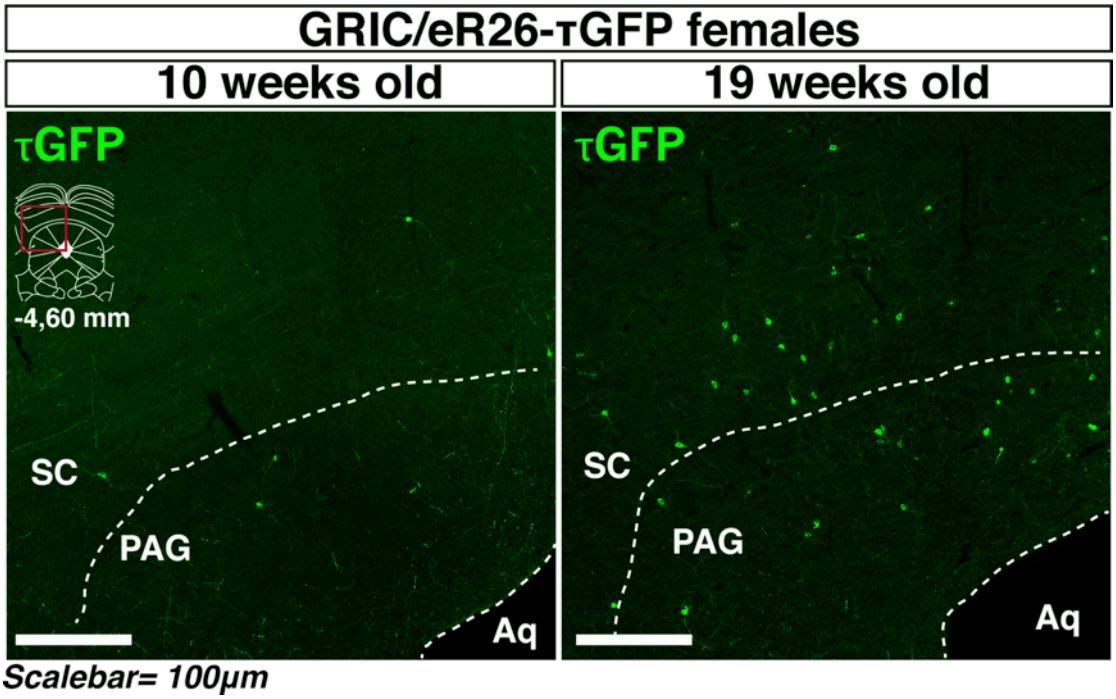

Figure 3.4 Representative 14 μm sections showing the PAG and superior colliculus 10 and 19 weeks old GRIC/eR26-τGFP females. SC: superior colliculus. Aq: aqueduct. PAG: periaqueductal gray.

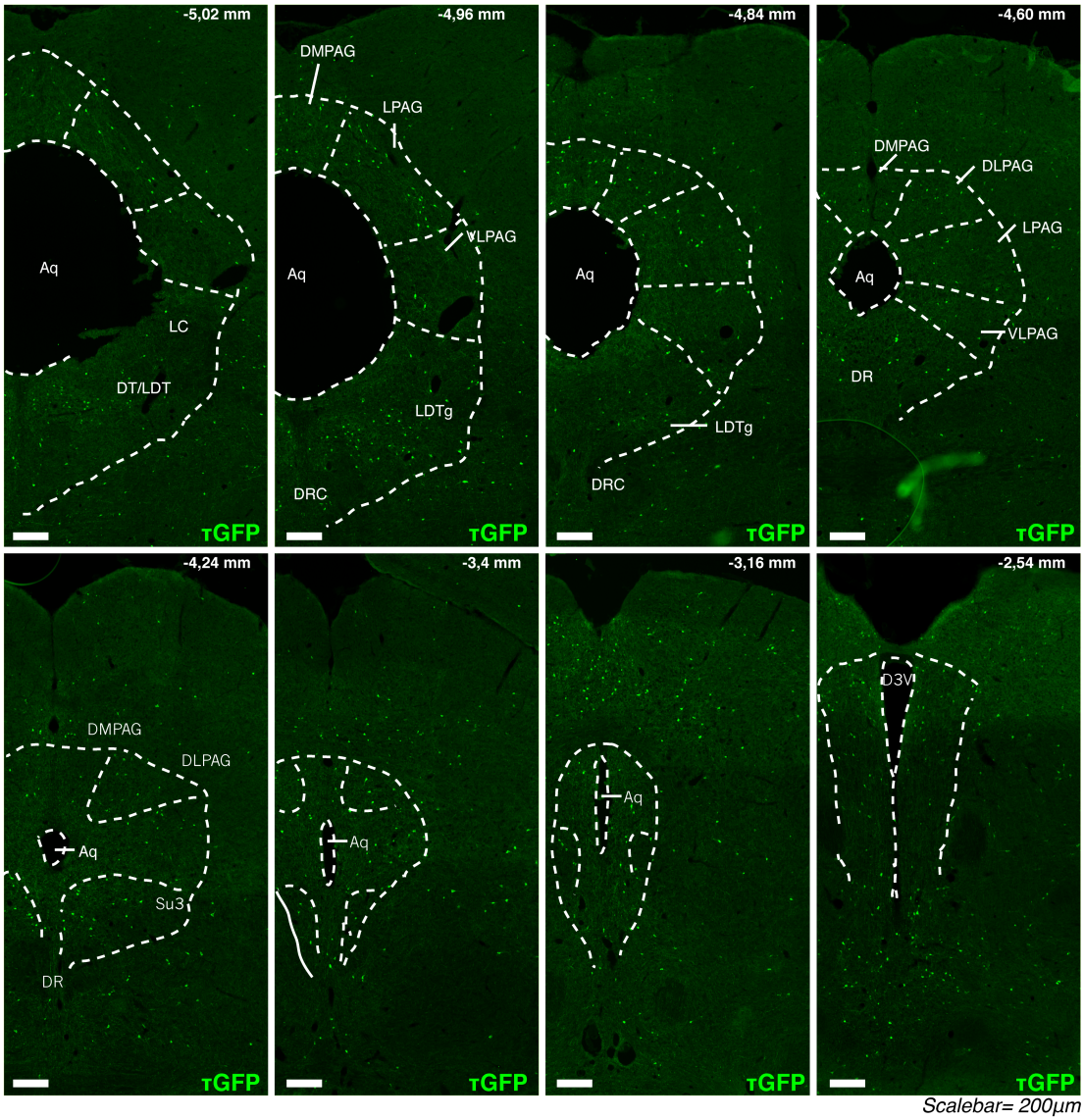

Figure 3.5 14 µm sections of the midbrain of an adult (12 weeks old) GRIC/eR26-τGFP female. Aq: aqueduct. LC: locus ceruleus. DTg: dorsal tegmentum. LDTg: laterodorsal tegmentum. DMPAG: dorsomedial periaqueductal gray. DLPAG: dorsolateral periaqueductal gray. LPAG: lateral periaqueductal gray. VLPAG: ventrolateral periaqueductal gray. DRC: dorsal raphe cap. DR: dorsal raphe. Su3: supraoculomotor central gray. D3V: dorsal 3rd ventricle.

3.1.1.1.1 τGFP neurons form a "stereotyped" map in the PAG and the midbrain of GRIC/eR26-τGFP female mice along the rostro-caudal axis.

Figure 3.5 shows the complete map of τGFP neurons along the PAG of an adult GRIC/eR26-τGFP female mouse. Especially in the more caudal moiety of the PAG, τGFP neurons appear clustered in the DMPAG and LPAG, whereas in the inferior

colliculus distribution is very low (in fig.3.5 see -5,02 and -4,96 mm). τGFP projections are densely distributed, forming a network that shapes the borders of periaqueductal gray (-5,02 mm to -4,84). Going rostrally, the distribution appears more scattered. Concomitantly, τGFP neurons appear to be more densely distributed as superior colliculus is expanding dorsally (starting at -4,84). Ventrally, the tegmental nucleus (LDTg and DT) is densely populated until its end at bregma -4,96 mm. As dorsal raphe enlarges and takes over the tegmentum, less τGFP neurons can be observed (-4,84 mm).

3.1.1.2 Phenotyping of τGFP neurons in the PAG of GRIC/eR26-τGFP female mice

3.1.1.2.1 GnRH fibers are absent from the posterior PAG

There is a great debate on how GnRH reaches its GnRHR target neurons (Schauer et al., 2015). I then asked whether GnRH formed direct contacts with the τGFP neurons or fibers that were observed in the hindbrain, into the more posterior parts of the PAG. Sections from GRIC/eR26-τGFP of the posterior part of the PAG were co-labeled for GnRH with a rabbit polyclonal antibody and for τGFP with chicken polyclonal antibody. As shown in figure 3.6, no detectable GnRH signal (red) was present in the posterior PAG, nor in the inferior colliculus and other nuclei present in the section of the midbrain, whereas τGFP neurons and projections were widely present (green).

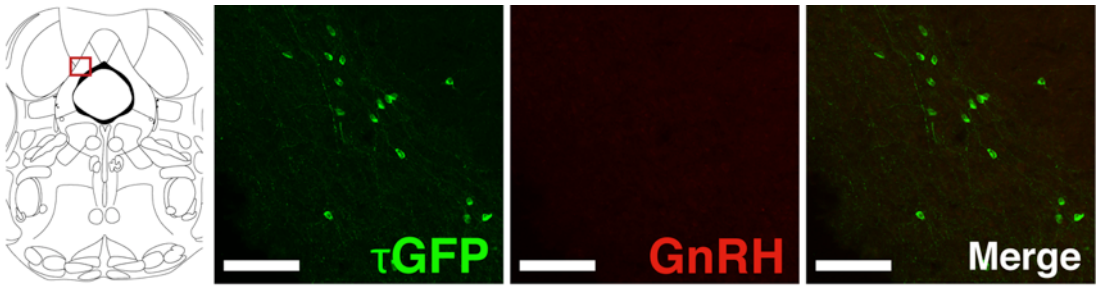

Figure 3.6 14 µm section showing the PAG of adult (12 weeks old) GRIC/eR26-τGFP female stained against τGFP (green) and GnRH (red). Scalebar: 100 µm.

3.1.1.2.2 Parallel regulatory role of ERα and GnRHR within the PAG

GnRH signal in the PAG is thought to enhance the estradiol modulatory effect onto a population of estradiol-sensitive neurons in the ventromedial hypothalamus to

promote female sexual receptivity (Saito and Moltz, 1986; Sakuma and Pfaff, 1980b, c), mainly through the ERα (Ogawa et al., 1999). However, ERα is also widely expressed in neurons in the PAG, (Loyd and Murphy, 2008), suggesting direct interaction at the level of the PAG. Next step was to assess whether GnRHR neurons in the PAG were regulated by estradiol, so I next examined if GnRHR neurons co-express ERα. Recently in our lab no ERα was detected in hypothalamic GnRHR neurons (Schauer et al., 2015). As shown in figure 3.7, although τGFP neurons (green) distribution strongly matched patterns of ERα nuclei in the LPAG, almost none of the τGFP neurons was ERα immunoreactive (the neuron shown in figure 3.7 is the sole detected in the section). These results showed that GnRHR neurons in the PAG do not coexpress ERα, showing no obvious evidence of a reciprocal regulation nor any direct interaction between neuronal GnRH signaling and genomic estradiol signaling in normal conditions within PAG GnRHR neurons. However, they may act in parallel to modulate the PAG neural network.

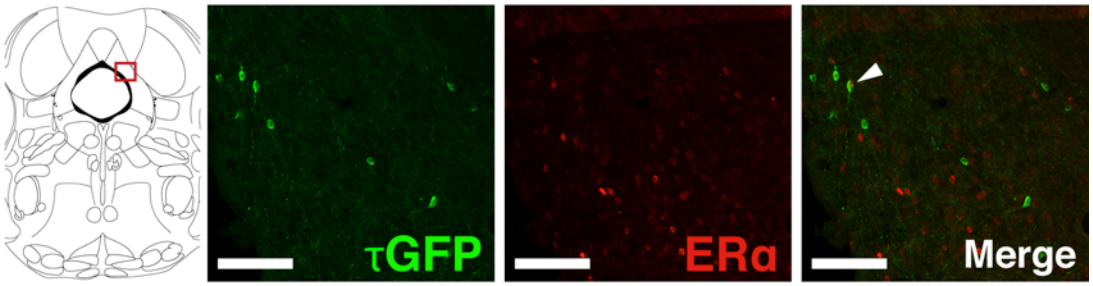

Figure 3.7 14 µm section showing the PAG of adult (12 weeks old) GRIC/eR26-τGFP female stained against τGFP (green) and ERα (red). One τGFP neuron is showing an ERα+ nucleus (white arrow). Scalebar: 100 µm

3.1.1.2.3 Non-overlapping neuronal populations within the PAG

nNOS neurons form a network clustered in the laterodorsal tegmentum (LDTg), highly matching the distribution of GnRHR neurons below the ventral wall of the IV ventricle (Gotti et al., 2005). By opposite, GnRHR neurons are poorly present in the nearby dorsal raphe (DR), mainly characterized by serotoninergic neurons (Clark et al., 2008). Since it was observed that GnRHR are specifically segregated in the lateral tegmentum rather than the dorsal raphe (DR) in the mesencephalic nuclei interfacing the IV ventricle, I examined more in detail how τGFP neurons are localized with respect to DR and LDTg. So, GRIC/eR26-τGFP sections were labeled for the neuronal nitric oxide synthase (nNOS) or for the second isoform of the tryptophan hydrolase (Tph2), the enzyme of the first step in serotonin (5-HT) biosynthesis and a

widely used marker for serotoninergic neurons (Clark et al., 2008), and for τGFP. Figure 3.8 shows that nNOS labeled intensively the LDTg (red). Although τGFP neurons (green) and nNOS neurons were in close vicinity to each other in LDTg, co-localization was rarely observed between the two populations, indicating indeed that GnRHR-specific τGFP neurons constitute a distinct population from nNOS neurons in the same nuclei. Interestingly, a difference in size could be noticed as well, with τGFP having smaller perikarya than nNOS+ neurons.

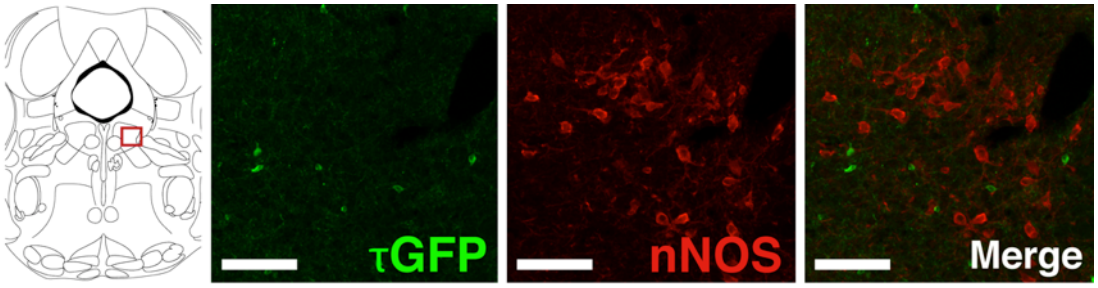

Figure 3.8 14 µm section showing the PAG of adult (12 weeks old) GRIC/eR26-τGFP female stained against τGFP (green) and nNOS (red). Scalebar: 100 µm.

Tph2 immunohistochemistry highlighted the DR, as shown in fig.3.9. As expected, DR was poor of τGFP neuronal somata.

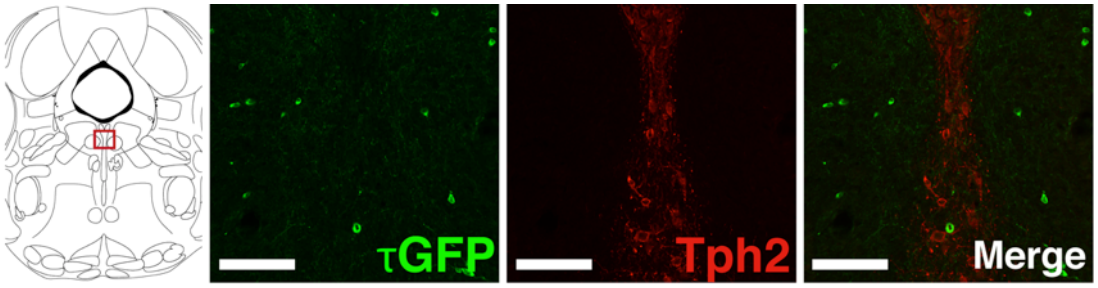

Figure 3.9 14 µm section showing the PAG of adult (12 weeks old) GRIC/eR26-τGFP female stained against τGFP (green) and Tph2 (red). Scalebar: 100 µm.

3.1.2 Manipulation *in vivo* of GnRHR-expressing neurons in the PAG of female mice.

3.1.2.1 GnRHR is acutely expressed in the dorsal periaqueductal gray neurons of the female.

In order to ablate GnRHR neurons in the dorsal PAG, the PAG was stereotaxically targeted at the rostrocaudal bregma coordinate -4,96 mm, were PAG is highly populated of GnRHR neurons, at the border between the DM- and the DLPAG.

According to the mapping results, age was strongly considered. Prior to the ablation experiment, in order to assess acute expression of GnRHR in the dorsal PAG of the adult female *in vivo,* an adult GnRHR-IRES-Cre female (17 wo) was stereotaxically injected with a cre-dependent mCherry AAV vector, then sacrificed 4 weeks after injection. The distribution of mCherry fibers and neurons could be observed in the dorsal midbrain (fig.3.10). mCherry fibers were scattered within the DM-, DL- and LPAG, starting at most posterior coordinates (bregma: - 5,02 mm, fig.3.10), although fewer neurons than expected were observed at this bregma position. More anteriorly, figure 3.10 shows a wide distribution of mCherry neurons and projection in the dorsal moiety of the PAG. Notably, the VLPAG completely lacked of mCherry labeling, indicating no spreading of the virus on the dorso-ventral axis. Labeling of the superior colliculus was also present at the level of the medial part of deep granular layer (DpG), in close contact with the DMPAG; by opposite, the inferior colliculus lacked mCherry neurons and projections. Dense network of projections and neurons spread through the DMPAG, DL/LPAG and DpG from bregma -4,84 mm to -4,16 mm (fig. 3.10), whereas in the more anterior bregma coordinates (-4,04 mm to -3,52 mm) mCherry neurons clustered in the DMPAG, to gradually decrease and being restricted dorsally in the DpG and the commissure of the superior colliculus (csc). Summarizing, cre-dependent AAV efficiently infected neurons in the midbrain and drives GnRHR-dependent expression of ChR2-(H134R)-mCherry fusion protein. These results confirmed acute GnRHR expression in PAG neurons from 17 to 21 weeks of age, indicating that the PAG and the surrounding superior colliculus are GnRH-sensitive in the adult female brain.

3.1.2.2 Genetic ablation of GnRHR-expressing neurons in the dorsal PAG.

To achieve temporal control of genetically defined GnRHR neurons ablation followed by sexual behavior assessment, adult sexually naive, OVX and estradiol-primed GRIC/eR26-τGFP females were injected stereotaxically with a cre-dependent AAV vector encoding for the procaspase 3, or with ACSF. After 3 weeks from the injection, females were tested for sexual behavior. Following behavior, females were sacrificed and τGFP neurons were quantified. In figure 3.11.A is shown the injection placement performed with methylene blue injection in one female, as control. The

injection site is shown at the left panel of figure 3.11.A, at bregma -4,96 mm. As shown, dye spreads in both dorsal PAG and colliculus between bregma -5,20 mm and -4,48 mm (coordinates that span the four panels of fig.3.11.A), being more intense around -4,96 mm to -4,84 mm (second and third panel of fig. 3.11.A), showing that injection correctly reached the dorsal PAG. In Cas3-injected GRIC/eR26-τGFP females, ablation was observed mostly in the DMPAG (fig.3.11.C). A significant reduction in the number of τGFP neurons was observed in the DMPAG from bregma -4,77 mm to -4,41 mm, being more drastic at -4,56 mm (from 16,33±0,88 in ACSF to 3±0,58 in AAV-Cas3; ***: p<0,001; fig.3.11.C) and -4,49 mm (11,67±1,2 in ACSF vs 3±1 in AAV-Cas3; **: p<0,01; fig.3.11.C), in AAV-Cas3 injected females. In DL/LPAG a significant reduction was observed only in bregma -4,85 mm (19±2,5 in ACSF vs 9±2,08 in AAV-Cas3; *: p<0,05; fig.3.11.D) and -4,28 mm (22±0,577 in ACSF vs 12,67±2,96 in AAV-Cas3; *: p<0,05; fig.3.11.D), whereas no change was observed in VLPAG (Fig.3.11.E). Ablation efficiency was calculated within the DMPAG (expressed as: % τGFP neurons counted in the AAV-Cas3 group out of the mean of the controls. Fig.3.11.F-I) within the interval of major reduction (highlighted with dark blue line in figure 3.11.F). A significant 68% reduction (**: p<0,01) was observed from bregma -4,77 to -4,41 mm (360 μm), whereas from bregma 4,93 mm to -4,41 mm (520 μm) GnRHR neurons were reduced by 60 % (**: p<0,01). Non-significant reduction (27%) of τGFP neurons was observed in the whole length of the DMPAG (fig.3.11. p=0,1125). Summarizing, acute, focal ablation in the posterior part of dorsal PAG caused a 68% reduction in the number of GnRHR neurons mostly in the DMPAG between bregma -4,77 mm to bregma -4,41 mm.

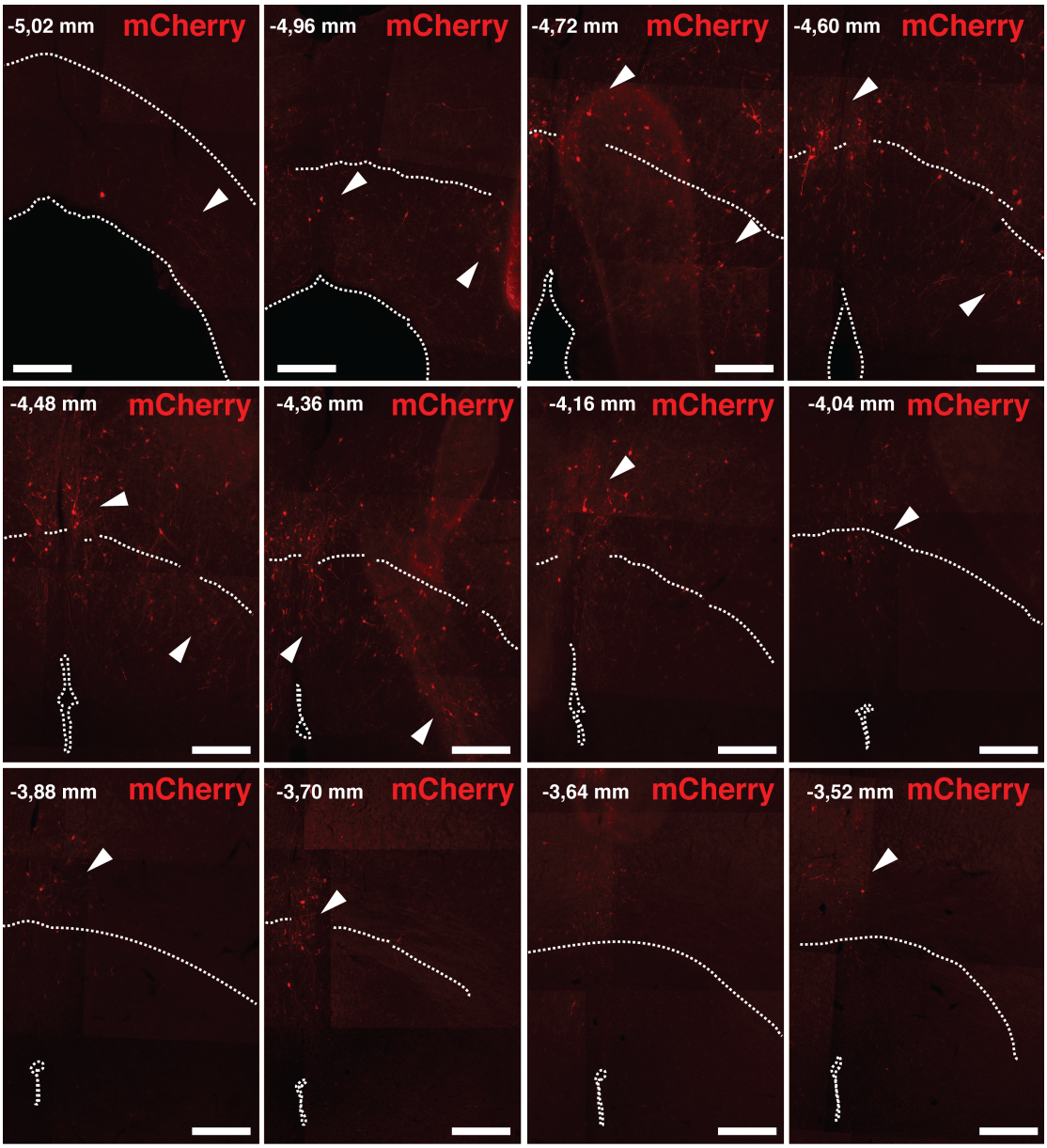

Figure 3.10 25 µm sections from a GRIC female injected with 0,2µl/side of AAv5-ChR2-mCherry in the dorsal PAG and stained anti-mCherry show cre-dependent distribution in the PAG and superior colliculus (white arrows). Scalebars: 200 µm.

3.1.2.2.1 Acute ablation of GnRHR-expressing neurons in the dorsal PAG has no effect on sexual behavior in OVX females primed with estradiol and progesterone.

Behavioral analysis of females which undergone GnRHR neurons ablation in the PAG together with ACSF controls is reported in figure 3.12. The number of mounting events was higher in the ACSF group in the first session, although only nearly significant (16±3,2 in ACSF vs 9,67±1,67; p=0,077). Similarly, ACSF group showed more rejection events with a nearly significant difference (13,67±2,186 in

ASCF vs 7,33±2,03 in AAV-Cas3; p=0,0504), perhaps mirroring the higher mounting activity from the males towards the females. Lordosis events seemed highly variable between the two groups. The lordosis quotient (LQ%) however, revealed that lordosis behavior is fully retained in AAV-Cas3 injected females (S.I: 18,93±14,67% in ACSF vs 20,5±20,5% in AAV-Cas3; p=0,47; S.II: 58,33±30,05% in ACSF vs 54,33±27,42 in AAV-Cas3; p=0,46), showing also increased receptivity between the first to the second session, similarly to ACSF controls. Notably the 2/3 of the females displayed sexual behavior at the second session in both groups, showing that the total number of receptive females was identical. The measurements of the total time spent in lordosis (S.I: 40,6±40 s in ACSF vs 42±42 s in AAV-Cas3; S.II: 79±47,7 s in ACSF vs 78,66±42,97 s in AAV-Cas3) and the lordosis duration per event (S.I: 4±3,5 s in ACSF vs 5,25±5,25 s in AAV-Cas3; S.II: 6,6±3,47 s in ACSF vs 9,1±5,09 s in AAV-Cas3), highlights that lordosis duration was undistinguishable from controls following GnRHR neurons ablation. Female receptivity results were corroborated by the number of intromissions by the male, which also were very similar in the two groups; ACSF and AAV-Cas3 injected females both displayed the same number of intromissions by the male both in the first and the second session (S.I: 1,66±1,66 s in ACSF vs 2,66±2,66 s in AAV-Cas3; S.II: 5,33±3,528 s in ACSF vs 5±3,06 s in AAV-Cas3), reflecting efficient lordosis execution. Male latency to mount was tendentially higher in Cas3 group in the first session (S.I: 55±3,2 s in ACSF vs 157,7±68,55 s in AAV-Cas3; p=0,1), but the time before showing lordosis (latency to lordosis) did not differ (S.I: 411,7±138,3 s in ACSF vs 447,3±152,7 s in AAV-Cas3; p=0,4; S.II: 300,3±154,5 s in ACSF vs 401,3±151,9 s in AAV-Cas3; p=0,3). In summary, results show that a 68% reduction of GnRHR neurons within the dorsal PAG between bregma -4,77 mm and bregma -4,41 mm did not interfere with estradiol and progesterone mediated induction of female sexual behavior.

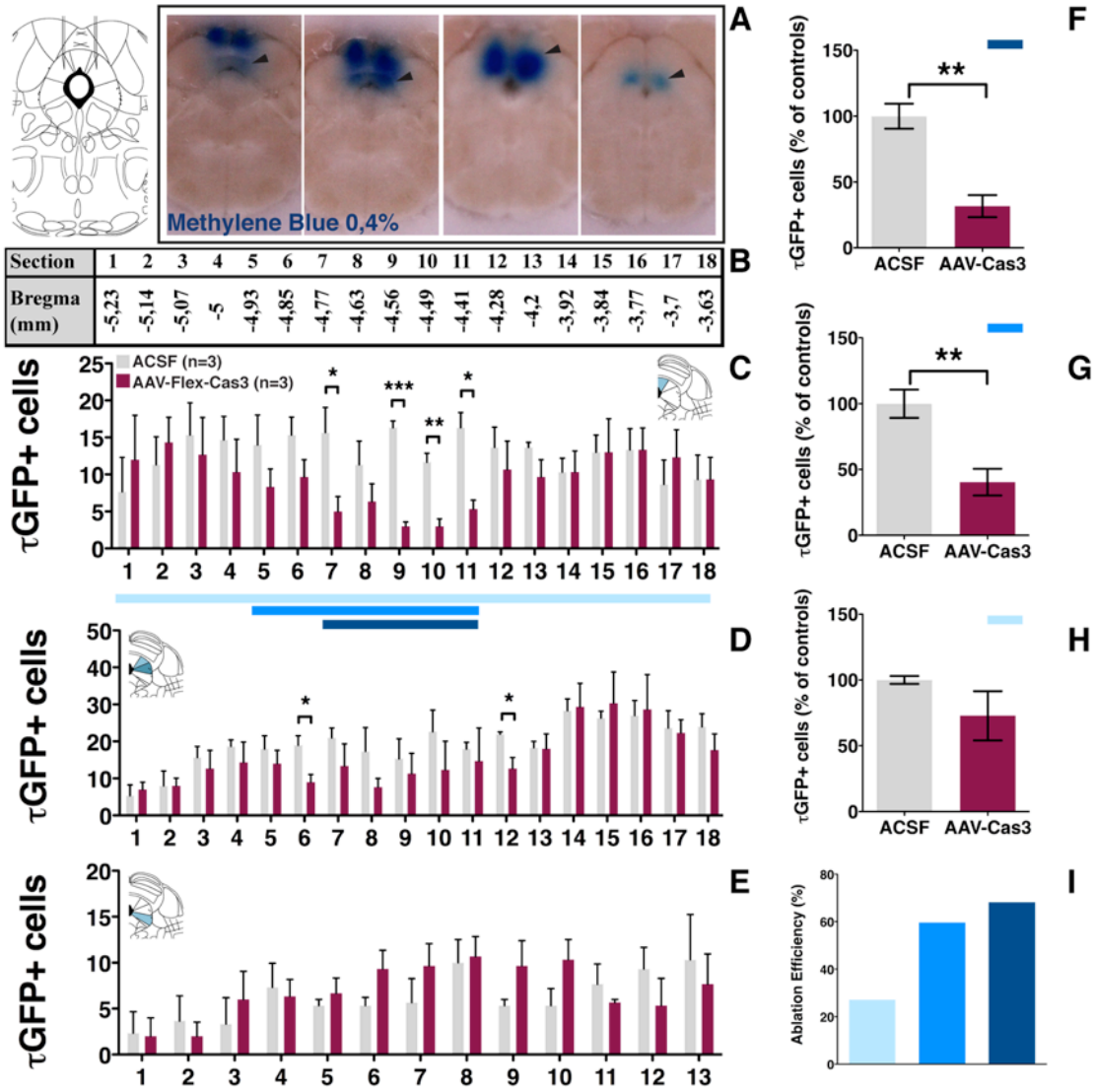

Figure 3.11 GnRHR neurons ablation in the dorsal PAG. A: Methylene blue injection in the dorsal PAG shows that injection procedure efficiently targets the dorsal PAG according to the atlas, although the injected "bolus" (in blue) spills over the superior colliculus. B-E: comparison of τGFP neurons between ACSF and AAV-Cas3 injected n the PAG subdivisions. Each bregma position represents a single 14 µm section for each experimental group. F-H; percent reduction of τGFP neurons in the DMPAG, within the three different intervals highlighted in C with three distinct colors. I: Ablation efficiency in the DMPAG. Colors of the columns match the intervals in C. Columns represent mean ±S.E.M apart from I (mean of percent values only). DMPAG: dorsomedial periaqueductal gray. DL/LPAG: dorsolateral and lateral periaqueductal gray. VLPAG: ventrolateral periaqueductal gray. Student's t test: *: p<0,05; **: p<0,01; ***: p<0,001.

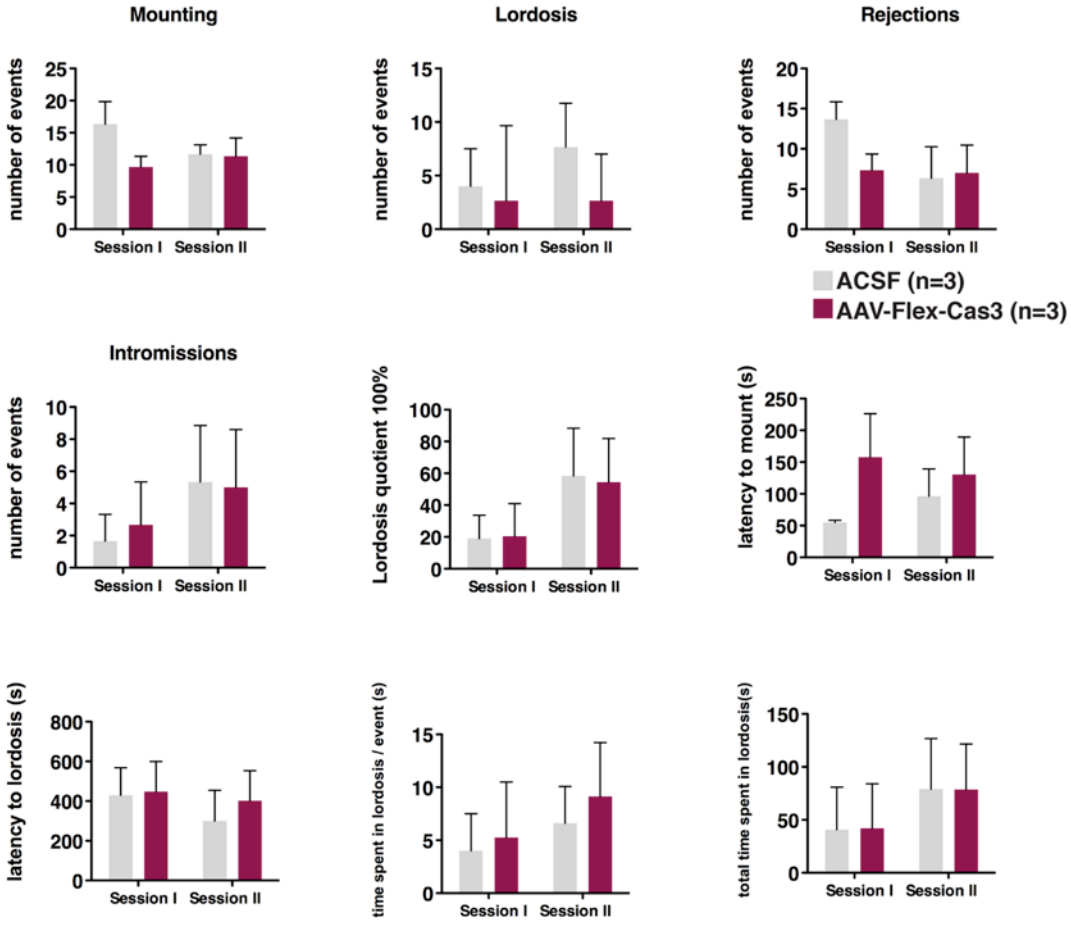

Figure 3.12 Behavioral phenotype following GnRHR neurons ablation in the dorsal PAG of females, displayed as mean ±S.E.M.

3.1.3 Assessing neural correlates of female sexual behavior: c-fos expression in the PAG of female mice following sexual behavior

Acute ablation of a portion of GnRHR-expressing neurons within the DMPAG did not affect female sexual receptivity in our experiment. Up regulation of c-fos in the lateral PAG following lordosis was reported in rats (Yamada and Kawata, 2014), suggesting activation of the lateral PAG during female receptivity. However, information is missing about the other PAG subdivisions. I therefore aimed to reproduce this experiment in wild type female mice and mapped the c-fos+ nuclei distribution within the midbrain. A total of four wild type OVX females (estrogen-primed) were primed with progesterone and then placed in the behavioral arena with clean bedding (controls) or with a sexually experienced male (lordosis). The females

in the lordosis group displayed a percent lordosis quotient of 85% and 72,22% respectively. As showed in table 3.1 and figure 3.13, c-fos signal was clearly increased in the PAG of females that displayed sexual behavior with respect to bedding controls. Higher number of c-fos+ nuclei was evident only in the caudal half of the PAG, whereas from bregma -3,88 mm to more anterior coordinates the two groups appeared equal. Increase was also evident in the superior colliculus, whereas no difference was evident within the nuclei ventral to the IV ventricle. Table.3.2 shows that c-fos was up regulated in all the columnar subdivisions: DMPAG, DL/LPAG and VLPAG. Summarizing, it was found a simultaneous c-fos activation in the caudal half of the DMPAG, DL/LPAG and VLPAG.

Table 3.1. number of c-fos+ nuclei following lordosis

	PAG				Colliculus				IV Ventricle Nuclei			
Bregma (mm)	Bedding		Lordosis		Bedding		Lordosis		Bedding		Lordosis	
-4,965	41	13	95	127	56	56	142	186	118	19	113	109
-4,821	35	18	214	178	81	68	262	195	117	2	16	65
-4,501	20	83	101	176	38	81	193	165	19	13	30	24
-4,18	27	14	158	141	66	5	226	24	3	0	24	17
-4,1	27	19	105	46	42	25	172	30	2	0	33	7
-4,02	23	21	100	99	35	15	99	108	0	2	32	65
-3,84	11	101	92	81	7	108	142	107	4	65	54	46
-3,76	50	72	103	46	35	54	130	41	14	108	39	17
-3,68	34	113	101	25	51	98	73	31	18	89	24	17
-3,6	49	51	52	39	39	84	66	59	4	93	49	57
-3,46	65	77	28	31	15	89	25	86	11	43	19	61
-3,33	27	61	22	48	11	110	33	103	0	37	0	63
-3,25	19	38	24	18	20	52	17	30	2	24	5	58
-2,92	6	18	9	13	40	48	20	26	0	0	8	0
-2,84	17	22	6	8	31	38	14	22	0	0	4	0
Total	451	721	1210	1076	567	931	1614	1213	312	495	450	606
Mean	586		1143		749		1414		404		528	
St.Dev.	191		94,8		257		284		129		110	
S.E.M.	135		67		182		201		91,2		78	

Table 3.2 number of c-fos+ nuclei following lordosis within PAG subdivisions

	DMPAG				DL/LPAG				VLPAG			
Bregma (mm)	Bedding		Lordosis		Bedding		Lordosis		Bedding		Lordosis	
-4,965	12	2	10	36	12	4	43	91	17	7	42	67
-4,821	7	6	41	29	16	12	122	117	12	0	51	32

-4,501	3	17	9	30	15	58	64	100	2	8	28	46
-4,18	8	8	35	23	15	6	64	48	4	0	59	70
-4,1	7	8	14	3	20	11	67	22	0	0	24	21
-4,02	1	10	25	13	18	11	52	56	4	0	23	30
-3,84	3	31	21	16	8	70	71	65				
-3,76	2	17	21	6	48	55	82	40				
-3,68	6	30	14	5	28	83	87	20				
-3,6	16	9	4	14	33	42	48	25				
-3,46	17	16	6	14	48	61	22	17				
-3,33	0	0	0	0	0	0	0	0				
-3,25	0	0	0	0	0	0	0	0				
-2,92												
-2,84												
Total	82	154	200	189	261	413	722	601	39	15	227	266
Mean	118		195		337		662		27		247	
St.Dev.	50,9		7,78		107		85,6		17		27,6	
S.E.M.	36		5,5		76		60,5		12		19,5	

3.1.3.1 c-fos expression in the PAG of GRIC/eR26-τGFP females following sexual behavior

To determine whether GnRHR neurons within the PAG take part to the neural correlates of lordosis within the PAG in mice, I quantified and statistically analyzed c-fos immunoreactive nuclei in the PAG of females from bregma -4,96 mm to bregma -3,88 mm. GRIC/eR26-τGFP females that encountered the males showed lordosis quotients percent of: 72% (18 lordosis events out of 25 total mounts), 59,6 % (17 lordosis events out of 29 total mounts) and 62,5 % (20 lordosis events out of 32 total mounts). The number of intromissions by the male were: 15 (out of 29 total mounts), 10 (out of 25 total mounts) and 15 (out of 32 total mounts), respectively, indicating clear receptivity of the females. Number of c-fos+ nuclei significantly increased by ≈ 1,9 fold in the PAG of females displaying lordosis behavior (811±82,5 in controls vs 1546±210,9 in lordosis; *: p<0,05; fig.3.14.A), notably between -4,88 mm to 4,4 mm (fig.3.14.E). Significant increase (by ≈ 3 fold) was observed in the overall colliculus, although evident only in the superior colliculus (419,3±90,69 in controls vs 1310±101,4 in lordosis; fig.3.14.B and F; **: p<0,01) and by ≈ 1,5 fold in the areas ventral to the IV ventricle (257±37,61 in controls vs 424±17,69 in lordosis;

fig.3.14.C and G; **: $p<0,01$). Detailed analysis revealed significant increase in c-fos+ nuclei in each PAG subdivision: by ≈ 2 fold in DMPAG (115±25,24 in controls vs 254,7±18,5 in lordosis; fig. 3.15.A; **: $p<0,01$), ≈ 1,8 fold in DL/LPAG (497,7±23,38 in controls vs 886,7±171,5 in lordosis; fig. 3.11.A fig.3.15.B; *: $p<0,05$) and ≈ 2 fold in VLPAG (198,3±34,72 in controls vs 404,3±27,83 in lordosis;

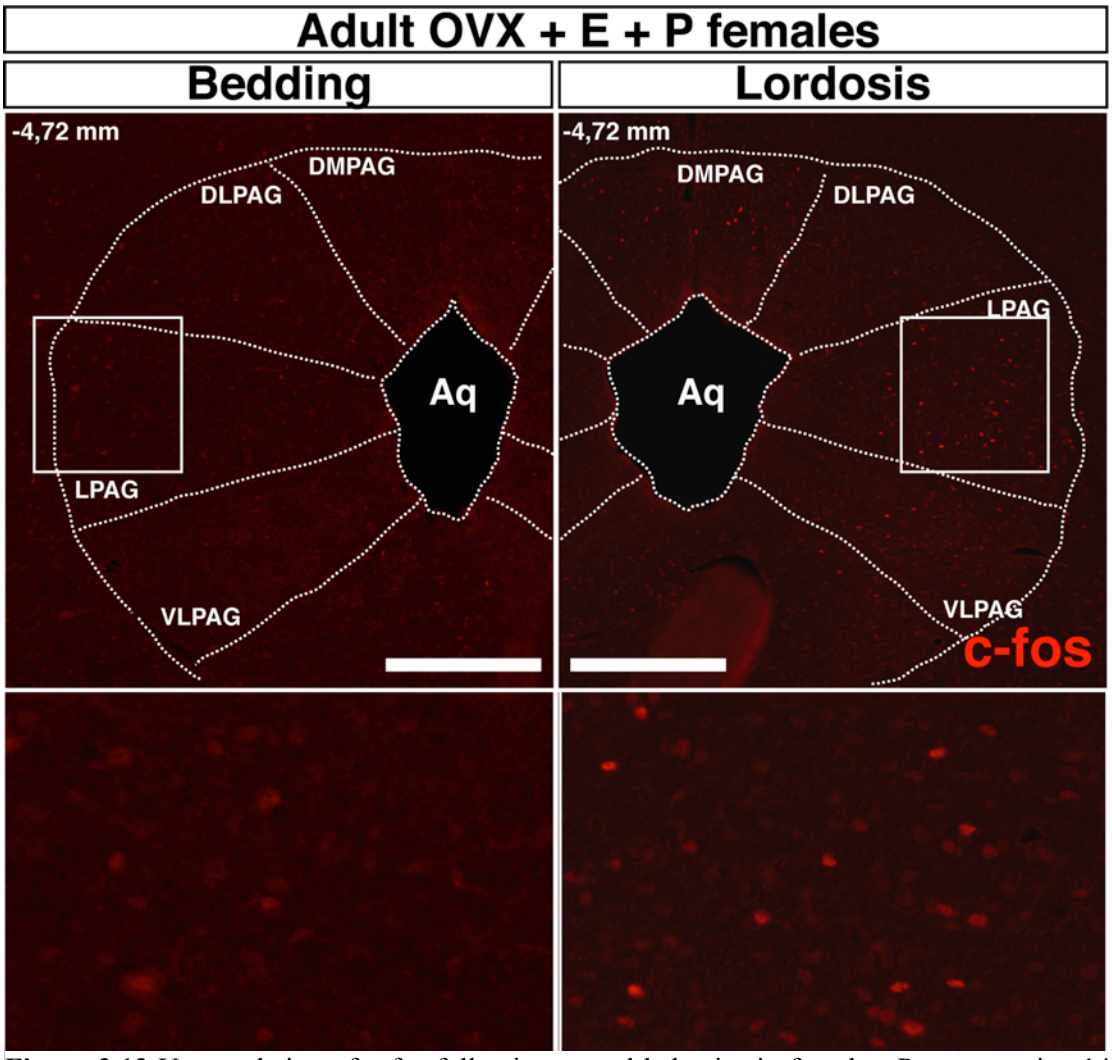

Figure 3.13 Up regulation of c-fos following sexual behavior in females. Representative 14 µm sections stained for rabbit anti c-fos and donkey anti-rabbit-488 (showed in pseudo-color red) in controls females (exposed to bedding) or lordosis females (exposed to a male showing lordosis). Aq: aqueduct. DMPAG: dorsomedial periaqueductal gray. DLPAG: dorsolateral periaqueductal gray. LPAG: lateral periaqueductal gray. VLPAG: ventrolateral periaqueductal gray. Scalebars: 200 µm (top images) and 100 µm (bottom images).

fig.3.14.C; **: $p<0,01$). c-fos increased significantly in all the PAG subdivisions (fig.3.14.A-BC). Analysis for each bregma position revealed increase in number of c-fos+ nuclei was restricted in the most posterior moiety of both the DMPAG and DL/LPAG (Fig.3.15.D and E), from bregma -4,93 to -4,80 mm, and from bregma

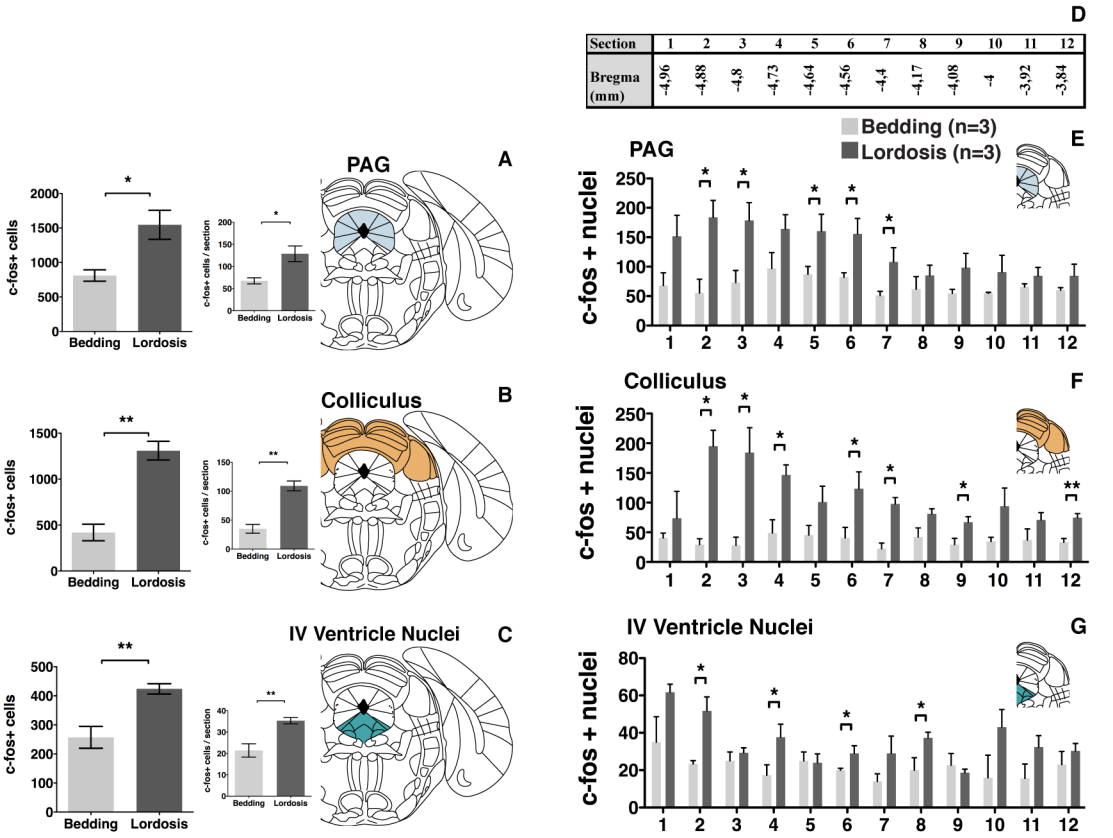

Figure 3.14 Statistical comparison of c-fos+ nuclei within the midbrain in controls females (exposed to bedding) or lordosis females (exposed to a male and showing lordosis). Columns represent mean ±S.E.M. Student's t test: *: p<0,05; **: p<0,01; ***: p<0,001. PAG: dorsomedial periaqueductal gray.

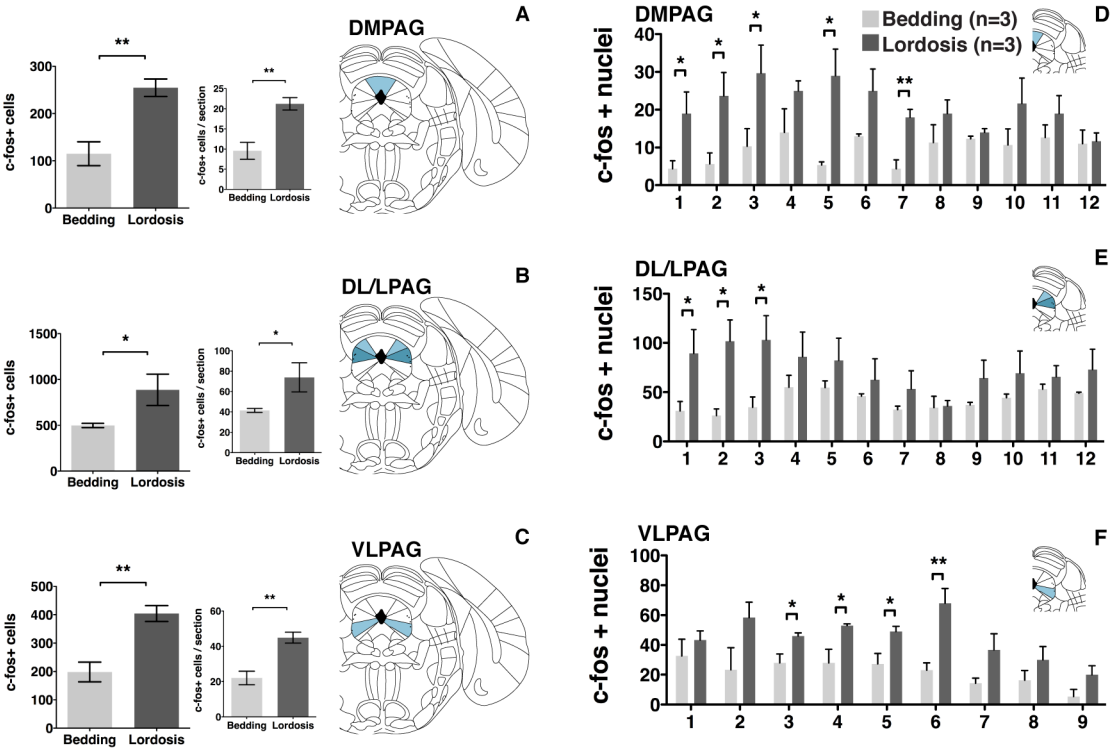

Figure 3.15 Statistical comparison of c-fos+ nuclei within the PAG subdivisions in controls females (exposed to bedding) or lordosis females (exposed to a male and showing lordosis).

Columns represent mean ±S.E.M. Student's t test: *: p<0,05; **: p<0,01; ***: p<0,001. DMPAG: dorsomedial periaqueductal gray. DL/LPAG: dorsolateral and lateral periaqueductal gray. VLPAG: ventrolateral periaqueductal gray.

-4,64 to -4,4 mm. Moreover the graphs of figures 3.15.D and E, confirmed simultaneous activation at the same bregma coordinate.

3.1.3.2 Assessment of PAG-GnRHR neurons activity during female sexual behavior

Parallel to c-fos analysis, the number of τGFP neurons that co-expressed c-fos was quantified. The percent of τGFP/c-fos+ co-expressing neurons out of the total of τGFP neurons was significantly increased in all the PAG subdivisions (Fig.3.16.D-F; *: p<0,05; **: p<0,01), and nearly significant in the colliculus (Fig.3.16.B; p=0,0563), but not ventrally to the IV ventricle (Fig.3.16.C; p=0,3195). However, the percent value and the neat number of τGFP neurons co-expressed c-fos following sexual behavior were very small: as shown in fig.3.16.F, the region with the higher percent of c-fos-expressing τGFP neurons was represented by the VLPAG showing a mean of ≈ 11 ± 2 % of the whole τGFP following lordosis, corresponding to a mean number of 3 ± 1 neurons.

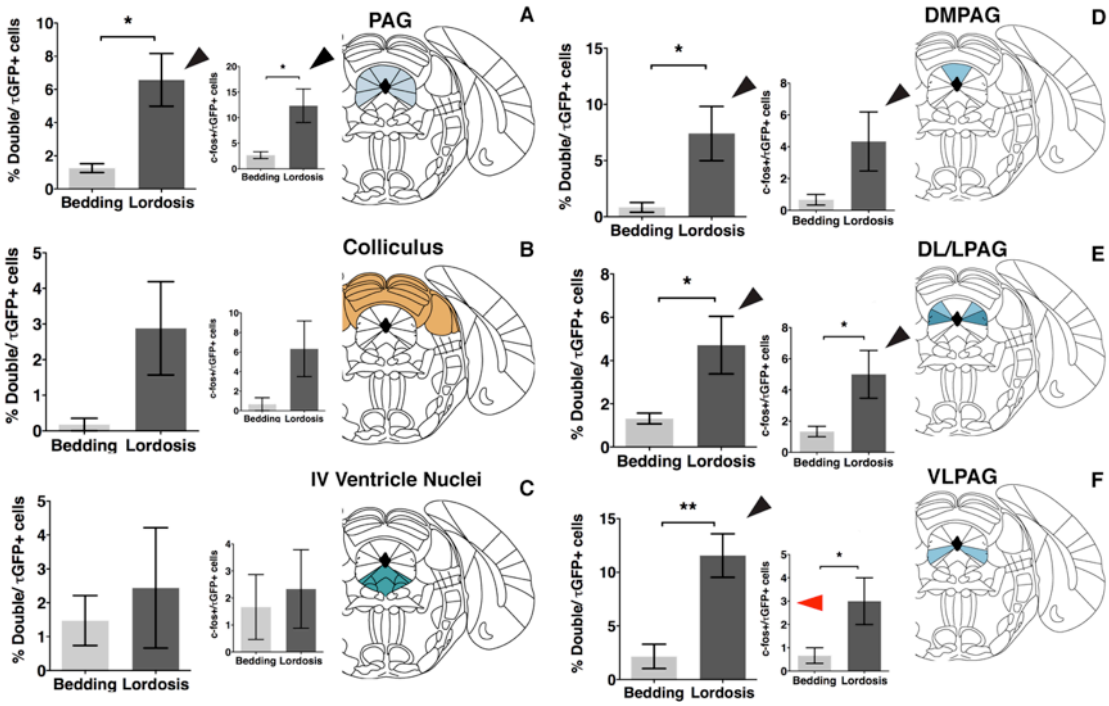

Figure 3.16 Statistical comparison between controls (exposed to bedding) or lordosis (exposed to a male and showing lordosis) GRIC/eR26-τGFP females of τGFP neurons which co-express c-fos within the midbrain and PAG subdivisions. Columns represent mean

±S.E.M. Student's t test : *: $p<0,05$; **: $p<0,01$; ***: $p<0,001$. PAG: periaqueductal gray. DMPAG: dorsomedial periaqueductal gray. DL/LPAG: dorsolateral and lateral periaqueductal gray. VLPAG: ventrolateral periaqueductal gray.

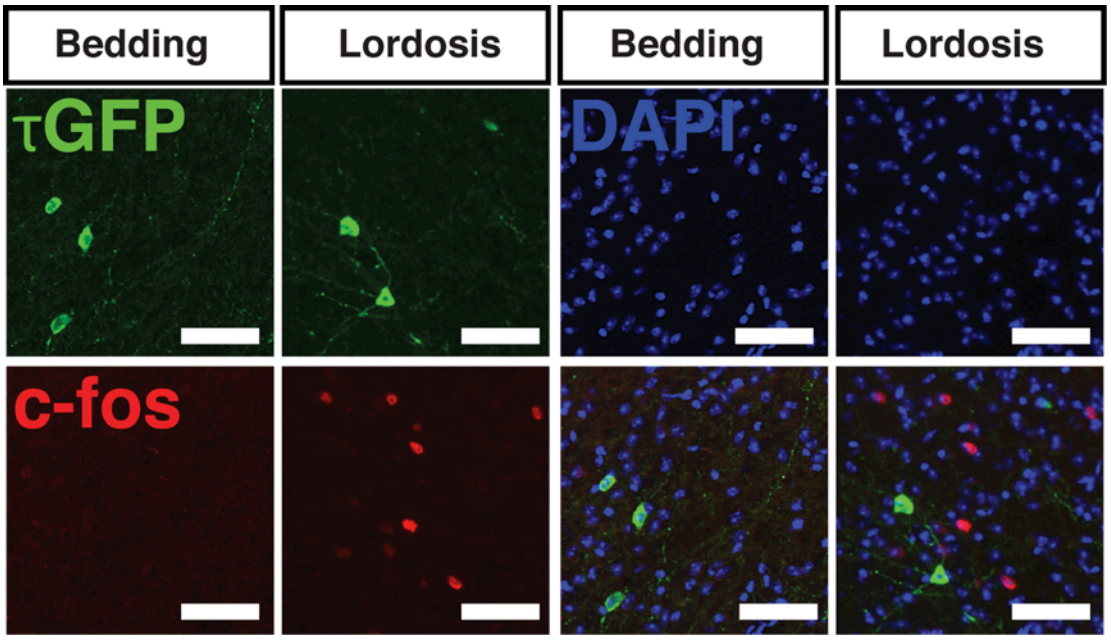

Figure 3.17 Representative 14 µm sections showing the PAG of controls (exposed to bedding) or lordosis (exposed to a male and showing lordosis) GRIC/eR26-τGFP females. Scalebars: 50 µm.

Notably, DMPAG and DL/LPAG strongly up-regulated c-fos expression following sexual behavior and exhibited higher distribution of τGFP neurons (compared to VLPAG), although the percent of τGFP neurons that co-expressed c-fos was even lower than VLPAG, *i.e.* ≈ 7 ± 2 % in the DMPAG and ≈ 5 ± 1 % in the DL/LPAG. Figure 3.17 further shows nearby τGFP neurons and c-fos+ nuclei in the PAG, although not colocalizing.

3.1.3.3 Correlation between sexual receptivity and activity-dependent c-fos increase in the PAG

To find out whether there was a link between the amount of receptivity and the increase in c-fos expression in the PAG, I plotted the single lordosis quotient values and the amount of c-fos (calculated as the percent of c-fos+ nuclei respect to the mean of c-fos+ nuclei in bedding-exposed controls) in the different brain areas as X and Y coordinates (fig.3.18). Unexpectedly, I observed that the higher the receptivity was, the less was the amount of c-fos+ nuclei present in the DMPAG and DL/LPAG. As shown in figure 3.18, the individual that showed a lordosis quotient of 58,6 % (the

lower value, left), displayed a c-fos increase by ≈ 240 % respect to the mean of the controls at the level of the DL/LPAG area, whereas the individual which showed a lordosis quotient of 62,5 % displayed a 176 % increase in c-fos. The higher value of lordosis quotient percent, 72 %, corresponded to an increase of only the ≈ 120 % respect to controls, close to the controls baseline (100%). The DMPAG showed the same trend. The distribution in c-fos in the VLPAG did not seem to follow the level of receptivity. Summarizing, I found that the c-fos increased in DMPAG and DL/LPAG inversely correlated with the level of sexual receptivity in females. This correlation study suggests that in less receptive females c-fos up-regulation may be consequent of some other behavior.

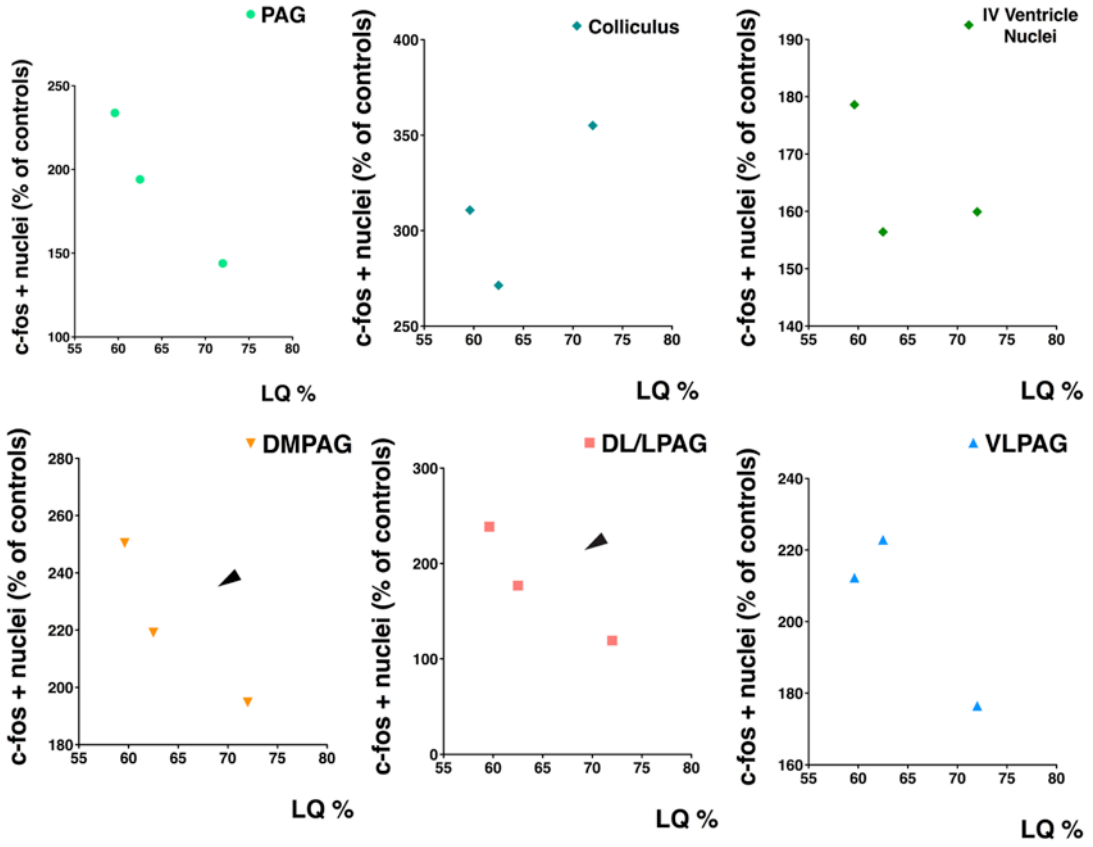

Figure 3.18 Graphs showing plots of the single lordosis quotients % and respective rise of c-fos+ nuclei for each female exposed to a male (lordosis group). DMPAG and DL/LPAG show a trend for inverse correlation (black arrows). PAG: periaqueductal gray. DMPAG: dorsomedial periaqueductal gray. DL/LPAG: dorsolateral and lateral periaqueductal gray. VLPAG: ventrolateral periaqueductal gray.

3.2 The role of mGluR5 in the initiation of puberty and reproductive function

In collaboration with Dr. Ioana Inta, it was analyzed the role of mGluR5 in the initiation of puberty and reproductive function. Vaginal opening (VO), an external hallmark of puberty onset (Mayer et al., 2010), uterine weight, estrus cyclicity and reproductive capacity were assessed in mGluR5 knockout females. Homozygous (-/-) mGluR5 KO females, but not mGluR5 heterozygous (+/-) KO mice exhibited marked delay in the time of vaginal opening (VO) and limited ovarian growth in peripubertal age. Adult mGluR5 -/- KO females exhibited impaired estrus cycle and loss of fertility, whereas mGluR5 +/- KO exhibited only a reduction in the litter size (unpublished data, from Dr. Ioana Inta). Together, these observations indicate defective maturation of the female reproductive axis and transition to adulthood in homozygous mGluR5 KO females.

3.2.1 Circulating pituitary hormone levels in adult female mice lacking the mGluR5 gene

A functional reproductive axis depends on highly regulated secretion of LH and FSH (Sisk and Foster, 2004). I therefore asked whether the reproductive phenotype of mGluR5 mutants was due to an altered LH and FSH secretion. In order to do this, I examined serum LH and FSH levels at three different time points, respectively at P30, P32 and P34 in wt, mGluR5 +/- and mGluR5 -/- female mice littermates, *i.e.* when reproductive age is already established in wild type females (Mayer et al., 2010). In order to have a complete profiling of the pituitary secretory function in the absence of the mGluR5 gene, I concomitantly measured the other pituitary hormones ACTH, prolactin, TSH and GH.

Serum levels of LH (fig.3.19.A) were not significantly altered in mGluR5 +/- (P30: 82,79 ± 12,97 pg/ml p=0,26. P32: 77,68 ± 16,75 pg/ml; p=0,7605. P34: 112,4 ± 20,35; p=0,447) and mGluR5 -/- (P30: 62,29 ± 7,4 pg/ml; p=0,56. P32: 83,68 ± 11,43 pg/ml; p=0,43. P34: 81,68 ± 14,12 pg/ml; p=0,65) with respect to wt (P30: 71,51 ± 10,52 pg/ml. P32: 71,39 ± 9,373 pg/ml. P34: 91,79 ± 16,24 pg/ml) from P30 to P34 (fig.3.19.A). FSH (fig.3.19.B) was also similar in mGluR5 +/- (P30: 226,7 ±

36,85 pg/ml; p=0,17. P32: 195,9 ± 17,16 pg/ml; p=0,52) and mGluR5 -/- (P30: 175,3 ± 15,55 pg/ml; p=0,93. P32: 204,6 ± 32,05 pg/ml; p=0,5) with respect to wt (P30: 173,2 ± 15,78 pg/ml. P32: 178,2 ± 20,74 pg/ml) in P30 and P32. Conversely, FSH levels dropped to a significant ≈ 50% reduction in mGluR5 -/- at P34 (134,9 ± 11,08 pg/ml) when compared to wt female mice (232,1 ± 26,38 pg/ml; **: p<0,01).

FSH serum concentration appeared significantly reduced between P32 and P34 in the -/- group as well (*: p<0,05). In contrast, mGluR5 +/- serum FSH concentration at P34 (297 ± 91,41 pg/ml; p=0,5) was very similar to wt. Summarizing, I found an age-related reduction in serum FSH concentration at P34 in female mice with homozygous mutation.

By opposite, TSH was increased significantly at P30 (104,9 ± 16,04 pg/ml; *: p<0,05) and P34 (153,7 ± 27,63 pg/ml; p<0,05) in mGluR5 -/- and nearly significant at P32 (173,7 ± 39,95; p=0,0503) respect to wild type females (P30: 56,86 ± 10,42 pg/ml; P32: 80,88 ± 12,08 pg/ml; P34: 78,55 ± 16,69 pg/ml ; fig.3.20.A).

Homozygous mGluR5 KO mutation did not affect GH serum concentration (P30: p=0,6; P32: p=0,37; P34: p=0,34), although heterozygous mGluR5 KO female displayed significant increase at P34 (mGluR5 -/-: 6870 ± 1477 pg/ml vs wt: 3173 ± 722,6 pg/ml; *: p<0,05; fig. 3.20.B).

ACTH was poorly present in serum, as the max concentration was < 25 pg/ml, as reported in figure 3.21.A. However, ACTH dropped significantly in wt from P30 (15,41 ± 1,593 pg/ml) to P32 (6,415 ± 1,754 pg/ml; **: p<0,01), but was not altered in mGluR5 mutants. Only at P34, mGluR5 +/- females had tendentially lower serum ACTH levels than wild type females (p=0,077). Prolactin was not affected as well in mGluR5 mutants (fig.3.21.B).

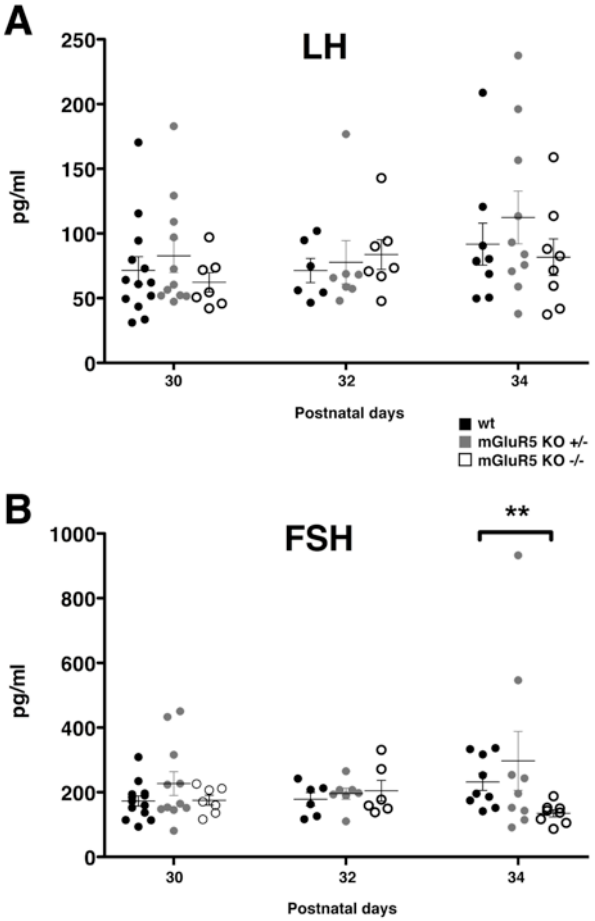

Figure 3.19 Serum levels of gonadotropins in pg/ml in wild type (wt), mGluR5 -/- KO and mGluR5 +/- KO female mice. at 30, 32 and 34 days old of age. A: luteinizing hormone (LH). B: follicle-stimulating hormone (FSH). Groups are displayed as scattered plots representing each sample and mean ± S.E.M. Student's t test: *: p<0,05; **: p<0,01; ***: p<0,001. LH: P30: n=13 wt, n=11 +/-, n=7 -/-. P32: n=6 wt, n=7 +/-, n=7 -/-. P34: n=9 wt, n=10 +/-, n=8 -/-. FSH: P30: n=13 wt, n=11 +/-, n=7 -/-. P32: n=6 wt, n=7 +/-, n=6 -/-. P34: n=9 wt, n=9 +/-, n=8 -/-.

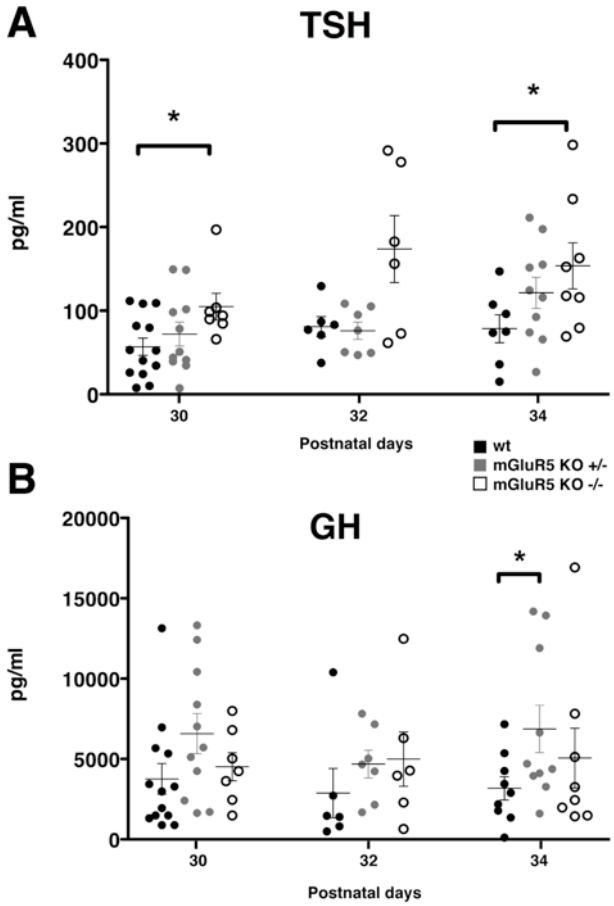

Figure 3.20 Serum levels of A: thyroid-stimulating hormone (TSH) and B: growth hormone (GH) in pg/ml. in wild type (wt), mGluR5 +/- and mGluR5 -/- females of 30, 32 and 34 days old. Groups are displayed as scattered plots representing each sample and mean ± S.E.M. Student's t test : *: $p<0,05$; **: $p<0,01$; ***: $p<0,001$. TSH: P30: n=13 wt, n=11 +/-, n=7 -/-. P32: n=6 wt, n=7 +/-, n=6 -/-. P34: n=7 wt, n=10 +/-, n=8 -/-. GH: P30: n=13 wt, n=11 +/-, n=7 -/-. P32: n=6 wt, n=7 +/-, n=6 -/-. P34: n=9 wt, n=10 +/-, n=8 -/-.

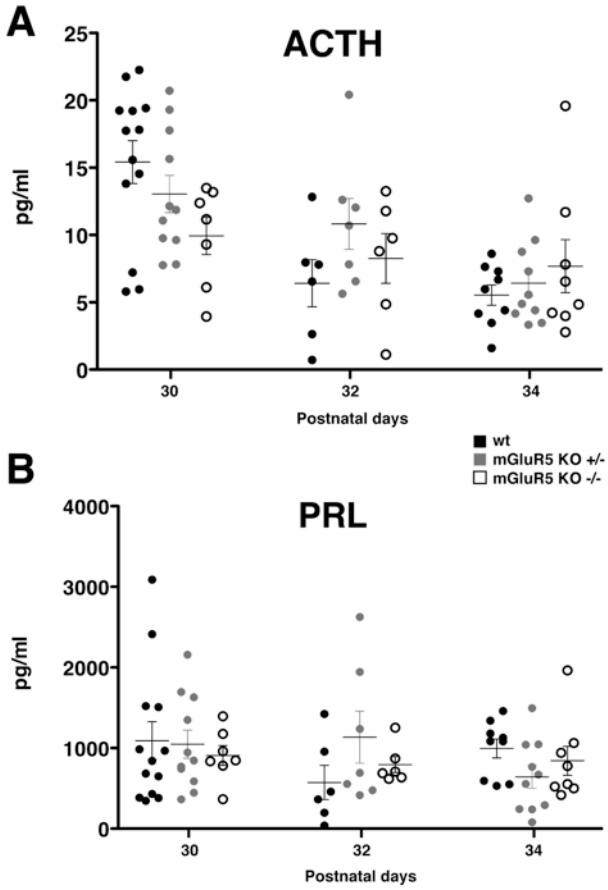

Figure 3.21 Serum levels of adrenocorticotropic hormone (ACTH) and prolactin (PRL) in pg/ml. in wild type (wt), mGluR5 +/- and mGluR5 -/- females of 30, 32 and 34 days old. Groups are displayed as scattered plots representing each sample and mean ± S.E.M. Student's t test: *: $p<0,05$; **: $p<0,01$; ***: $p<0,001$. ACTH: P30: n=13 wt, n=11 +/-, n=7 -/-. P32: n=6 wt, n=7 +/-, n=6 -/-. P34: n=9 wt, n=10 +/-, n=8 -/-. PRL: P30: n=13 wt, n=11 +/-, n=7 -/-. P32: n=6 wt, n=7 +/-, n=6 -/-. P34: n=9 wt, n=10 +/-, n=8 -/-.

4 Discussion

4.1 Characterization of the GnRHR network within the PAG of the female

In this study it was employed for the first time a genetically defined approach to study the GnRH network in the central nervous system, in order to investigate the postulates implicating that GnRH plays a determinant function in sexual receptivity. The traditional model establishes that the hormonal feedback from the gonads, driven by the GnRH-dependent gonadotropins release, is responsible for the neural modulation of sexual behavior (Ferrero and Liberles, 2013; Pfaff and Sakuma, 1979a; Pfaus et al., 2003; Yang et al., 2013). Several studies also proposed a direct, together with the indirect, role of GnRH as a neuromodulator in sexual behavior, selectively in the PAG (Meredith, 1998; Meredith and Howard, 1992; Saito and Moltz, 1986; Sakuma and Pfaff, 1980c), introducing GnRH as a main integrator of sexual communication by tuning behavioral responses with reproduction. However, these classical models were largely incomplete, due to technical limitations at different levels. For example, brain lesions and electrical stimulations employed in these studies indiscriminately targeted the whole pool of neuronal populations, leading to an imprecise functional mapping. Moreover, GnRH administrations prevented the characterization of the endogenous GnRH. Previous attempts to identify the neural targets of GnRH by characterizing the GnRHR expression in the brain were hampered by aberrant expression of the transgenic constructs employed (Granger et al., 2004).

The GnRHR-IRES-Cre/eR26-τGFP and GnRHR-IRES-Cre/R26-YFP mouse lines enabled the reliable visualization of GnRHR cells, unveiling the neural targets of GnRH in addition to gonadotropes in the pituitary. Previous work on these mouse lines already showed direct neural modulation by GnRH in synchrony with the estrus cycle (Schauer et al., 2015). This binary genetic approach offered the possibility to manipulate the GnRHR network *in vivo* with genetic, temporal and spatial definition and without interfering with the hpg axis.

In the present study I used a combinatorial approach to *functionally* describe the GnRHR network within the periaqueductal gray of the female mouse: I first visualized the GnRHR-IRES-Cre/eR26-τGFP female midbrain then by cre-dependent AAV delivery into the PAG I visualized adult GnRHR expression, then induced GnRHR neuron ablation. In this way, I could affect the PAG network in the adult female and study the effect on sexual behavior.

4.1.1 Age-dependent increase of GnRHR neurons in the female midbrain

I characterized the distribution of GnRHR neurons in the PAG by visualizing τGFP neurons in the adult, intact GnRHR-IRES-Cre/eR26-τGFP female mouse. This allowed me to identify regions with higher GnRHR neuron density, in order to achieve more efficient manipulation. GnRHR neurons in the midbrain of the 10 wo female were present in the DM, DL/LPAG and superior colliculus mainly, whereas in the VLPAG and inferior colliculus GnRHR neurons were poorly distributed. This pattern of distribution is similar to previously described distribution in the midbrain of the male GnRHR-IRES-Cre/eR26-τGFP mouse (Wen et al., 2011). Other than scattered, GnRHR neurons in the midbrain have stereotyped, well-defined patterns of distribution that are similar in males and females.

Unexpectedly, older 19 wo females showed higher distribution, suggesting an age-dependent increase in GnRHR neurons within the midbrain, which occurs in the adulthood within a relatively short period of time. This effect was observed in the superior colliculus and, within the PAG, only in DMPAG, DL/LPAG, but not in the VLPAG, *i.e.* the areas containing more GnRHR neurons within the midbrain in younger females. Compared to the embryonic onset of GnRH expression and functional peptide (Wray et al., 1989; Wu et al., 1997) and pituitary GnRHR expression (Wen et al., 2010), the neuronal GnRHR onset is dramatically delayed at postnatal day 16. This late onset in the appearing of GnRHR expression in neurons in the adult could be caused by a neuron-specific restraining mechanism to achieve GnRH sensitivity only in the adult, probably through tissue-specific regulation. Heterologous expression studies reported that *cis*-elements within the GnRHR promoter (Granger et al., 2004) could direct brain GnRHR expression, probably through Steroidogenic factor 1 (SF-1) or the LIM-homeodomain factor Lhx5 which

are important in shaping the development of the VMH and hippocampus, respectively (Ikeda et al., 1995; Zhao et al., 1999), as well as and for GnRHR promoter activity in the pituitary (Granger et al., 2004). However, the early role of these transcriptional factors cannot solely explain the adult onset of GnRHR expression.

Which factors could then contribute to the increase in sensitivity to GnRH? These observations indicates that prominent increase occurs within the reproductive age of the females, suggesting that the estrus cycle could set the priming to GnRH sensitivity. In the pituitary gland, the GnRHR mRNA is up regulated upon ovulation, in the morning of the proestrus (Bauer-Dantoin et al., 1993), and is strongly down regulated in OVX females, although with mechanisms independent from the classical estradiol pathways (Couse et al., 2003).

Should be considered that the current observations are based on τGFP visualization, which does not follow fluctuations in GnRHR expression. Whereas τGFP neurons increase, it could be the case that GnRHR expression is cyclically suppressed, leading not to an overall increased GnRH sensitivity, but an "alternated" GnRH sensitivity within the PAG.

Similar phenomena of adult onset were also identified concerning pheromone detection. Interestingly, recent evidence indicates that the production of some members of a family of sexually relevant peptide-derived pheromones is strikingly related to age, having "juvenile" specific (such ESP22) and adult specific (ESP24) pheromones (Ferrero et al., 2013). The juvenile pheromone ESP22 indeed, has an inhibitory effect of adult males towards juvenile mice. Retaining this logical view, it is likely the process that primes the brain for sex could also be restrained until fertility is established by an evolutionary selected mechanism.

4.1.2 Absence of GnRH fibers from the PAG of the mouse

Previous studies identified long-distance GnRH projections in the PAG of the female rat (Merchenthaler et al., 1984). In mice, however, GnRH fibers don't reach the midbrain but are limited to the amygdala, thalamus, BNST and hypothalamus (Boehm et al., 2005). I examined GnRH signal in the PAG of the GnRHR-IRES-

Cre/eR26-τGFP female, to assess whether GnRH directly contacts GnRHR neurons in the PAG. As expected, GnRH fibers were completely absent from the PAG at a coordinate of a high density of GnRHR-dependent τGFP somata and fibers, confirming that in female mice GnRH neurons don't make long-distance projections to the midbrain, nor directly contact GnRHR neurons at their somata or projections at the level of the PAG.

This result supports the hypothesis that GnRH could be sensed through the vasculature or the cerebrospinal fluid. Previous studies in ewes showed that GnRH pulse propagates from the hypophyseal portal vasculature in the cerebrospinal fluid, with a time lapse in between within minutes (Caraty and Skinner, 2008). However, recent characterization of hypothalamic GnRHR neurons in GnRHR-IRES-Cre/eR26-τGFP showed that GnRHR neuron fibers form both close appositions with blood capillaries and GnRH fibers (Schauer et al., 2015). Whether GnRH could be sensed through the cerebrospinal fluid, would be through a "volume transmission" to all the GnRHR expressing neurons present in the brain (Caraty and Skinner, 2008). However, τGFP does not reflect the exact localization of the functional GnRHR protein; given this, is not possible however to exclude that PAG GnRHR neurons form long distance projections towards GnRH terminals-containing areas, where the functional receptor could putatively be localized.

4.1.3 The neuronal GnRHR as a parallel GnRH feedback within the PAG

The peak in estradiol prior to ovulation primes the brain for sexual arousal through ERα neurons within the VMH. Concomitantly, feedbacks mediated by estradiol triggers GnRH release that in turn potentiates lordosis behavior, acting on the periaqueductal gray. These two events mediated by estradiol may act synergistically to switch neuronal circuits towards a sexual arousal state, as hypothesized before (Saito and Moltz, 1986). The presence of ERα neurons in the PAG suggests an additional level of regulation by estradiol (Loyd and Murphy, 2008). The visualization of GnRHR neurons in the female midbrain by genetic τGFP labeling in the GnRHR-IRES-Cre/eR26-τGFP led me to investigate how the ERα and GnRHR patterns are related to each other. To do this, I visualized co-expression of τGFP and

ERα in the PAG of a GnRHR-IRES-Cre/eR26-τGFP female. GnRHR neurons and ERα cells are clustered within the same neural circuit but they are not co-expressed within the same neuron. This result showed for the first time that estradiol and GnRH could act in parallel at the periaqueductal gray to modulate PAG neural activity, and that genomic estradiol and GnRHR can be independently regulated. Given this, ERα is unlikely a candidate that drives the shaping of the GnRHR network in the adult female. This is also consistent with the phenotype of global ERαKO mice, in which pituitary GnRHR gene expression is unaffected (Couse et al., 2003).

An important role in sexual arousal is played by the nitric oxide (NO), synthesized by neurons that express the neuronal isoform nitric oxide synthase (nNOS) enzyme (Mani et al., 1994). These neurons are found clustered in the LDTg, a nuclei at the ventral surface of the IV ventricle, which is involved in the modulation of sexual behavior in female and male rats (Shimura and Shimokochi, 1990; Yamanouchi and Arai, 1985). GnRHR neurons form an independent network in the LDTg and CTg but are poorly expressed in the nearby DR. Together, these data show that GnRHR neurons are preferentially present within sexually-relevant neural circuits and exhibit a parallel anatomical organization with respect to nNOS neurons.

4.1.4 Is GnRH in the PAG necessary to the induction of female sexual receptivity?

The PAG plays a major role in modulating hormone-dependent sexual receptivity in females (Sakuma and Pfaff, 1979). Furthermore, GnRH injections in the dorsal PAG could positively modulate lordosis in OVX estradiol-primed female rats, whether anti GnRH globulin, a GnRH antagonist, disrupts sexual receptivity (Sakuma and Pfaff, 1980c). Studies on mice were inconclusive whether GnRH is necessary to lordosis, due to employment of a mouse model presenting a global loss of GnRH. I then aimed to test whether a selective loss of GnRH sensitivity within the dorsal PAG could affect lordosis, by ablating the local GnRHR neurons. I did not employed GnRH administration in order to understand the role of endogenous GnRH. Preliminary data revealed broad mCherry expression in the dorsal PAG neurons of the adult GnRHR-IRES-Cre female, indicating that those neurons do express significant levels of the GnRHR gene. Ovaries removal (OVX) resulted the best strategy to reliably induce

sexual receptivity in rodents, by dissociating it from the estrus cycle. OVX disrupts the estradiol and progesterone feedbacks and required replacement of continuous estradiol and acute progesterone to induce receptivity. This procedure did not affect the distribution of GnRHR neurons in controls, showing a robust GnRHR network.

Comparison between lordosis responses and rejective responses in controls revealed a mutually exclusive relationship, consistently with previous findings that show lordosis arising from an ERα-dependent suppression of rejective behavior towards the male (Musatov et al., 2006). Ablation of GnRHR neurons in the dorsal PAG did not affect lordosis behavior, either receptivity in general, as shown by the multiple intromissions from the males observed. Rather, GnRHR-ablated display strong lordosis behavior. Given that dorsal PAG is central in the sexual response in rats, and rapid response was elicited with focal GnRH injections, it was expected that a focal ablation of GnRHR neurons could produce a change in the lordosis response.

However, I could not find any genetic evidence in the support on this model. It seems more likely that GnRH in the brain could have a facilitating rather than crucial, permissive role in female receptivity.

4.1.5 Activity patterns in the PAG following female sexual behavior, but not in GnRHR neurons

The genetically-defined method used in this study to dissect the GnRH network failed to support the classic postulates of an essential role of GnRH in sexual behavior *in vivo*. I used then a strategy based on fluorescent visualization of neural activity to assess if GnRHR neurons in the PAG participate to sexual behavior. The early gene c-fos expression was found to be dependent on high neural activity (Dragunow and Faull, 1989), and became a reliable probe of neural activity following behavioral performances in animal models (Cruz et al., 2013). Although DMPAG and LPAG simultaneously activate during sexual behavior, the GnRHR neurons present in those area didn´t up regulate c-fos expression during female sexual behavior, indicating no considerable underlying neural activity. Nearby cells instead, strongly up-regulated c-fos. Moreover, c-fos up-regulation negatively correlates with sexual receptivity only in DMPAG and DL/LPAG subdivisions, collectively the dorsal PAG. This

correlation study suggests that in less receptive females c-fos up-regulation may be consequent of some other behavior. Nevertheless, GnRHR ablation neurons was mostly in the DMPAG, and correlated with a tendentially reduced rejective behavior. Rejections are mutually exclusive respect to lordosis, and an ERα-dependent neural switch within the VMH positively modulates behavior towards receptivity rather then rejections in females (Musatov et al., 2006). In males, ERα neurons in the VMHvl could both coordinate aggression and mounting behavior (Lee et al., 2014). The VMHvl-dorsal PAG pathway has also been implicated in processing fear of conspecifics (Silva et al., 2013), indicating multiple overlapping behavioral outcomes arising from the same pathways.

The genetic evidence that GnRH neurons are wired to vomeronasal pathways (Boehm, 2006) suggests the involvement of GnRH in the behavioral response to individual recognition, in addition to an endocrine response. Although GnRH was found not to have a role in mediating sexual preference (Dudley and Moss, 1985), in fishes a segregated subpopulation of neurons expressing GnRH-III facilitates copulation by mediating partner familiarization (Okuyama et al., 2014). Consistent with this, GnRH could have an earlier role in the processing of the recognition of the male, being than released prior to sexual behavior activation, promoting receptivity by the suppressing of the rejective responses. GnRH could provide further regulatory priming towards a behavioral selection among the vast repertoire within the neural circuits that modulate instinctual behavioral responses necessary for social interactions.

4.2 mGluR5, a novel molecule in puberty onset

mGluR5 -/- KO female mice exhibit severe infertility phenotype whereas mGluR5 +/- KO mutants exhibit only a slight reduction in litter size. Moreover, mGluR5 -/- KO exhibit delayed vaginal opening and first estrus as well as a reduced ovarian growth together with an impairment of the estrus cycle. Pituitary hormones analysis revealed a selective reduction in FSH and no changes in LH serum levels in the peripubertal age only in mGluR5 -/- KO mutants, however with a concomitant increase in TSH. This phenotype strongly suggests impairment in the onset and progression of puberty by a reduced release in FSH. Importantly, this phenotype requires an homozygous

loss of function of the mGluR5 gene, since +/- mGluR5 KO females show unaltered maturation of the hpg axis, although with a reduction in litter size. It is ignored whether deregulated TSH could be due to the global loss of mGluR5 (therefore involving all tissues), or to a specific interaction between FSH and TSH. This can be addressed only by conditional mGluR5 KO.

Puberty consists in the activation of the hpg axis and the entering in the reproductive age (Sisk and Foster, 2004). Although the main candidate for the central regulation of puberty onset is kisspeptin and its receptor GPR54, it was shown that female with chronic genetic ablation of kisspeptin neurons are fertile, suggesting a compensatory mechanism (Mayer and Boehm, 2011). Glutamate inputs to GnRH neurons were reported as well as the expression of NMDA receptors on GnRH neurons (Iremonger et al., 2010). Importantly, studies on the metabotropic glutamate receptor 1 (mGluR1) revealed a role in regulating GnRH neurons excitability (Chu and Moenter, 2005) and identified two distinct GnRH neurons subpopulation based on the selective responsiveness to kisspeptin or to a mGluR1 agonist (Dumalska et al., 2008). This model proposed a parallel feedback onto GnRH neurons by kisspeptin and glutamate. However, so far there was no evidence of a role of metabotropic glutamate receptors in the regulation of puberty. In particular, mGluR5 could lead to a preferential regulation of the synthesis and/or secretion of FSH instead of LH.

Together with Dr.Ioana Inta, we first described an involvement of a metabotropic glutamate receptor subtype in the regulatory mechanisms of puberty and fertility. Further experiments will aim to delineate the effects of glutamate exerted by mGluR5. Phenotype and hormonal levels will be also analyzed in females mice lacking the NMDA receptor NR2A subunit (NR2A KO) will be performed, in order to examine the role of NMDA receptor in puberty and fertility.

These findings could contribute to the growing information in the genetics of puberty and the mechanisms that regulate fertility (Boehm et al., 2015), and could help to develop new effective treatments for puberty disorders.

4.3 Future experiments

4.3.1 Further investigation of the brain GnRHR system

The present study provides new insights in the knowledge of the GnRHR network in the brain. First, it revealed an adult-restricted establishment of GnRH responsive neurons in midbrain areas. Next experiments will provide complete information about the whole female brain, to investigate whether this phenomenon is extended to the rest of the brain or is restricted only to a subset of nuclei. Moreover, is unknown whether a post-pubertal increase of GnRHR neurons occurs also in males. Next experiments will aim to address these questions in age-matched mice.

As previously shown, ovariectomy induces a decrease in the GnRHR gene expression in the pituitary. Reliable visualization of the GnRHR expression in neurons will allow understanding whether the feedback from the ovaries is required for the shaping of the GnRHR network, by analyzing the GnRHR neurons map in OVX females at different ages.

Combining different strategies to either ablate or examine activation of GnRHR neurons revealed that GnRHR neurons do not participate in the induction of sexual behavior in females. These findings brought into question an entire field of research that states GnRH as a main trigger of lordosis execution. Further experiments are needed to elucidate the functional role of GnRH in the brain.

Subsequent examinations need to address an involvement of GnRHR neurons in processing odor information, by using the activity marker c-fos. Moreover, it will be tested the ability of systemic GnRH injections to trigger GnRHR neurons activation or to facilitate lordosis in females where GnRHR neurons in the dorsal PAG were previously ablated. Moreover, cre-dependent optogenetic tools will be stereotaxically delivered into the dorsal PAG of GnRHR-IRES-Cre and/or GnRHR-IRES-Cre/eR26-τGFP females to stimulate or inhibit GnRHR neurons during sexual intercourse using light.

5 Summary

To determine whether GnRH signaling is needed in the PAG to the display in lordosis in mice, I visualized and specifically ablated the GnRHR neurons in the dorsal PAG of GnRHR-IRES-Cre/eR26-τGFP females. Females with GnRHR neurons ablation within the dorsal PAG exhibit a strong lordosis behavior undistinguishable from controls, indicating that neurons downstream to GnRH in the dorsal PAG are not required for lordosis behavior. Moreover, up regulation of neural activity within the PAG evidenced by c-fos analysis following sexual behavior did not involve fluorescently labeled GnRHR neurons. These results are in sharp contrast with the established paradigm that proposes GnRH as a central molecule in the modulation of sexual receptivity, as a neurotransmitter.

Characterization of the GnRHR network in the PAG of the female mouse revealed a post pubertal, adult age-dependent establishment of a GnRHR network within the midbrain. GnRHR neurons form a non-overlapping neural network together with hormone-related neuronal populations, such as ERα and nNOS neurons, suggesting parallel permissive hormonal cues within these neural circuits. However, the role of GnRHR neurons in the brain remains unknown and requires further characterization.
The GnRHR-IRES-Cre/eR26-τGFP model revealed to be extremely useful for characterization at different reproductive stages within the pituitary. In the present study has been successfully employed for the characterization in the brain *in vivo*. The use of cre-driven genetic tools will allow the further characterization of the function of GnRHR neurons in reproductive behavior.

The combination of a genetic knockout strategy and a method to measure simultaneously the whole pool of pituitarian hormones allowed me to identify an exact time point in which the mGluR5 is involved in the regulation of FSH release, but not of LH, that correlates with delayed puberty and impaired fertility. The next step will aim to clarify the level of the hpg axis in which the mGluR5 is involved. However, the generation of a conditional knock out mouse strain for the mGluR5 gene is necessary the specificity of the mGluR5-mediated effect on the release of FSH. Nevertheless, simultaneous hormonal measurement protocol is an extremely useful tool that provides full information about pituitary hormone fluctuations, thus

allowing improved description and correlation between the distinct hormonal systems.

6 Bibliography

Alim, Z., Hartshorn, C., Mai, O., Stitt, I., Clay, C., Tobet, S., and Boehm, U. (2012). Gonadotrope plasticity at cellular and population levels. Endocrinology *153*, 4729-4739.

Arendash, G.W., and Gorski, R.A. (1983). Suppression of lordotic responsiveness in the female rat during mesencephalic electrical stimulation. Pharmacology, biochemistry, and behavior *19*, 351-357.

Atasoy, D., Aponte, Y., Su, H.H., and Sternson, S.M. (2008). A FLEX switch targets Channelrhodopsin-2 to multiple cell types for imaging and long-range circuit mapping. The Journal of neuroscience : the official journal of the Society for Neuroscience *28*, 7025-7030.

Baba, Y., Matsuo, H., and Schally, A.V. (1971). Structure of the porcine LH- and FSH-releasing hormone. II. Confirmation of the proposed structure by conventional sequential analyses. Biochemical and biophysical research communications *44*, 459-463.

Bakker, J., Honda, S., Harada, N., and Balthazart, J. (2002). The aromatase knock-out mouse provides new evidence that estradiol is required during development in the female for the expression of sociosexual behaviors in adulthood. The Journal of neuroscience : the official journal of the Society for Neuroscience *22*, 9104-9112.

Bandler, R., and Shipley, M.T. (1994). Columnar organization in the midbrain periaqueductal gray: modules for emotional expression? Trends in neurosciences *17*, 379-389.

Bauer-Dantoin, A.C., Hollenberg, A.N., and Jameson, J.L. (1993). Dynamic regulation of gonadotropin-releasing hormone receptor mRNA levels in the anterior pituitary gland during the rat estrous cycle. Endocrinology *133*, 1911-1914.

Beitz, A.J., and Shepard, R.D. (1985). The midbrain periaqueductal gray in the rat. II. A Golgi analysis. The Journal of comparative neurology *237*, 460-475.

Bingel, A.S. (1974). Timing of LH release and ovulation in 4- and 5-day cyclic mice. Journal of reproduction and fertility *40*, 315-320.

Boehm, U. (2006). The vomeronasal system in mice: from the nose to the hypothalamus- and back! Seminars in cell & developmental biology *17*, 471-479.

Boehm, U., Bouloux, P.M., Dattani, M.T., de Roux, N., Dode, C., Dunkel, L., Dwyer, A.A., Giacobini, P., Hardelin, J.P., Juul, A.*, et al.* (2015). Expert consensus document: European Consensus Statement on congenital hypogonadotropic hypogonadism--pathogenesis, diagnosis and treatment. Nature reviews Endocrinology *11*, 547-564.

Boehm, U., Zou, Z., and Buck, L.B. (2005). Feedback loops link odor and pheromone signaling with reproduction. Cell *123*, 683-695.

Boyd, S.K., and Moore, F.L. (1985). Luteinizing hormone-releasing hormone facilitates the display of sexual behavior in male voles (Microtus canicaudus). Hormones and behavior *19*, 252-264.

Brock, O., Baum, M.J., and Bakker, J. (2011). The development of female sexual behavior requires prepubertal estradiol. The Journal of neuroscience : the official journal of the Society for Neuroscience *31*, 5574-5578.

Bronson, F.H., and Whitten, W.K. (1968). Oestrus-accelerating pheromone of mice: assay, androgen-dependency and presence in bladder urine. Journal of reproduction and fertility *15*, 131-134.

Caligioni, C.S. (2009). Assessing reproductive status/stages in mice. Current protocols in neuroscience / editorial board, Jacqueline N Crawley [et al] *Appendix 4*, Appendix 4I.

Campos, P., and Herbison, A.E. (2014). Optogenetic activation of GnRH neurons reveals minimal requirements for pulsatile luteinizing hormone secretion. Proceedings of the National Academy of Sciences of the United States of America *111*, 18387-18392.

Candlish, M., De Angelis, R., Gotz, V., and Boehm, U. (2015). Gene Targeting in Neuroendocrinology. Comprehensive Physiology *5*, 1645-1676.

Canteras, N.S., Simerly, R.B., and Swanson, L.W. (1994). Organization of projections from the ventromedial nucleus of the hypothalamus: a Phaseolus vulgaris-leucoagglutinin study in the rat. The Journal of comparative neurology *348*, 41-79.

Caraty, A., and Skinner, D.C. (2008). Gonadotropin-releasing hormone in third ventricular cerebrospinal fluid: endogenous distribution and exogenous uptake. Endocrinology *149*, 5227-5234.

Cardin, J.A., Carlen, M., Meletis, K., Knoblich, U., Zhang, F., Deisseroth, K., Tsai, L.H., and Moore, C.I. (2009). Driving fast-spiking cells induces gamma rhythm and controls sensory responses. Nature *459*, 663-667.

Charlton, H. (2004). Neural transplantation in hypogonadal (hpg) mice - physiology and neurobiology. Reproduction *127*, 3-12.

Chu, A., Zhu, L., Blum, I.D., Mai, O., Leliavski, A., Fahrenkrug, J., Oster, H., Boehm, U., and Storch, K.F. (2013). Global but not gonadotrope-specific disruption of Bmal1 abolishes the luteinizing hormone surge without affecting ovulation. Endocrinology *154*, 2924-2935.

Chu, Z., and Moenter, S.M. (2005). Endogenous activation of metabotropic glutamate receptors modulates GABAergic transmission to gonadotropin-releasing hormone neurons and alters their firing rate: a possible local feedback circuit. The Journal of neuroscience : the official journal of the Society for Neuroscience *25*, 5740-5749.

Clark, J.A., Flick, R.B., Pai, L.Y., Szalayova, I., Key, S., Conley, R.K., Deutch, A.Y., Hutson, P.H., and Mezey, E. (2008). Glucocorticoid modulation of tryptophan hydroxylase-2 protein in raphe nuclei and 5-hydroxytryptophan concentrations in frontal cortex of C57/Bl6 mice. Molecular psychiatry *13*, 498-506.

Clarkson, J., d'Anglemont de Tassigny, X., Colledge, W.H., Caraty, A., and Herbison, A.E. (2009). Distribution of kisspeptin neurones in the adult female mouse brain. J Neuroendocrinol *21*, 673-682.

Couse, J.F., Yates, M.M., Walker, V.R., and Korach, K.S. (2003). Characterization of the hypothalamic-pituitary-gonadal axis in estrogen receptor (ER) Null mice reveals hypergonadism and endocrine sex reversal in females lacking ERalpha but not ERbeta. Molecular endocrinology *17*, 1039-1053.

Cruz, F.C., Koya, E., Guez-Barber, D.H., Bossert, J.M., Lupica, C.R., Shaham, Y., and Hope, B.T. (2013). New technologies for examining the role of neuronal ensembles in drug addiction and fear. Nature reviews Neuroscience *14*, 743-754.

d'Anglemont de Tassigny, X., Fagg, L.A., Dixon, J.P., Day, K., Leitch, H.G., Hendrick, A.G., Zahn, D., Franceschini, I., Caraty, A., Carlton, M.B.*, et al.* (2007). Hypogonadotropic hypogonadism in mice lacking a functional Kiss1 gene. Proceedings of the National Academy of Sciences of the United States of America *104*, 10714-10719.

Daniels, D., Miselis, R.R., and Flanagan-Cato, L.M. (1999). Central neuronal circuit innervating the lordosis-producing muscles defined by transneuronal transport of pseudorabies virus. The Journal of neuroscience : the official journal of the Society for Neuroscience *19*, 2823-2833.

de Roux, N., Genin, E., Carel, J.C., Matsuda, F., Chaussain, J.L., and Milgrom, E. (2003). Hypogonadotropic hypogonadism due to loss of function of the KiSS1-derived peptide receptor GPR54. Proceedings of the National Academy of Sciences of the United States of America *100*, 10972-10976.

de Roux, N., Young, J., Misrahi, M., Genet, R., Chanson, P., Schaison, G., and Milgrom, E. (1997). A family with hypogonadotropic hypogonadism and mutations in the gonadotropin-releasing hormone receptor. The New England journal of medicine *337*, 1597-1602.

Devall, A.J., and Lovick, T.A. (2010). Differential activation of the periaqueductal gray by mild anxiogenic stress at different stages of the estrous cycle in female rats.

Neuropsychopharmacology : official publication of the American College of Neuropsychopharmacology *35*, 1174-1185.

DiBenedictis, B.T., Ingraham, K.L., Baum, M.J., and Cherry, J.A. (2012). Disruption of urinary odor preference and lordosis behavior in female mice given lesions of the medial amygdala. Physiology & behavior *105*, 554-559.

Dragunow, M., and Faull, R. (1989). The use of c-fos as a metabolic marker in neuronal pathway tracing. Journal of neuroscience methods *29*, 261-265.

Dudley, C.A., and Moss, R.L. (1985). LHRH and mating behavior: sexual receptivity versus sexual preference. Pharmacology, biochemistry, and behavior *22*, 967-972.

Dulac, C., and Kimchi, T. (2007). Neural mechanisms underlying sex-specific behaviors in vertebrates. Current opinion in neurobiology *17*, 675-683.

Dumalska, I., Wu, M., Morozova, E., Liu, R., van den Pol, A., and Alreja, M. (2008). Excitatory effects of the puberty-initiating peptide kisspeptin and group I metabotropic glutamate receptor agonists differentiate two distinct subpopulations of gonadotropin-releasing hormone neurons. The Journal of neuroscience : the official journal of the Society for Neuroscience *28*, 8003-8013.

Ferrero, D.M., and Liberles, S.D. (2013). Animal behavior: shifting neural circuits with sex hormones. Current biology : CB *23*, R621-623.

Ferrero, D.M., Moeller, L.M., Osakada, T., Horio, N., Li, Q., Roy, D.S., Cichy, A., Spehr, M., Touhara, K., and Liberles, S.D. (2013). A juvenile mouse pheromone inhibits sexual behaviour through the vomeronasal system. Nature *502*, 368-371.

Floody, O.R., and DeBold, J.F. (2004). Effects of midbrain lesions on lordosis and ultrasound production. Physiology & behavior *82*, 791-804.

Fortune, J.E. (2003). The early stages of follicular development: activation of primordial follicles and growth of preantral follicles. Animal reproduction science *78*, 135-163.

Gotti, S., Sica, M., Viglietti-Panzica, C., and Panzica, G. (2005). Distribution of nitric oxide synthase immunoreactivity in the mouse brain. Microscopy research and technique *68*, 13-35.

Granger, A., Ngo-Muller, V., Bleux, C., Guigon, C., Pincas, H., Magre, S., Daegelen, D., Tixier-Vidal, A., Counis, R., and Laverriere, J.N. (2004). The promoter of the rat gonadotropin-releasing hormone receptor gene directs the expression of the human placental alkaline phosphatase reporter gene in gonadotrope cells in the anterior pituitary gland as well as in multiple extrapituitary tissues. Endocrinology *145*, 983-993.

Haga, S., Hattori, T., Sato, T., Sato, K., Matsuda, S., Kobayakawa, R., Sakano, H., Yoshihara, Y., Kikusui, T., and Touhara, K. (2010). The male mouse pheromone ESP1 enhances female sexual receptive behaviour through a specific vomeronasal receptor. Nature *466*, 118-122.

Halem, H.A., Cherry, J.A., and Baum, M.J. (2001). Central forebrain Fos responses to familiar male odours are attenuated in recently mated female mice. The European journal of neuroscience *13*, 389-399.

Hardy, D.F., and Debold, J.F. (1971). Effects of mounts without intromission upon the behavior of female rats during the onset of estrogen-induced heat. Physiology & behavior *7*, 643-645.

Herbison, A.E. (2015). Gonadotropin-releasing hormone neuronal network. In Knobil and Neill's Physiology of Reproduction, 4th edition, pp. 399-467.

Herde, M.K., Geist, K., Campbell, R.E., and Herbison, A.E. (2011). Gonadotropin-releasing hormone neurons extend complex highly branched dendritic trees outside the blood-brain barrier. Endocrinology *152*, 3832-3841.

Herde, M.K., Iremonger, K.J., Constantin, S., and Herbison, A.E. (2013). GnRH neurons elaborate a long-range projection with shared axonal and dendritic functions. The Journal of neuroscience : the official journal of the Society for Neuroscience *33*, 12689-12697.

Hubscher, C.H., Brooks, D.L., and Johnson, J.R. (2005). A quantitative method for assessing stages of the rat estrous cycle. Biotechnic & histochemistry : official publication of the Biological Stain Commission *80*, 79-87.

Ikeda, Y., Luo, X., Abbud, R., Nilson, J.H., and Parker, K.L. (1995). The nuclear receptor steroidogenic factor 1 is essential for the formation of the ventromedial hypothalamic nucleus. Molecular endocrinology *9*, 478-486.

Iremonger, K.J., Constantin, S., Liu, X., and Herbison, A.E. (2010). Glutamate regulation of GnRH neuron excitability. Brain research *1364*, 35-43.

Jemiolo, B., Harvey, S., and Novotny, M. (1986). Promotion of the Whitten effect in female mice by synthetic analogs of male urinary constituents. Proceedings of the National Academy of Sciences of the United States of America *83*, 4576-4579.

Kaiser, U.B., Zhao, D., Cardona, G.R., and Chin, W.W. (1992). Isolation and characterization of cDNAs encoding the rat pituitary gonadotropin-releasing hormone receptor. Biochemical and biophysical research communications *189*, 1645-1652.

Kavanaugh, S.I., Nozaki, M., and Sower, S.A. (2008). Origins of gonadotropin-releasing hormone (GnRH) in vertebrates: identification of a novel GnRH in a basal vertebrate, the sea lamprey. Endocrinology *149*, 3860-3869.

Kim, E.J., Horovitz, O., Pellman, B.A., Tan, L.M., Li, Q., Richter-Levin, G., and Kim, J.J. (2013). Dorsal periaqueductal gray-amygdala pathway conveys both innate and learned fear responses in rats. Proceedings of the National Academy of Sciences of the United States of America *110*, 14795-14800.

Kumar, D., Candlish, M., Periasamy, V., Avcu, N., Mayer, C., and Boehm, U. (2015). Specialized subpopulations of kisspeptin neurons communicate with GnRH neurons in female mice. Endocrinology *156*, 32-38.

Lee, H., Kim, D.W., Remedios, R., Anthony, T.E., Chang, A., Madisen, L., Zeng, H., and Anderson, D.J. (2014). Scalable control of mounting and attack by Esr1+ neurons in the ventromedial hypothalamus. Nature *509*, 627-632.

Leinders-Zufall, T., Brennan, P., Widmayer, P., S, P.C., Maul-Pavicic, A., Jager, M., Li, X.H., Breer, H., Zufall, F., and Boehm, T. (2004). MHC class I peptides as chemosensory signals in the vomeronasal organ. Science *306*, 1033-1037.

Leinders-Zufall, T., Ishii, T., Chamero, P., Hendrix, P., Oboti, L., Schmid, A., Kircher, S., Pyrski, M., Akiyoshi, S., Khan, M.*, et al.* (2014). A family of nonclassical class I MHC genes contributes to ultrasensitive chemodetection by mouse vomeronasal sensory neurons. The Journal of neuroscience : the official journal of the Society for Neuroscience *34*, 5121-5133.

Lohman, R.J., Liu, L., Morris, M., and O'Brien, T.J. (2005). Validation of a method for localised microinjection of drugs into thalamic subregions in rats for epilepsy pharmacological studies. Journal of neuroscience methods *146*, 191-197.

Lombardi, J.R., and Vandenbergh, J.G. (1977). Pheromonally induced sexual maturation in females: regulation by the social environment of the male. Science *196*, 545-546.

Lovick, T.A., and Devall, A.J. (2009). Progesterone withdrawal-evoked plasticity of neural function in the female periaqueductal grey matter. Neural plasticity *2009*, 730902.

Low, K., Aebischer, P., and Schneider, B.L. (2013). Direct and retrograde transduction of nigral neurons with AAV6, 8, and 9 and intraneuronal persistence of viral particles. Human gene therapy *24*, 613-629.

Loyd, D.R., and Murphy, A.Z. (2008). Androgen and estrogen (alpha) receptor localization on periaqueductal gray neurons projecting to the rostral ventromedial medulla in the male and female rat. Journal of chemical neuroanatomy *36*, 216-226.

Lu, Y.M., Jia, Z., Janus, C., Henderson, J.T., Gerlai, R., Wojtowicz, J.M., and Roder, J.C. (1997). Mice lacking metabotropic glutamate receptor 5 show impaired learning and reduced CA1 long-term potentiation (LTP) but normal CA3 LTP. The Journal of neuroscience : the official journal of the Society for Neuroscience *17*, 5196-5205.

Maeda, K., Ohkura, S., Uenoyama, Y., Wakabayashi, Y., Oka, Y., Tsukamura, H., and Okamura, H. (2010). Neurobiological mechanisms underlying GnRH pulse generation by the hypothalamus. Brain research *1364*, 103-115.

Maggi, R., Cariboni, A.M., Marelli, M.M., Moretti, R.M., Andre, V., Marzagalli, M., and Limonta, P. (2016). GnRH and GnRH receptors in the pathophysiology of the human female reproductive system. Human reproduction update *22*.

Mani, S.K., Allen, J.M., Rettori, V., McCann, S.M., O'Malley, B.W., and Clark, J.H. (1994). Nitric oxide mediates sexual behavior in female rats. Proceedings of the National Academy of Sciences of the United States of America *91*, 6468-6472.

Mathews, D., and Edwards, D.A. (1977). Involvement of the ventromedial and anterior hypothalamic nuclei in the hormonal induction of receptivity in the female rat. Physiology & behavior *19*, 319-326.

Mayer, C., Acosta-Martinez, M., Dubois, S.L., Wolfe, A., Radovick, S., Boehm, U., and Levine, J.E. (2010). Timing and completion of puberty in female mice depend on estrogen receptor alpha-signaling in kisspeptin neurons. Proceedings of the National Academy of Sciences of the United States of America *107*, 22693-22698.

Mayer, C., and Boehm, U. (2011). Female reproductive maturation in the absence of kisspeptin/GPR54 signaling. Nature neuroscience *14*, 704-710.

Merchenthaler, I., Gorcs, T., Setalo, G., Petrusz, P., and Flerko, B. (1984). Gonadotropin-releasing hormone (GnRH) neurons and pathways in the rat brain. Cell and tissue research *237*, 15-29.

Meredith, M. (1998). Vomeronasal, olfactory, hormonal convergence in the brain. Cooperation or coincidence? Annals of the New York Academy of Sciences *855*, 349-361.

Meredith, M., and Howard, G. (1992). Intracerebroventricular LHRH relieves behavioral deficits due to vomeronasal organ removal. Brain research bulletin *29*, 75-79.

Morrell, J.I., and Pfaff, D.W. (1982). Characterization of estrogen-concentrating hypothalamic neurons by their axonal projections. Science *217*, 1273-1276.

Moss, R.L., and McCann, S.M. (1973). Induction of mating behavior in rats by luteinizing hormone-releasing factor. Science *181*, 177-179.

Musatov, S., Chen, W., Pfaff, D.W., Kaplitt, M.G., and Ogawa, S. (2006). RNAi-mediated silencing of estrogen receptor {alpha} in the ventromedial nucleus of hypothalamus abolishes female sexual behaviors. Proceedings of the National Academy of Sciences of the United States of America *103*, 10456-10460.

Novotny, M., Jemiolo, B., Harvey, S., Wiesler, D., and Marchlewska-Koj, A. (1986). Adrenal-mediated endogenous metabolites inhibit puberty in female mice. Science *231*, 722-725.

Novotny, M.V., Ma, W., Wiesler, D., and Zidek, L. (1999). Positive identification of the puberty-accelerating pheromone of the house mouse: the volatile ligands associating with the major urinary protein. Proceedings Biological sciences / The Royal Society *266*, 2017-2022.

Ogawa, S., Chan, J., Chester, A.E., Gustafsson, J.A., Korach, K.S., and Pfaff, D.W. (1999). Survival of reproductive behaviors in estrogen receptor beta gene-deficient (betaERKO) male and female mice. Proceedings of the National Academy of Sciences of the United States of America *96*, 12887-12892.

Ogawa, S., Eng, V., Taylor, J., Lubahn, D.B., Korach, K.S., and Pfaff, D.W. (1998). Roles of estrogen receptor-alpha gene expression in reproduction-related behaviors in female mice. Endocrinology *139*, 5070-5081.

Okabe, M., Ikawa, M., Kominami, K., Nakanishi, T., and Nishimune, Y. (1997). 'Green mice' as a source of ubiquitous green cells. FEBS letters *407*, 313-319.

Okuyama, T., Yokoi, S., Abe, H., Isoe, Y., Suehiro, Y., Imada, H., Tanaka, M., Kawasaki, T., Yuba, S., Taniguchi, Y.*, et al.* (2014). A neural mechanism underlying mating preferences for familiar individuals in medaka fish. Science *343*, 91-94.

Ordog, T., and Knobil, E. (1995). Estradiol and the inhibition of hypothalamic gonadotropin-releasing hormone pulse generator activity in the rhesus monkey. Proceedings of the National Academy of Sciences of the United States of America *92*, 5813-5816.

Parkash, J., Messina, A., Langlet, F., Cimino, I., Loyens, A., Mazur, D., Gallet, S., Balland, E., Malone, S.A., Pralong, F.*, et al.* (2015). Semaphorin7A regulates neuroglial plasticity in the adult hypothalamic median eminence. Nature communications *6*, 6385.

Parker, K.L., Rice, D.A., Lala, D.S., Ikeda, Y., Luo, X., Wong, M., Bakke, M., Zhao, L., Frigeri, C., Hanley, N.A.*, et al.* (2002). Steroidogenic factor 1: an essential mediator of endocrine development. Recent progress in hormone research *57*, 19-36.

Pfaff, D.W. (1973). Luteinizing hormone-releasing factor potentiates lordosis behavior in hypophysectomized ovariectomized female rats. Science *182*, 1148-1149.

Pfaff, D.W., and Sakuma, Y. (1979a). Deficit in the lordosis reflex of female rats caused by lesions in the ventromedial nucleus of the hypothalamus. The Journal of physiology *288*, 203-210.

Pfaff, D.W., and Sakuma, Y. (1979b). Facilitation of the lordosis reflex of female rats from the ventromedial nucleus of the hypothalamus. The Journal of physiology *288*, 189-202.

Pfaus, J.G., Kippin, T.E., and Coria-Avila, G. (2003). What can animal models tell us about human sexual response? Annual review of sex research *14*, 1-63.

Qiao, S., Nordstrom, K., Muijs, L., Gasparoni, G., Tierling, S., Krause, E., Walter, J., and Boehm, U. (2016). Molecular Plasticity of Male and Female Murine Gonadotropes Revealed by mRNA Sequencing. Endocrinology *157*, 1082-1093.

Radovick, S., Levine, J.E., and Wolfe, A. (2012). Estrogenic regulation of the GnRH neuron. Frontiers in endocrinology *3*, 52.

Roberts, E.K., Lu, A., Bergman, T.J., and Beehner, J.C. (2012). A Bruce effect in wild geladas. Science *335*, 1222-1225.

Rodriguez, I., Feinstein, P., and Mombaerts, P. (1999). Variable patterns of axonal projections of sensory neurons in the mouse vomeronasal system. Cell *97*, 199-208.

Saito, T.R., and Moltz, H. (1986). Sexual behavior in the female rat following removal of the vomeronasal organ. Physiology & behavior *38*, 81-87.

Sakuma, Y., and Pfaff, D.W. (1979). Facilitation of female reproductive behavior from mesensephalic central gray in the rat. The American journal of physiology *237*, R278-284.

Sakuma, Y., and Pfaff, D.W. (1980a). Covergent effects of lordosis-relevant somatosensory and hypothalamic influences on central gray cells in the rat mesencephalon. Experimental neurology *70*, 269-281.

Sakuma, Y., and Pfaff, D.W. (1980b). Excitability of female rat central gray cells with medullary projections: changes produced by hypothalamic stimulation and estrogen treatment. Journal of neurophysiology *44*, 1012-1023.

Sakuma, Y., and Pfaff, D.W. (1980c). LH-RH in the mesencephalic central grey can potentiate lordosis reflex of female rats. Nature *283*, 566-567.

Schally, A.V., Arimura, A., Baba, Y., Nair, R.M., Matsuo, H., Redding, T.W., and Debeljuk, L. (1971). Isolation and properties of the FSH and LH-releasing hormone. Biochemical and biophysical research communications *43*, 393-399.

Schauer, C., Tong, T., Petitjean, H., Blum, T., Peron, S., Mai, O., Schmitz, F., Boehm, U., and Leinders-Zufall, T. (2015). Hypothalamic gonadotropin-releasing hormone (GnRH) receptor neurons fire in synchrony with the female reproductive cycle. Journal of neurophysiology *114*, 1008-1021.

Seminara, S.B., Messager, S., Chatzidaki, E.E., Thresher, R.R., Acierno, J.S., Jr., Shagoury, J.K., Bo-Abbas, Y., Kuohung, W., Schwinof, K.M., Hendrick, A.G.*, et al.* (2003). The GPR54 gene as a regulator of puberty. The New England journal of medicine *349*, 1614-1627.

Shimura, T., and Shimokochi, M. (1990). Involvement of the lateral mesencephalic tegmentum in copulatory behavior of male rats: neuron activity in freely moving animals. Neuroscience research *9*, 173-183.

Silva, B.A., Mattucci, C., Krzywkowski, P., Murana, E., Illarionova, A., Grinevich, V., Canteras, N.S., Ragozzino, D., and Gross, C.T. (2013). Independent hypothalamic circuits for social and predator fear. Nature neuroscience *16*, 1731-1733.

Sisk, C.L., and Foster, D.L. (2004). The neural basis of puberty and adolescence. Nature neuroscience *7*, 1040-1047.

Skinner, D.C., Caraty, A., Malpaux, B., and Evans, N.P. (1997). Simultaneous measurement of gonadotropin-releasing hormone in the third ventricular cerebrospinal fluid and hypophyseal portal blood of the ewe. Endocrinology *138*, 4699-4704.

Smith, J.T., Popa, S.M., Clifton, D.K., Hoffman, G.E., and Steiner, R.A. (2006). Kiss1 neurons in the forebrain as central processors for generating the preovulatory luteinizing hormone surge. The Journal of neuroscience : the official journal of the Society for Neuroscience *26*, 6687-6694.

Smith, M.S., Freeman, M.E., and Neill, J.D. (1975). The control of progesterone secretion during the estrous cycle and early pseudopregnancy in the rat: prolactin, gonadotropin and steroid levels associated with rescue of the corpus luteum of pseudopregnancy. Endocrinology *96*, 219-226.

Soriano, P. (1999). Generalized lacZ expression with the ROSA26 Cre reporter strain. Nature genetics *21*, 70-71.

Staley, K., and Scharfman, H. (2005). A woman's prerogative. Nature neuroscience *8*, 697-699.

Topaloglu, A.K., Tello, J.A., Kotan, L.D., Ozbek, M.N., Yilmaz, M.B., Erdogan, S., Gurbuz, F., Temiz, F., Millar, R.P., and Yuksel, B. (2012). Inactivating KISS1 mutation and hypogonadotropic hypogonadism. The New England journal of medicine *366*, 629-635.

Tsai, H.C., Zhang, F., Adamantidis, A., Stuber, G.D., Bonci, A., de Lecea, L., and Deisseroth, K. (2009). Phasic firing in dopaminergic neurons is sufficient for behavioral conditioning. Science *324*, 1080-1084.

Walmer, D.K., Wrona, M.A., Hughes, C.L., and Nelson, K.G. (1992). Lactoferrin expression in the mouse reproductive tract during the natural estrous cycle: correlation with circulating estradiol and progesterone. Endocrinology *131*, 1458-1466.

Ward, B.J., and Charlton, H.M. (1981). Female sexual behaviour in the GnRH deficient, hypogonadal (hpg) mouse. Physiology & behavior *27*, 1107-1109.

Wen, S., Ai, W., Alim, Z., and Boehm, U. (2010). Embryonic gonadotropin-releasing hormone signaling is necessary for maturation of the male reproductive axis. Proceedings of the National Academy of Sciences of the United States of America *107*, 16372-16377.

Wen, S., Gotze, I.N., Mai, O., Schauer, C., Leinders-Zufall, T., and Boehm, U. (2011). Genetic identification of GnRH receptor neurons: a new model for studying neural circuits underlying reproductive physiology in the mouse brain. Endocrinology *152*, 1515-1526.

Wen, S., Schwarz, J.R., Niculescu, D., Dinu, C., Bauer, C.K., Hirdes, W., and Boehm, U. (2008). Functional characterization of genetically labeled gonadotropes. Endocrinology *149*, 2701-2711.

Wray, S., Grant, P., and Gainer, H. (1989). Evidence that cells expressing luteinizing hormone-releasing hormone mRNA in the mouse are derived from progenitor cells in the olfactory placode. Proceedings of the National Academy of Sciences of the United States of America *86*, 8132-8136.

Wu, T.J., Gibson, M.J., Rogers, M.C., and Silverman, A.J. (1997). New observations on the development of the gonadotropin-releasing hormone system in the mouse. Journal of neurobiology *33*, 983-998.

Yamada, S., and Kawata, M. (2014). Identification of neural cells activated by mating stimulus in the periaqueductal gray in female rats. Frontiers in neuroscience *8*, 421.

Yamanouchi, K., and Arai, Y. (1985). The role of mesencephalic tegmentum in regulating female rat sexual behaviors. Physiology & behavior *35*, 255-259.

Yang, C.F., Chiang, M.C., Gray, D.C., Prabhakaran, M., Alvarado, M., Juntti, S.A., Unger, E.K., Wells, J.A., and Shah, N.M. (2013). Sexually dimorphic neurons in the ventromedial hypothalamus govern mating in both sexes and aggression in males. Cell *153*, 896-909.

Yizhar, O., Fenno, L.E., Davidson, T.J., Mogri, M., and Deisseroth, K. (2011). Optogenetics in neural systems. Neuron *71*, 9-34.

Zhao, Y., Sheng, H.Z., Amini, R., Grinberg, A., Lee, E., Huang, S., Taira, M., and Westphal, H. (1999). Control of hippocampal morphogenesis and neuronal differentiation by the LIM homeobox gene Lhx5. Science *284*, 1155-1158.

7 Acknowledgments

My deepest gratitude goes to Prof. Dr. Ulrich Boehm, for giving me the opportunity to join his team and for his continuous help during my PhD work. I gained so much experience working with him.

I am especially grateful to our collaborator Dr. Ioana Inta for her major contributions to the collaborative project.

I am grateful to Prof. Dr. Veit Flockerzi for providing the mCherry antibody for my project.

My gratitude goes to Dr. Petra Weissgerber and to the all the UkS mouse facility group in the Forschungsgebäude, Uniklinikum Homburg (Saar). In particular, I would like to mention Oliver Glaser for his great professionality and support.

I would like to thank Martin Simon-Thomas and Katrin Schetting for their daily support.

I wish to thank Leon Mujis for his irreplaceable role in the lab.

I am grateful to all my colleagues, which I had the honor to work with. I am grateful for the time shared in and out of the lab, for the whole scientific discussions, as well as for personal support. In particular Devesh Kumar, Soumya Kusumakshi, Oliver Mai, Mari Aoki, Amanda Wyatt, Viktoria Götz, Qiao Sen, Sarah-Louise Candlish, Mona Grünewald, Phillipp Wartenberg and Qiang Yu. Special thanks are for Michael Candlish for his constant support and willingness to help, and for his precious advice as a native English speaker.

I would like to extend my sincere gratitude to all my family and to Valentina for their endless support, encouragement and participation.

Finally, I dedicate this thesis to my mother.

8 List of publications

1. Candlish M., **De Angelis R.**, Götz V., Boehm U. (2015) "Gene targeting in neuroendocrinology". Comprehensive Physiology. 2015 Sept 20th; 5(4):1645-1676.